DISSERTATION

PROBING BACTERIA LIFE STAGES AND QUANTITATIVE ASSAYS USING MATERIAL PLATFORMS

Submitted by

Bella Hirschl Neufeld

Department of Chemistry

In partial fulfillment of the requirements

For the Degree of Doctor of Philosophy

Colorado State University

Fort Collins, Colorado

Summer 2018

Doctoral Committee:

Advisor: Melissa M. Reynolds

Thomas Borch
Ellen Fisher
Ketul Popat
Alan Van Orden

ABSTRACT

PROBING BACTERIA LIFE STAGES AND QUANTITATIVE ASSAYS USING MATERIAL PLATFORMS

The growing concern associated with nosocomial infections has been attributed to both the increasing prevalence of superbugs that are resistant to one or more antibiotic and the decreased susceptibility of bacteria to therapeutics once in biofilm form. Nosocomial infections are a particular concern with implanted biomaterials as the material surface is ideal for bacterial attachment and biofilm formation. Thus, there remains a significant need to modify current biomaterials to either prevent or kill bacteria in the biofilm stage. The focus of this work is specific to polymer systems most commonly associated with applications such as extracorporeal circuitry, catheters, and wound dressings, all of which are known to undergo complications from bacterial infections.

The ability to probe the different life stages of bacteria (planktonic, initial attachment, and mature biofilm) to elicit a desired biological effect requires discrete methodologies that are presented herein. Additionally, accurate measurements of complex biological systems using *in vitro* assays are utilized both for antibacterial studies as well as an in-depth analysis of potential interferences arising from these techniques. Specifically, the potent antibacterial agent nitric oxide (NO) is employed in two ways to determine efficacy against planktonic and mature biofilm bacteria (the former being utilized in a blended film and the latter by addition as a solution). These presented studies demonstrate the ability to target different bacteria life stages using the same therapeutic administered in different forms. They also provide quantification for the

amount of NO necessary to impose antibacterial action, whether in planktonic or biofilm states. Another presented study explores the attachment stage of biofilm formation through the use of a water-stable metal composite material. A copper-based metal-organic framework is incorporated into a chitosan matrix and the materials demonstrate a remarkable ability to impede bacterial attachment. These composite materials are also shown to be reusable, highlighting their ability to be employed in an antibacterial surface fashion. Finally, two *in vitro* assays that exploit chemical spectroscopic transformations in the presence of cellular activity are analyzed for potential interferences. The assay starting reagents are placed in solution with 19 small molecules in the absence of cells and deviations from the control solutions are determined via absorbance measurements. This critical study (which ultimately revealed a high occurrence of false responses in the presence of multiple tested compounds) highlights the importance of implementing proper control studies when using these types of techniques. Overall, a combination of polymer-bacteria systems are presented using *in vitro* techniques to continue to mitigate the prevalence of clinical infections. As a result of the findings presented herein, there is a significantly deeper understanding of the susceptibility of bacteria both in their planktonic and biofilm states that will ultimately lead to an enhanced ability to target and effectively kill bacteria throughout their life stages.

ACKNOWLEDGEMENTS

I am extremely grateful for my friends and family who have been supportive of me during my graduate career. I want to specifically thank Brian David Woodward (my phenomenal husband and best friend), Shona Hirschl Neufeld (my sister, confidant, and person who keeps me eternally laughing), my parents, Meta Chaya Hirschl and Leo Abraham Neufeld (both of whom give me endless inspiration to keep pushing on), and my grandparents (Harry Hirschl and Patricia Brown) who are likely my biggest supporters. I am endlessly appreciative for the many ways in which you have all made this graduate experience infinitely better. I also feel very fortunate to have a support system within the TMBR group and friends to share beers with at Ramskeller. Finally, I want to hugely thank my mentor and advisor, Melissa Reynolds, for providing me the support and flexibility to structure my own graduate career. Her endless confidence in me gave me the strength to carry on, even in the darkest of times. Thank you!

Nevertheless, science persisted!

TABLE OF CONTENTS

CHAPTER 1

INTRODUCTION

1.1 INTERSECTION OF BIOMATERIALS AND BACTERIA

1.1.1 The fate of biomaterials. The use of biomaterials (broadly defined as any synthetic or naturally derived material that will come into contact with a biological system) has been a key component of medicine for centuries in every region of the world. Biomaterials such as contact lenses and bandages to artificial hip replacements have helped revolutionize medical advances in their ability to enhance a person's quality of life.[1,2] With these scientific advances, however, comes a host of biological complications (known as the foreign body response) that require improvements in the field of biomaterials. One specific area within biomaterials that has been deemed critical to further a materials' performance is implantable medical devices.[3-5]

When a medical device is implanted within the body, a number of adverse biological responses can ensue. These include protein adsorption followed by platelet adhesion and activation onto the surface, ultimately resulting in blood clot formation, or bacterial attachment onto the surface, leading to biofilm formation. These described biological interactions can lead to biofouling of the device, in which the material is rejected from the body due to explicit complications.[5] In some scenarios, this requires post-operative surgery to remove and ultimately replace the device, but in more severe cases, can lead to patient death.[6] One of the leading causes of patient mortality associated with biomaterials is attributed to clinical infections, or hospital acquired infections (HAIs). Indeed, HAIs are the sixth leading cause of death in Western industrialized countries and affect ~5 out of every 100 hospital visits. Of these HAIs, roughly half of them are associated with some type of implantable device.[5-9]

1.1.2 Bacteria life stages. Given the risk associated with clinical infections, there is immense research being conducted to mitigate the likelihood for these infections to occur. To understand the current approaches associated with the interaction of bacteria and biomaterials, it is useful and necessary to identify the life stages associated with bacteria. These stages ultimately impact the methods implemented to evaluate the antibacterial efficacy of the tested system.

Bacteria exist in two forms – planktonic and biofilm (Figure 1.1). The planktonic form is associated with free-floating bacteria that are loosely associated with one another. Planktonic bacteria exist in the solution or liquid phase of the biological system and are therefore often associated with bloodstream infections. Once planktonic bacteria identify a surface, they proceed to attach to it, and begin the process of forming a biofilm. Biofilm formation is thought to occur broadly in three steps – attachment, growth, and dispersal.[10-12]

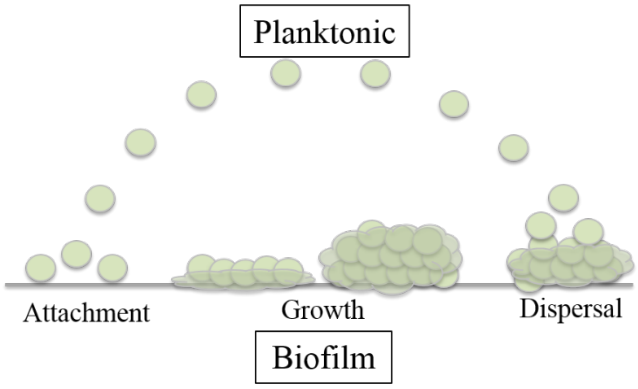

Figure 1.1 Bacteria life stages: planktonic bacteria are considered free-floating and loosely associated with one another, while biofilm is the attachment and growth of bacteria onto a surface. The biofilm stage can be divided into three parts consisting of attachment, growth (marked by the excretion of extracellular polymeric substances), and dispersal.

Bacterial attachment. The initial step in biofilm formation is the physical and chemical attachment of bacteria onto a surface. The exact mechanisms of this process are not fully understood and appear to depend greatly on the specific bacteria species. On a large scale, these

interactions are generally thought to involve proteins, polysaccharides, pili, fimbria and adhesins (surface ligands and host receptors).[13] On the molecular level, the attachment stage is considered to be driven by long-range van der Waals forces likely dictated by Brownian motion.[14] Regardless of the exact mechanisms of adhesion, this initial step is considered the foundation for the development of infections. Additional factors for determining bacterial attachment onto a surface include hydrophobicity, charge, roughness, chemical composition, and presence of additional bacteria species. Based on the relatively weak interactions associated with the initial attachment, this step is considered reversible.[13-16]

Biofilm growth and maturation. The second step in biofilm formation is growth of the biofilm. This is marked by the excretion of a sticky substance made up of extracellular DNA, proteins, and polysaccharides, known as extracellular polymeric substances (EPS). The EPS plays a significant role in biofilm formation as it can produce extra sites for polysaccharide - substrate interactions, aid in cell to cell signaling, and provide a protective coating for the bacteria existing within the biofilm.[10,11] Likewise to the initial attachment step, the exact molecular interactions of this stage are still a debated topic. It is hypothesized that additional van der Waals forces coupled with strong hydrogen bonding interactions is an essential component. Given the number of interactions possible between large polysaccharide and protein residues, the resulting effect is robust and indeed considered irreversible.[14] The critical aspect of this stage in the biofilm life cycle is that the presence of the EPS and resulting biofilm maturation are marked by the impenetrability of the biofilm to traditional antibiotics. Once the bacteria have reached this stage, there is little ability to kill or break up the biofilm, resulting in substantially increased likelihood of prolonged or even deadly infections.[17]

Biofilm dispersal. Once a biofilm has grown to maturity, it will reach a point where resources (namely food and space) are scarce, leading to a dispersal phase. At this time, biofilms detach a portion of the bacteria cells back into the planktonic phase in order to colonize a new area or a new surface altogether.[10,18] This is likely the least understood stage in the biofilm life cycle, but also in some ways, the most critical. When the biofilm is in its dispersal phase, it is considered much more susceptible to traditional antibiotics, and is therefore the topic of many research studies.[19,20] Although a promising avenue for new research, this stage was not utilized in the upcoming studies and, therefore, will not be discussed at length.

Targeting bacteria life stages. Each aspect of the planktonic and biofilm life stages can be targeted using discrete experimental conditions to probe the desired phase. This is important because it is hypothesized that both the planktonic and biofilm bacteria have different susceptibilities at each stage. Hence, the cells may require a different amount of therapeutic agent depending on the targeted phase and possible application of the therapeutic agent in a different form.[11] Not only may the stages require different therapeutic quantities, the desired reduction in cellular viability is not constant throughout all the phases. For example, the industry standard for efficacy against planktonic bacteria is considered a log-3 reduction in viability (or 99.9% decrease), however many research groups have demonstrated even higher reductions.[21-25] When it comes to reduction in biofilms, however, the expected results are much less severe. Reductions observed for killing a mature biofilm (particularly when using more robust bacteria strains) rarely reach greater than log-1 or log-2 reductions (representing 90 or 99% decrease).[26,27] Finally, demonstrating a modest 50% reduction in bacterial attachment can be considered an achievement within this field, as this is often one of the most challenging yet critical steps in halting biofilm formation.[23,28-31]

In general, evaluation of the cellular viability in the solution around a tested biomaterial gives insight into planktonic bacteria, while evaluation of the viable bacteria remaining on a surface of the biomaterial provides information on the biofilm bacteria. Specific to biofilm studies, determination of bacterial attachment onto a biomaterial versus the ability to reduce a mature biofilm also requires discrete experimental methods. To study the effects of the initial step in biofilm formation, it is useful to impregnate the substrate with the therapeutic agent to evaluate its ability to impede the attachment of the chosen bacteria, while determining the efficacy of a therapeutic agent on a mature biofilm requires some initial growth period on the given substrate in the absence of the therapeutic agent. This dissertation will examine three stages of the bacteria life cycle: planktonic, bacterial attachment, mature biofilm.

1.2 INFECTION MITIGATION

There are three main approaches to control the interaction of bacteria and biomaterials – biocidal or drug-eluting surfaces, bacteria repelling surfaces, and contact killing surfaces. The latter two strategies contain similar qualities and can broadly be defined as non-biocidal eluting surfaces.[32,33] Therefore, a discussion and comparison between biocidal/drug-eluting surfaces and non-biocidal/drug-eluting surfaces (Figure 1.2) are presented below.

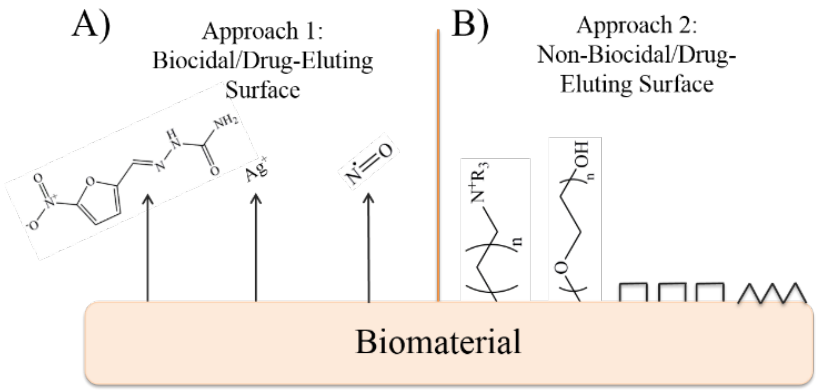

Figure 1.2 Current approaches to mitigate infections associated with biomaterials separated by A) biocidal/drug-eluting surface and; B) non-biocidal/drug-eluting surface. The left side (A) is marked by the release of a therapeutic agent into the tested system, including traditional antibiotics (nitrofurazone shown), silver, and nitric oxide. The right side (B) includes implementation of charged moieties onto the surface (generic quaternary ammonium compound shown), adding long, hydrophilic chains (such as polyethylene glycol) to the surface, and texturizing surfaces.

1.2.1 Approach 1: Biocidal/Drug-Eluting Surfaces. The first approach, related to biocidal or drug-eluting surfaces, describes when a host material is implanted with some type of therapeutic agent that is subsequently released from the system when in contact with a biological environment. The use of drug-eluting materials can be useful in identifying the efficacy against planktonic bacteria or the ability to control bacterial attachment. This first approach most commonly utilizes either antibiotic or silver releasing systems (as these devices have undergone clinical testing) in applications such as cardiac and urinary catheters.[34-36] Although there is concern with acquired resistance when implanting traditional antibiotics (most attributable to having a single antibacterial mechanism of action), some studies show the initial effectiveness of antibiotics exceeds that seen with using silver as the drug-eluting agent.[37,38] Some of the most commonly used antibiotics in catheter applications are nitrofural, sparfloxacin, minocycline, and rifampin, and each work by a different mechanism of action against Gram-positive and negative

bacteria.[36] Effectiveness of these impregnated materials has been demonstrated against both planktonic and biofilm bacteria of *Escherichia coli (E. coli), Staphylococcus aureus (S. aureus)*, *Proteus mirabilis* (*P. mirabilis),* and *Pseudomonas aeruginosa* (*P. aeruginosa)* strains at varying concentrations and contact times.[37-40] There is a desire within the field to investigate alternative approaches rather than utilizing antibiotic releasing surfaces in an effort to decrease the prevalence of superbugs (bacteria strains resistant to one or more antibiotic). This is especially relevant as a greater understanding of the increased tolerance of biofilms (versus planktonic bacteria) is understood, requiring higher and higher doses of antibiotics to be used effectively.[41] Additionally, these materials are often synthetically challenging and costly to produce.[42]

Silver represents an attractive alternative to antibiotics, as it includes multiple mechanisms of killing action, including membrane and protein disruption as well as inducing overall oxidative stress.[43,44] Additionally, silver can be incorporated into a medical device via multiple forms, with the most prevalent being nanoparticles and coatings.[45-50] It has also been shown to be a broad-spectrum antibacterial agent, effectively killing both Gram-positive and negative bacteria such as *E. coli, S. aureus* (including MRSA), *P. aeruginosa,* and *Acinetobacter baumannii,* as examples.[44,45,47] One of the current challenges, however, with the use of silver eluting surfaces, is the ability to control the rate of release from the given material, as this will ultimately have drastic effects on the efficacy of the substrate as an antibacterial surface. Some current strategies to overcome this are adding top coatings, altering the hydrophobicity of the surface to impede leaching, and altering the properties of the polymer itself.[51-53] There have been a number of studies comparing the antibacterial activity of traditional antibiotics and silver and, in some cases, the antibiotics seem to be more effective. However, the decreased likelihood for

developed resistance and the cost analysis in using silver has deemed it an advantageous candidate to be used for catheter applications.

Other drug-eluting strategies have been employed for medical devices outside of catheters that include additional metal ions (such as copper and zinc), peptides, halogens (such as chlorine), and nitric oxide (abbreviated NO and will be discussed in depth later in this section).[54-58] There is extensive research surrounding these alternative approaches, though few have made it through FDA approval. With regard to the two most prominent strategies (implantation of antibiotics and metal ions), there remains a need to enhance these surfaces to make them less prone to developed resistance and minimize the likelihood for cytotoxicity issues.[34] The biomolecule NO presents an attractive alternative to antibiotics due to its multiple mechanisms of antibacterial action and decreased concern with toxicity issues that may be observed with the use of silver. As such, NO will be a major focus of this dissertation.

Nitric oxide. Impregnating a biomaterial with a therapeutic that can release upon entering a physiological environment is an attractive approach to mitigating infection due to the localized interaction between the material (and biocidal agent) and incoming bacteria (as opposed to systemic administration).[32] Additionally, by integrating the therapeutic agent directly into the material substrate, it becomes possible to probe the initial stage of biofilm formation by monitoring the attachment of bacteria in the presence of the released therapeutic. As mentioned, some of these biocidal agents may include traditional antibiotics or metallic ions (specifically silver). One therapeutic that has received much attention for its role in numerous biological processes is NO. This small molecule was found to be the endothelium-derived relaxing factor in the 1980s and was later the subject of the 1998 Nobel Prize for Physiology and Medicine (received by Dr. Robert F. Furchgott, Dr. Louis J. Ignarro, and Dr. Ferid Murad).[59-60] Since this

discovery, NO has been rigorously studied for its role in angiogenesis, neurotransmission, and antimicrobial action. It is produced endogenously through an enzymatic pathway between L-arginine and nitric oxide synthases. Certain mammalian cells release NO under biological stress and, in particular, in response to bacterial colonization.[61-63] Therefore, researchers attempt to mimic these natural cellular processes by developing materials that are capable of releasing similar amounts of NO.[64,65] This is of significant importance when the body either cannot produce enough due to a weakened immune system or in the presence of opportunistic, nosocomial pathogens (such as those found in hospital settings) or both.[66,67]

NO donors. Administration of NO within a material substrate requires the tethering of the molecule to a secondary compound. These secondary compounds that contain NO moieties are generally called NO donors and come in a variety of forms. *S*-nitrosothiols (or RSNOs) and *N*-diazeniumdiolates are some of the most common types of NO donors used in antibacterial applications (Figure 1.3), with both capable of existing as small molecules or macromolecules, such as polymers.[68] While each of these NO donors has associated advantages and disadvantages, the focus of the work presented herein will be the utilization of RSNOs. These specific NO donors form by the nitrosation of a thiol moiety to form an S-N bond that can break and release NO under physiological conditions (37 °C, pH 7.4), making them ideal candidates for biocidal-releasing biomaterials. The decomposition of two RSNOs yields two moles of NO and the formation of a disulfide bond (as shown in reaction **1.1**).[69,70]

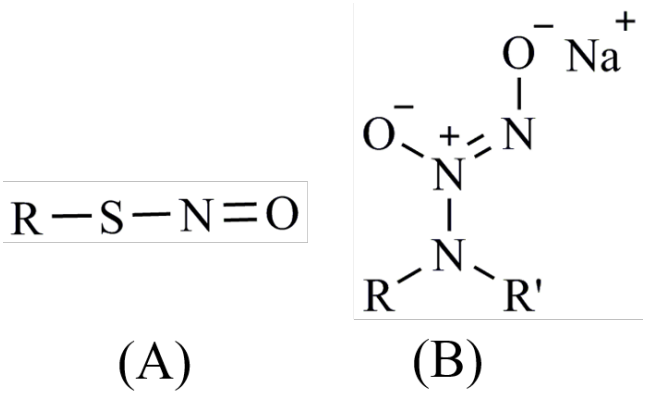

Figure 1.3 General form of common NO donors used in biomedical applications – (A) *S*-nitrosothiol (RSNO); (B) *N*-diazeniumdiolate.

$$2RSNO \rightarrow 2NO + RS\text{-}SR \qquad \textbf{(1.1)}$$

The two most common nitrosating agents for RSNOs are *t*-butyl nitrite and nitrous acid, the former being preferable in organic conditions and the latter in aqueous environments.[69,70] While RSNOs liberate NO under slightly elevated temperatures and neutral pH, there are a number of other methods by which they can decompose that should be taken into consideration. It has been shown that exposure to copper (specifically in the +1 oxidation state), light, pH, and the availability of oxygen significantly affects the stability of the S-N bond. A final consideration when utilizing RSNOs is the availability of non-nitrosated thiol compounds that may be present (i.e. RSH). These can lead to transnitrosating conditions, where the liberated NO from an initial RSNO moiety attaches to an RSH, forming a new RSNO and limiting the overall availability of NO.[71-74]

NO as an antibacterial agent. Whether blended into a polymer substrate, added in solution form, or administered in its native gaseous form, NO has been shown to be a highly effective broad-spectrum antimicrobial agent. This has been shown for both Gram-positive and Gram-negative bacteria (including those strains highly resistant to antibiotics), throughout many model systems (through the use of dendrimers, functionalized metal surfaces, hydrogels, thin films, etc.) and

demonstrated with *in vivo* studies.[75-78] The Schoenfisch Laboratory at University of North Carolina, Chapel Hill is one of the leading research groups that fabricates new NO-releasing materials and demonstrates the resultant antibacterial efficacy against both planktonic and biofilm bacteria. They have utilized numerous platforms for NO release including electrospun polyurethane fibers embedded with NO-releasing dendrimers to determine the effect on planktonic bacteria, polyvinyl chloride films embedded with NO-releasing sol-gels to examine bacterial adhesion, and extensive work using chitosan-based materials in both planktonic and biofilm bacteria studies.[79-83]

A team of researchers from the University of South Wales (including Dr. Nicolas Barraud, Dr. Scott A. Rice, and Dr. Staffan Kjelleberg) have performed immense work understanding the relationship between NO and microbiological systems. For example, they have conducted considerable research on the mechanisms associated with biofilm dispersal events, including methods for examining these events. They were also some of the first to determine the extensive role that NO plays in the natural dispersal events in bacteria (specifically in *P. aeruginosa* but also in multi-species biofilms).[20,84,85] Since this discovery they have designed synergistic systems that can induce dispersal through the presence of NO and kill the subsequently released planktonic bacteria by eluting antibiotics from the same system.[26]

While the above mentioned *in vitro* assays show great promise towards mitigating clinical infections, *in vivo* testing is necessary to advance these therapies to clinical testing. Towards this end, the Meyerhoff group from the University of Michigan has conducted some of the most extensive research of NO-releasing materials in animal models (not just for antibacterial applications but also for antithrombotic applications). They have demonstrated efficacious NO-releasing materials in multiple animal models (including mice and sheep) and, perhaps most

impressively, have shown a reduction in bacterial attachment onto NO-releasing catheters for 7 days implanted into sheep.[86-89] Although a review of this work shows that the current state of NO-releasing materials for antibacterial applications is vast, many questions remain unanswered. The work presented in Chapters 2 and 3 explore some of these remaining questions.

NO mechanism of action. The complex reactivity of NO (particularly in biological settings) makes the exact mechanism of antibacterial action difficult to determine. It is clear that conversion of NO to other oxidative and nitrosative species (namely peroxynitrite, dinitrogen trioxide, and nitrogen dioxide) can impart antibacterial activity, but to what extent each of these components is directly attributable is unclear (reactions 1.2-1.4). Likewise, species involved in these reactions, such as hydrogen peroxide and superoxide, have been shown to have antibacterial activity on their own and may also contribute to the observed effects. Lastly, it has been shown that NO itself can diffuse through bacterial cell membranes and cause irreversible DNA damage, though this too may be the result of further conversion to oxidative and nitrosative species.[58,90-92] The complexities associated with NO as an antibacterial agent are exaggerated further since its efficacy is varied from bacteria strain to strain. For instance, it is thought that NO itself may not impart a negative effect on *E. coli* cells, but rather the reactive oxygen species that increase in the presence of NO likely impart antibacterial activity.[93] Another example of the intricacies of this agent is in the case of *S. aureus*, where both NO and RSNOs are effective at killing the cells, but peroxynitrite (a species that increases in the presence of NO) does not seem to impart this effect to the same extent.[94] Regardless of the exact mechanism of action, NO is an incredibly potent antibacterial therapeutic agent.

$$NO + O_2^- \rightarrow {}^-OONO \quad \textbf{(1.2)}$$

$$2NO + O_2 \rightarrow 2NO_2 \quad \textbf{(1.3)}$$

$$NO + NO_2 \rightarrow N_2O_3 \quad \textbf{(1.4)}$$

NO detection methods. With the vast research conducted regarding NO as an antibacterial agent, the ability to accurately detect and report the amounts of deliverable NO is crucial. A quantitative discussion on the relative amounts of NO needed to elicit a desired biological effect is vital when comparing results across the field. Even more imperative, it is critical to determine what optimal amounts of NO are needed to move forward with *in vivo* and clinical testing. Indeed it is still unclear what levels of NO are necessary to induce various biological functions under each clinically relevant circumstance. Generally ranges of low concentrations of NO (pM-nM) are thought to result in a positive biological response (associated with vasodilation and angiogenesis) while high concentrations of NO (μM-mM) are thought to cause apoptosis of cells.[95,96] To enhance our understanding of the complex reactivity of NO and NO byproducts in biological systems and to make comparisons across the literature, it is important to report the amount of NO utilized in each study. It is also critical to recognize that reporting the NO donor concentration used cannot be a replacement for reporting available NO concentrations, since it has been shown that these values are not necessarily equivalent, particularly when performing the measurements in biological media.[97,98]

Spectroscopic and electrochemical methods are currently the most common techniques for the detection and quantification of NO. Within spectroscopic detection, absorbance and chemiluminescence based measurements are utilized the most frequently.[96,99] One NO detection method currently employed is the Griess assay, where NO is converted to nitrite (in the presence of oxygen), followed by nitrite reacting with the Griess reagents (sulfanilamide and *N*-1-napthylethylenediamene). This reaction results in an azo dye that can be monitored spectroscopically at 540 nm. Based on a generated calibration curve, the absorbance

measurement can be used to calculate the amount of nitrite that was initially present, which is directly attributed to the starting amount of NO. [100,101] While the Griess assay is a useful method based on ease, cost, and high throughput of samples, it also contains limitations. The limit of detection associated with the assay is in the μM range (reported as 2.5 μM), which is only useful for certain applications (as mentioned above, some biological effects are thought to occur in the pM or nM levels of NO).[96] Additionally, this indirect method of NO detection can lead to substantial false positives, as nitrite may exist in the system prior to the conversion of NO to nitrite. Indeed, the nitrosating conditions to make RSNOs often utilize nitrite and it is possible to have some unreacted nitrite leftover after the synthesis is complete. This assay can additionally lead to false negatives if NO continues to react to form nitrate instead of nitrite, leading to superficially depressed signals.[102] For these reasons, the Griess assay was not used in the studies presented in this dissertation, although it is a very common technique currently employed and can be performed under oxygenated conditions (a useful attribute when attempting to mimic experimental conditions).

Chemiluminescence detection of NO using a Nitric Oxide Analyzer (NOA) is another method that can be employed using a variety of material platforms. Though rather costly and difficult to operate (making it less commonly utilized), this technique has many beneficial properties.[96] This method employs a reaction chamber, in which the released NO is reacted with ozone to produce nitrogen dioxide in an excited state. The conversion from the excited to ground state produces a photon which can be subsequently detected.[103] This approach has many advantages, particularly in its selectivity and sensitivity towards NO. Not only is the chemiluminescent reaction specific to NO and ozone, a filter is placed between the reaction chamber and the detector to ensure any photons not associated with the reaction are not included

in the measurement. With regards to sensitivity, the limit of detection for this technique is in the nM range (reported as ~30 nM) and therefore can be employed for many applications and systems with very low but prolonged NO release.[96] The value obtained (while initially in a ppb or ppm value) can be converted to multiple reportable units (such as mols or flux), which ultimately aids in the desire to compare NO values across the literature. The experimental setup for this method also allows for many types of samples to be analyzed, including solution and film, various solvents (such as ethanol or complex media), and elevated temperatures, all of which help to mimic experimental conditions associated with biological studies. One major consideration when performing NOA studies is the requirement to perform them under deoxygenated conditions. While this ensures the released NO reaches the reaction chamber and then to the detector, it does not allow for an exact mimic of the biological experimental conditions. Overall, the versatility of NOAs for many material platforms over a wide range of experimental conditions, coupled with the selectivity and sensitivity of the instrument, led to extensive use of this method throughout this dissertation when reporting NO values.

The final method employed for NO detection is based on electrochemical sensors, in which the released NO can either be oxidized to nitrate or reduced to hyponitrite ($N_2O_2^{2-}$).[96] As with many electrochemical detection methods, the advantage lies in its ability to make extremely sensitive measurements (reported as low as ~80 pM), however the disadvantage comes in the way of selectivity. This is particularly challenging when attempting to conduct measurements in complex biological media, as many interfering species may exist (namely nitrite) that will cause artificially high responses.[104] Current research seeks to improve upon the problematic interferences faced by electrochemical sensors, and indeed this is a commonly utilized approach due to its ease of use and small size.[105,106] While not used in the work presented in this

dissertation, these sensors are a useful and common approach for the detection of NO and should be considered, especially when requiring low NO flux values in the presence of aerated conditions.

Utilization of NO. The work presented throughout this dissertation will utilize RSNOs in small molecule form (such as *S*-nitrosoglutathione, [GSNO]). The approach for implementation of NO within a biomaterial is often dictated by the intended application. The two main studies presented in this dissertation regarding NO administration for antibacterial action focus on (1) the applications of extracorporeal circulation, which uses modified polyvinyl chloride as its primary component, and (2) catheters, materials generally made of medical grade polyurethanes. In the first mentioned study, RSNOs were directly impregnated into the polymer substrate and the effect of released NO on two planktonic bacteria strains were studied to mimic the conditions associated with bloodstream infections. This particular study used two different amounts of blended RSNO (and therefore NO) and highlights the extreme difference in antibacterial efficacy on planktonic bacteria between the two amounts (no observed reduction in viable bacteria versus 99.999999% reduction in cellular viability).[107] The second study pertaining to NO administration differed in that a biofilm was allowed to grow on the polymer substrate, forming a mature biofilm, before the addition of solution-phase RSNO, to study the quantity of NO necessary to cause a reduction in the pre-formed biofilm. The mature biofilm consisting of *P. aeruginosa* was exposed to varying concentrations of RSNO (and therefore NO) to determine the amount necessary to cause a 90% reduction in the viable biofilm cells.[98] These two studies (discussed in Chapters 2 and 3) highlight the ability to probe certain phases in the bacteria life stages based on both the form of administered therapeutic (impregnated into a solid substrate versus in solution)

and the assessment of remaining viable bacteria after the challenge period (in solution versus on the polymer substrate).

1.2.2 Approach 2: Non-Biocidal/Drug-Eluting Surfaces. There are many strategies that can be employed to the material surface itself to either kill or inhibit the viability of prevalent bacteria, without the need for drug release.[108] This is ultimately a very attractive approach to mitigating infections, as there is not a finite reservoir of active agent that will be depleted, making these non-biocidal releasing materials theoretically infinitely reusable. Adding charged compounds to the surface of materials allows for direct disruption of the bacterial cell wall without the need for the compounds to leave the surface. One of the most common examples that employ this method is through the use of cationic species, such as quaternary ammonium compounds.[109-111] Bacteria repelling surfaces (also called antifouling) is another common approach and includes adding long hydrophilic chains to the surface of materials (such as polyethylene glycol), polyzwitterions, increasing the hydrophilicity of the surface (through plasma treatment), and texturized surfaces (such as adding nano- or micro- scale structures).[112-116] It is not entirely clear how these antifouling surfaces work to impede bacterial attachment, but it is often attributed to the more favorable thermodynamics of having a hydration layer surrounding the material which ultimately repel the proteins associated with biofilm formation. It could be more likely, however, that steric repulsion inhibits the bacteria's ability to begin the initial stages of biofilm formation.[14,113,117] Because these approaches have had mixed results in their ability to impede or kill bacteria, it remains difficult to predict the effect surface modifications will have on the bacteria and can lead to a trial and error (empirical) experimental procedure. This final approach may seem counterintuitive, since in some cases the cells ultimately remain intact and viable. Driving bacteria to remain in the planktonic form rather than the biofilm state, however, is a very useful

technique, as the planktonic bacteria are more susceptible to therapeutic agents than once encased in the biofilm matrix. Indeed, even the use of traditional antibiotics may be administered if the bacteria remain in the planktonic state, as very low doses of the drug can be effective.[118,119]

The successful use of metals in antibacterial applications, in tandem with the metal-based materials synthesized in our laboratory, led to an investigation of copper-based biomaterials as antibacterial surfaces. One focus area in this dissertation is the conversion of a metal-eluting surface (representing approach 1) to a metal-stable surface (encompassing approach 2), exploiting the known antibacterial activity of metals.

Metal–organic frameworks. While surfaces that release therapeutic agents are beneficial for localized delivery of highly concentrated antibacterial agents, identification of a surface with inherent properties to repel or kill bacteria is ultimately the goal to minimize HAIs. This is due to the finite reservoir of biocide stored within the biomaterial that will eventually become depleted and could lead to regrowth of bacteria around a wound site.[32] The concept behind a true antibacterial surface lies in its ability to be reused without loss of function towards the attachment and survival of viable bacteria. Identification of such a surface will be the focus of Chapter 4 in this dissertation.

Given the known antibacterial activity of metal ions, research has focused on blending or incorporating metals into polymer substrates to help mitigate infection associated with the parent polymer. The idea behind this incorporation is the slow and deliberate release of the metals into a bacterial solution to negatively impact the present cells and cause a decrease in bacterial viability (ultimately representing approach 1: a biocidal/drug-eluting surface). As mentioned previously, metals can be integrated in multiple forms, including nanoparticles.[120-123] An emerging area of research for metal incorporation is the use of metal–organic frameworks (MOFs), as these

distinct structures contain extensive metal sites and tunable properties based on the chosen organic linkers. MOFs are a unique class of hybrid materials that combine metal centers with organic ligands to form highly crystalline structures.[124-126] While MOFs are currently utilized in a variety of applications (ranging from biosensors to gas storage), they have predominantly been explored for their antibacterial action in the form of a biocidal or drug-eluting surface. This is attributable to the inherent instability of most MOFs in aqueous environments, ultimately making them ideal for this type of approach.[127] For example, multiple silver-based MOFs have shown efficacy against planktonic *E. coli*, *S. aureus*, and *P. aeruginosa*, while two cobalt-based MOFs and one zinc-based MOF have shown reactivity against multiple bacteria strains, including *E. coli*, *Pseudomonas putida* (*P. putida*) *S. aureus*, and *Staphylococcus epidermis* (*S. epidermis*), as well as others.[128-132]

One copper-based MOF that has been utilized in this area is copper benzene-1,3,5-tricarboxylate (also called Cu-BTC or HKUST-1), one of the most widely used MOFs due to its extensive characterization and commercial availability.[133,134] Cu-BTC has been shown to exhibit antibacterial activity in solution, and after growth on both silk and cellulose fibers. Rodriguez et al. immobilized Cu-BTC onto cellulose fibers and exposed the materials to solutions of *E. coli* for 1 h. They used multiple techniques (including colorimetric cellular viability and zone of inhibition assays) to determine antibacterial efficacy against planktonic *E. coli* and attributed the observed reduction to the MOF interaction with the bacterial solution.[135] Likewise, Abbasi et al. grew Cu-BTC onto silk fibers that were subsequently placed on agar containing *E. coli* and *S. aureus*. The zone of inhibition of bacteria around each Cu-BTC fiber was assessed the following day and again attributed to the slow and deliberate release of copper ions into the agar.[136]

The key component of the above mentioned studies is that the antibacterial nature is attributable primarily to the breakdown of the MOF upon entering the water-based environment, causing the deliberate release of the metal centers. While these show promising efficacy towards multiple bacteria strains, this approach still raises concern with the finite reservoir of available metal ions that will eventually become depleted and the limited ability to tune the rate of release of the metals. Therefore, a goal of the work presented in this dissertation (Chapter 4) was to utilize MOFs in such a way that the MOF would not degrade and the metal sites would not become depleted over time. To make a true antibacterial surface in which the metal sites remain intact and the material can be reused, it is necessary to identify a MOF that is both water stable and contains a metal with known antibacterial activity. Chapter 4 of this dissertation utilizes a copper-based MOF that has been shown to be extremely stable under aqueous environments, even under harsh conditions (immersion in blood and boiling in water). Copper 1,3,5-benzene-tris-triazole (known as Cu-BTTri) was loaded into a chitosan matrix and tested for its ability to both kill bacteria in solution and prevent the attachment of *P. aeruginosa* after 6 and 24 h exposure periods. This work presented the first account of utilizing a copper-based MOF as an antibacterial surface in which the substrate was shown to be effective against the tested bacteria strain after a second round of testing. Additionally, the antibacterial activity could not be attributed to the slow and deliberate release of metal centers, as this particular MOF does not undergo substantial degradation in aqueous environments.[137] This is an exciting step towards mitigating infection as there is no longer concern associated with a finite reservoir of therapeutic agent and it shows the ability to impede the first step in biofilm formation.

1.3 DETERMINATION OF ANTIBACTERIAL EFFICACY

To mitigate the infections associated with clinically relevant bacteria strains, quantitative measurements must be performed to understand and evaluate the antibacterial efficacy of a novel therapeutic or novel system. The complex system in place between the biomaterial being tested, the nutrient broth media utilized to assist growth of the bacteria, the chosen reagent to quantify viability, and the presence of living organisms makes this detection challenging from an analytical standpoint. Specifically, reproducibility of the data and the risk of false positives or false negatives that may exist in the presence of the sample analyte are prevalent concerns. This is particularly worrisome with the implementation of *in vitro* assays that rely on spectroscopic detection of cellular activity. While a rigorous study of these interferences is contained in Chapter 5, a short review of common viability assays is necessary first.

1.3.1 Methods for bacterial growth. A number of experimental methods are currently in place to grow and test bacteria in both the planktonic and biofilm forms. The American Society for Testing and Materials has determined four standard procedures for *in vitro* biofilm growth, including a drip flow reactor, flow reactor, CDC reactor, and microplate method.[138] The first three are similar in that they implement a flow system, while the final method employs a static setup. The notable difference here in the flow setup is a continuous circulation of media constantly being exposed to the growing bacteria, ultimately allowing for longer incubation periods (up to weeks), thus providing a better mimic for a wound site that has continuous biological fluid flowing over it. With a static setup, the bacteria are generally grown in one environment (often a petri dish or well plate) with the growth confined to that specific space. The limitation with the static system is the assay time (usually one week or less) and that it is not as comparable to an *in vivo* setup. The advantage is finer control over the system with regards to

both the bacteria present and the therapeutic agent tested.[139,140] The studies discussed throughout this dissertation will use a static set up for bacterial growth for both planktonic and biofilm experiments.

1.3.2 Methods to determine cellular viability. The general outline for testing antibacterial efficacy is to grow an applicable bacteria strain, expose the healthy bacteria to the sample analyte for a clinically relevant time period (known as the challenge period), and evaluate the remaining viable bacteria cells after this exposure period. Some of the most common methods are quantification of cellular activity by assessment of bacterial viability and visualization of the biofilm using microscopy.[118,141]

Microscopy. A number of microscopy techniques exist for the visualization of biofilms (for all stages of the life cycle), however fluorescence detection is most commonly employed. This can be achieved using confocal laser scanning microscopy or widefield microscopy, the former employed for establishing a 3D representation of the biofilm. To obtain representative images of a biofilm, the bacteria are exposed to stains, imaged, and a comparison is made between the control biofilm and the biofilm after exposure to the tested therapeutic.[142] These stains often come in the form of LIVE/DEAD dyes, such as SYTO 9 and DAPI (4',6-diamidino-2-phenylindole) acting as the LIVE stain and propidium iodide (PI) and SYTOX representing the DEAD stain. The LIVE stains can permeate all cellular membranes (whether intact or not), while the DEAD stains cannot permeate intact membranes. With the differing fluorescence spectra of the LIVE and DEAD dyes, those bacteria which have intact versus non-intact membranes can be visualized. Thus the combination of these stains together gives some insight into the cellular viability of the bacteria, as intact versus broken cellular membrane is considered one indication of this.[143,144] This technique is often reported in conjunction with other quantitative methods for

cellular viability, however a more quantitative assessment of the live versus dead cells is possible via pixel quantification and comparison to control samples. Other microscopy techniques employed for biofilm studies include scanning electron microscopy, atomic force microscopy, and optical microscopy (such as crystal violet staining), all of which have their own advantages and disadvantages and should be considered for future studies.[140]

One of the challenges with using fluorescence microscopy is the consideration of the solid substrate on which to grow and image the biofilm. The materials employed in the studies throughout this dissertation use polymers that tend to autofluoresce and/or incorporate the dye into the polymer backbone, making the bacteria difficult to distinguish from the material itself. This has been shown to be especially problematic when exciting with wavelengths associated with UV (<400 nm), blue (400-500 nm), or green light (450-500 nm).[145,146] Unfortunately, both SYTO9 and DAPI fall within these categories, making the use of LIVE staining rather challenging on polymer-based materials. To circumvent this issue, a DEAD stain only (PI) was utilized in Chapter 3 to visualize the immense difference between a mature biofilm grown on polyurethane substrates and one exposed to NO. Quantification of the pixels was not employed, however, as there was no counterstain to determine the number of remaining living cells.[98] This challenge with implementation of polymer substrates is underreported in the literature, though the use of only one stain (either LIVE or DEAD) in multiple studies would perhaps indicate that this issue is indeed prevalent.

Spectroscopic detection. For more quantitative assessment, sensitive and selective measurements of bacterial activity in the presence of therapeutics are necessary to accurately evaluate potential improvements in biomaterials. This can come in many forms, but the use of spectroscopic detection to signify cellular viability is widespread in the field of microbiology, primarily

because these assays allow for a high throughput of samples with minimal time and difficulty.[147] Indeed, the development of spectroscopic *in vitro* assays has truly revolutionized the ability to quickly and accurately detect cytotoxicity and cellular viability with novel therapeutics that would previously have required expensive and controversial *in vivo* testing to prove compatibility. These assays rely on the ability for healthy, metabolically active cells to convert one starting compound to a final compound. The absorbance or fluorescence properties associated with the starting or final reagent can be measured to gain insight into the viability of the exposed cells. While there are many *in vitro* methods that work by this overarching principle, the two that will be the focus of this work are the resazurin-resorufin (sold as either CellTiter Blue or Alamar Blue) and MTT (3-(4,5-dimethylthiazol-2-yl)-2,5-diphenyl-tetrazolium bromide) assays. There are numerous other viability assays based on tetrazolium salts (abbreviated MTAs for microculture tetrazolium assays), which include MTS (3-(4,5-dimethylthiazol-2-yl)-5-(3-carboxymethoxyphenyl)-2(4-sulfonyl)-2*H*-tetrazolium), XTT (2,3-bis-(2-methoxy-4-nitro-5-sulfophenyl)-2*H*-tetrazolium-5-carboxanilide), WST-1 (2-(4-iodophenyl)-3-(4-nitrophenyl)-5-(2,4-disulfophenyl)-2*H*-tetrazolium), WST-3 (2-(4-iodophenyl)-3-(2,4-dinitrophenyl)-5-(2,4-disulfophenyl)-2*H*-tetrazolium), and WST-8 (2-(2-methoxy-4-nitrophenyl)-3-(4-nitrophenyl)-5-(2,4-disulfophenyl)-2*H*-tetrazolium).[148] MTAs all rely on the ability for metabolically-active organisms to chemically transform the initial salt into a brightly colored formazan product that can be easily measured using a spectrophotometer. While the use of these detection methods provide invaluable insight into the interaction between materials and cells, Chapter 5 highlights the many interferences that exist in the presence of the initial and final compounds that can lead to substantial false negatives and positives without the need for cellular activity.

Agar plating. Spectroscopic detection induced by metabolically active cells is not the only method to determine cellular viability. The use of agar plating is also a common approach in microbiological techniques. Agar plates can be utilized to determine zones of inhibition (also known as agar diffusion method), where discs are impregnated with an antibacterial agent and placed on an agar plate that has been inoculated with bacteria. After an incubation period, a ring with a distinct diameter will form around the impregnated disc if that specific agent contains antibacterial properties. Given the zone of inhibition diameter, established guidelines can determine whether the tested therapeutic is considered resistant, intermediate, or susceptible towards a particular bacteria strain.[21] Although this method was not utilized in the work presented herein, it is a very common method employed for initial screening studies.

Due to the complexities associated with biofilm formation and the interferences that may occur when working with spectroscopic detection, a secondary technique was employed in the studies presented to verify results associated with resazurin and MTT assays. One common method is to enumerate the number of viable bacteria cells by plating on agar. To perform this assay, remaining bacteria are streaked onto agar plates and those that are viable will grow into colony-forming units (CFUs). The CFUs that are observed after an extended growth period (18-24 h) can be counted and normalized by either volume or area.[21,118,149] This is advantageous compared with spectroscopic techniques because it allows for extremely sensitive detection of bacteria relative to a control. It also reduces concerns associated with false responses due to the removal of a detector reagent. Unlike the resazurin and MTT assays, however, it is extremely time consuming and can result in large variability within a dataset.

It is critical to recognize that regardless of which assay is employed, all measurements are related back to a positive control sample. This control can be either the bacteria in the

absence of the therapeutic agent or the bacteria in the presence of the parent compound (non-derivatized therapeutic agent). This signifies that all reported cellular viabilities have no inherent meaning of their own, but are always relative to a control value. Hence, a decrease in cellular activity indicates an increase in antibacterial efficacy of the tested compound. Taken together, these two methods (spectroscopic detection and agar plating) should corroborate to give definitive results of bacterial viability after exposure to a therapeutic agent.

1.4 DISSERTATION OUTLINE

The dissertation presented herein utilizes a range of clinically relevant polymer substrates assessed in the presence of multiple bacteria strains under varying conditions. The method of therapeutic incorporation and assessment of bacteria viability exploit the ability to probe discrete stages in the bacteria life cycle given the desired application.

Chapter 2. An examination of the antibacterial efficacy of different amounts of NO against planktonic forms of *E. coli* and *S. aureus* is conducted. Specifically, a Tygon® substrate (proprietary blend of polyvinyl chloride) is impregnated with a small molecule RSNO and the release of NO is correlated to a planktonic kill rate. The cellular viability of the bacteria is evaluated after exposure to two films containing the different amounts of RSNO after 2, 4, 24, and 72 h using the agar plating method (Figure 1.4). It is demonstrated that no antibacterial efficacy against either strain is achieved at the lower amount of RSNO incorporation (5% w/w RSNO, corresponding to $0.38 \pm 0.04 \times 10^{-5}$ mols NO over 24 h), but achieves log-8 reductions for both bacteria strains using the higher amount of NO loading (20% w/w RSNO, corresponding to $1.31 \pm 0.13 \times 10^{-5}$ mols NO over 24 h). **The enormous loss in cellular viability represents one of the highest bacterial reductions to date.** Although the difference in tested RSNO amounts is relatively small (5 versus 20%), the resulting effect on planktonic bacteria is

substantial, ultimately giving insight into the amount of NO necessary to elicit antibacterial action.

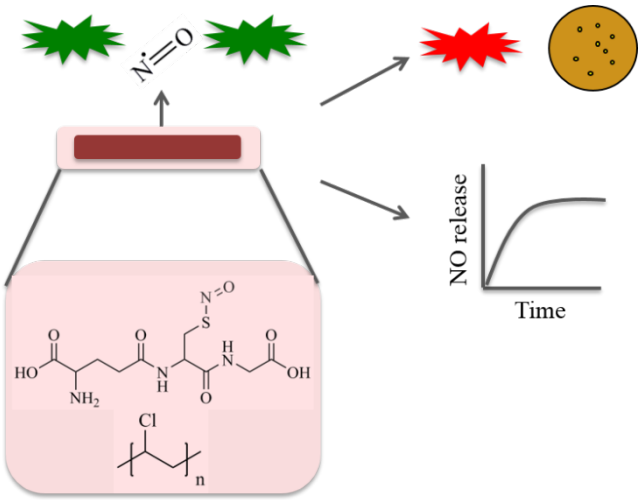

Figure 1.4 Schematic of study described in Chapter 2 where a Tygon® substrate is impregnated with *S*-nitrosoglutathione and the antibacterial efficacy is tested against planktonic bacteria.

Chapter 3. The third chapter of this dissertation utilizes NO in a different manner from Chapter 2, by studying its effects on a pre-formed biofilm rather than planktonic bacteria. A solution of *P. aeruginosa* is exposed to polyurethane substrates for 24 h to grow a mature biofilm and mimic conditions associated with catheter infections. Once the biofilm is formed, various concentrations of RSNO (in solution phase) are added to the biofilm for an additional 24 h before quantifying the remaining cellular viability by both agar plating and spectroscopic detection methods (Figure 1.5). The most efficacious concentration is found to be 10 mM RSNO, corresponding to 2.73 ± 0.31 μmol NO/mL NBM (or 1.09 ± 0.12 x 10^{-5} mol NO) over the 24 h challenge period and led to a 90% reduction in biofilm bacteria. This amount of NO is administered to the pre-formed biofilm and cellular viability is measured after 4, 8, 12, and 16 h of exposure (in addition to the original 24 h) to determine when the 90% reduction in viability occurs. This is found to be after 12 h of exposure to NO and corresponds to 1.49 ± 0.17 μmol

NO/mL NBM (or 5.97 ± 0.66 x 10^{-6} mol NO). **This represents the first report of the critical amount of NO necessary to elicit the desired biological effect on a medically relevant polymer and the described method can be applied to similar systems to determine the critical amount for inhibition and dispersal or for different polymer substrates.**

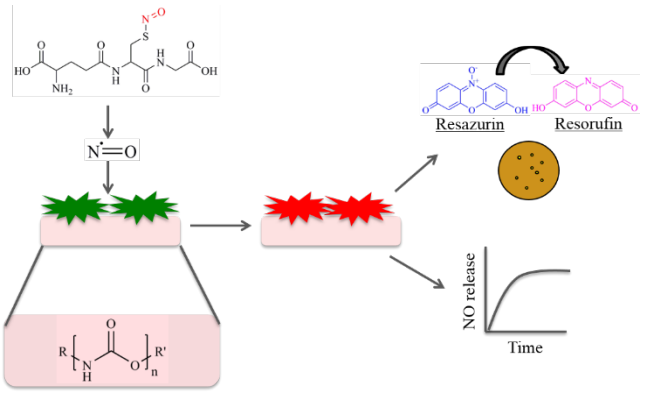

Figure 1.5 Schematic of study described in Chapter 3 where a mature biofilm is grown on a polyurethane substrate before the addition of solution-phase *S*-nitrosoglutathione to cause a reduction in biofilm viability.

Chapter 4. An exploration of a metal-based material impregnated into a chitosan matrix is studied. A copper-based MOF is embedded into a chitosan matrix and tested for properties related to bacterial attachment inhibition. The films are exposed to solutions of *P. aeruginosa* for 6 and 24 h and the resulting attached bacteria is quantified (Figure 1.6). The MOF-chitosan films demonstrate an impressive 85% reduction in attached bacteria (compared to control films) and are able to perform in a similar fashion after a second round of testing. These films demonstrate the ability to inhibit bacterial attachment (the first step towards biofilm formation) against a particularly robust bacteria strain without the need for a biocidal releasing agent. **This study represents the first use of a water-stable MOF to inhibit bacterial attachment onto a polymer surface.**

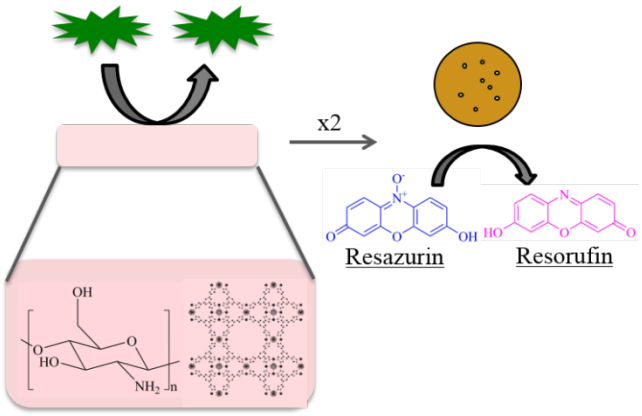

Figure 1.6 Schematic of study described in Chapter 4 where a copper-based metal-organic framework is embedded into a chitosan matrix to inhibit bacterial attachment.

Chapter 5. The fifth chapter is an investigation into small molecule interferences of two common *in vitro* assays (one of which is extensively used in the previously mentioned experiments) to delineate possible sources of deviations that may arise during experimentation. To determine the prevalence and extent of interferences on the resazurin and MTT assays in the absence of viable cells, 19 small molecules were tested at 6 concentrations (1 μM – 100 mM) (Figure 1.7). Interestingly, 16 of the 19 tested analytes cause deviations from the control when tested against resazurin, and all 19 cause deviations when tested in the presence of the MTT assay. The findings also show that the deviations were much more significant for MTT (some molecules were >3000%) than in the presence of resazurin (largest ~150%). Additional testing using UV-Visible and mass spectrometric analyses were performed on 4 or 5 of the tested analytes that displayed significant deviations in an attempt to delineate the pathway for interference. Those samples that contained thiol and carboxylic acid chemical functionalities were the most attributable sources of interference, while amine and amide functional groups appeared to play a less significant role. **This represents the first rigorous study of small molecule interferences on these two assays and highlights the importance of performing proper control studies in**

order to obtain useful and accurate *in vitro* data. This is of particular significance if the ultimate goal is to move forward to *in vivo* studies.

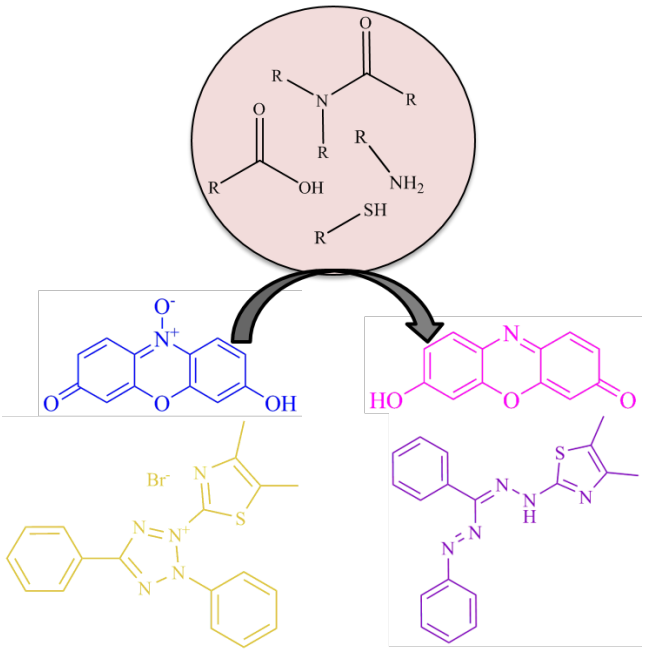

Figure 1.7 Schematic of study described in Chapter 5 where resazurin and MTT assay reagents are exposed to sample molecules containing a variety of functional groups in the absence of cells to determine potential interferences.

Summarizing remarks. This dissertation presents studies describing the intersection of biomaterials and bacteria through a variety of polymeric platforms to address the concerns of clinical infections associated with superbugs and biofilm formation. Implementation of an NO-releasing surface within a Tygon® substrate resulted in a log-8 reduction in planktonic bacteria viability, representing progress towards surfaces that can mitigate bloodstream infections associated with extracorporeal circuitry. Next, an approach to combat a mature biofilm of a robust bacteria strain on catheter-like surfaces was determined using critical amounts of NO, providing a potential solution to this common clinical infection. Additionally, an antibacterial surface composed of a copper-based material was evaluated for bacterial inhibition properties, aiding in the concerns associated with bacterial colonization of wound dressings. Finally, a better

understanding of potential interferences in the presence of common assay reagents was discovered to enable better translation from *in vitro* to *in vivo* studies of novel therapeutics. Collectively, the projects and findings outlined in this dissertation progress the field of biomaterials and, specifically, aid in the search to mitigate clinical infections associated with biomedical devices.

CHAPTER 1 – REFERENCES

1. Ratner, B.D.; Bryant, S.J., *Annu. Rev. Biomed. Eng.* **2004**, 6, 41-75.
2. Huebsch, N.; Mooney, D.J., *Nature* **2009**, 462(*7272*), 426-432.
3. Zimmerli, W.; Trampuz, A. *Biomaterials Associated Infection: Immunological Aspects and Antimicrobial Strategies*. Springer: New York, 2013.
4. Luttikhuizen, D.T.; Harmsen, M.C.; Van Luyn, M.J. *Tissue Eng.* **2006**, 12(*7*), 1955-1970.
5. Anderson, J.M.; Rodriguez, A.; Chang, D.T. *Semin. Immunol.* **2008**, 20(*2*), 86-100.
6. Jarvis, W.R. *Infect. Control Hosp. Epidemiol.* **1996**, 17(*8*), 552-557.
7. Scott, R.D. The Direct Medical Costs of Healthcare-Associated Infections in U.S. Hospitals and the Benefits of Prevention. Centers for Disease Control and Prevention (2009).
8. Robson, M.C. *Surg. Clin. North Am.* **1997**, 77(*3*), 637-650.
9. Percival, S.L.; Suleman, L.; Vuotto, C.; Donelli, G. *J. Med. Microbiol.* **2015**, 64, 323-334.
10. O'Toole, G.; Kaplan, H.B.; Kolter, R. *Annu. Rev. Microbiol*. **2000**, 54, 49-79.
11. Stoodley, P.; Sauer, K.; Davies, D.G.; Costerton, J.W. *Annu. Rev. Microbiol,* **2002**, 56, 187-209.
12. Hall-Stoodley, L.; Costerton, J.W.; Stoodley, P. *Nature Rev Microbiol*. **2004**, 2 95-108.
13. Pizarro-Cerda, J.; Cossart, P. *Cell* **2006**, 124, 715-727.
14. An, Y.H.; Friedman, R.J. *Handbook of Bacterial Adhesion: Principles, Methods, and Applications*. Humana Press: New Jersey, 2000.
15. Busscher, H.J.; van der Mei, H.C. *PLOS Pathog.* **2012**, 8(*1*), e1002440.

16. Garrett, T.R.; Bhakoo, M.; Zhang, Z. *Prog. Nat. Sci. Mater. Int.* **2008**, 18, 1049-1056.

17. Limoli, D.H.; Jones, C.J.; Wozniak, D.J. *Microbiol. Spectr.* **2015**, 3(3),

18. Kaplan, J.B. *J. Dent. Res.* **2010**, 89(*3*), 205-218.

19. Guilhen, C.; Forestier, C.; Balestrino, D. *Mol. Microbiol.* **2017**, 105(*2*), 188-210.

20. Baraud, N.; Kelso, M.J.; Rice, S.A.; Kjelleberg, S. *Curr. Pharm. Des.* **2015**, 21, 31-42.

21. Coyle, M.B. *Manual of Antimicrobial Susceptibility Testing;* American Society for Microbiology, 2005.

22. Levison, M.E.; Levison, J.H. *Infect. Dis. Clin. North Am.* **2013**, 23(*4*), 791-820.

23. Regev-Shoshani, G.; Ko, M.; Miller, C.; Av-Gay. *Antimicrob. Agents Chemother.* **2010**, 54(*1*), 273-279.

24. Pegalajar-Jurado, A.; Wold, K.A.; Joslin, J.M.; Neufeld, B.H.; Arabea, K.A.; Suazo, L.A.; McDaniel, S.L.; Bowen, R.A.; Reynolds, M.M *J. Control. Release* **2015**, 217, 228-234.

25. Wiegand, C.; Abel, M.; Ruth, P.; Elsner, P.; Hipler, U. *J. Mater. Sci. Mater. Med.* **2015**, 26(*1*), 18-31.

26. Nguyen, T.; Selvanayagam, R.; Ho, K.K.K.; Chen, R.; Kutty, S.K.; Rice, S.A.; Kumar, N.; Barraud, N.; Duong, H.T.T.; Boyer, C. *Chem. Sci.* **2016**, 7, 1016-1027.

27. Panmanee, W.; Taylor, D.; Shea, C.J.A; Tang, H.; Nelson, S.; Seibel, W.; Papoian, R.; Kramer, R.; Hassett, D.J.; Lamkin, T.J. *J. Biomol. Screen.* **2013**, 18(*7*), 820-829.

28. Hasan, S.; Thomas, N.; Thierry, B.; Prestidge, C.A. *J. Mater. Chem. B.* **2017**, 5, 1005-1014.

29. Dosler, S.; Karaaslan, E. *Peptides* **2014**, 62, 32-37.

30. Dobmeier, K.P.; Schoenfisch, M.H. *Biomacromolecules* **2004**, 5, 2493-2495.

31. Wo, Y.; Xu, L.; Li, Z.; Matzger, A.J.; Meyerhoff, M.E.; Siedlecki, C.A. *Biomater. Sci.* **2017**, 5, 1265-1278.

32. Cloutier, M.; Mantovani, D.; Rosei, F. *Trends Biotechnol.* **2015**, 33(*11*), 637-652.

33. Neoh, K.G.; Li, M.; Kang, E.; Chiong, E.; Tambyah, P.A. *J. Mater. Chem. B* **2017**, 5, 2045-2067.

34. Singha, P.; Locklin, J.; Handa, H. *Acta Biomater.* **2017**, 50, 20-40.

35. Anagnostakos, K.; Furst, O.; Kelm, J. *Acta. Orthop.* **2006**, 77(*4*), 628-637.

36. Paladini, F.; Pollini, M.; Sannino, A.; Ambrosio, L. *Biomacromolecules* **2015**, 16(*7*), 1873-1885.

37. Johnson, J.R.; Johnston, B.; Kuskowski, M.A. *Antimicrob. Agents Chemother.* **2012**, 56(*9*), 4969-4972.

38. Regev-Shoshani, G.; Ko, M.; Crowe, A.; Av-Gay, Y. *Urology* **2011**, 78(*2*), 334-339.

39. Salvarci, A.; Koroglu, M.; Gurpinar, T. *J. Pak. Med. Assoc.* **2015**, 65(*2*), 115-119.

40. Fisher, L.E.; Hook, A.L.; Ashraf, W.; Yousef, A.; Barrett, D.A.; Scurr, D.J.; Chen, X.; Smith, E.F.; Fay, M.; Parmenter, C.D.J.; Parkinson, R.; Bayston, R. *J. Contol. Release* **2015**, 202, 57-64.

41. Stewart, P.S. *Int. J. Med. Microbiol.* **2002**, 292(*2*), 107-113.

42. O'Neill, J. *Securing New Drugs for Future Generations: The Pipeline of Antibiotics;* The Review on Antimicrobial Resistance, 2015.

43. Lemire, J.A.; Harrison, J.J.; Turner, R.J. *Nat. Rev. Microbiol.* **2013**, 11, 371-384.

44. Jung, W.K.; Koo, H.C.; Kim, K.W.; Shin, S.; Kim, S.H.; Park, Y.H. *Appl. Environ. Microbiol.* **2008**, 74(*7*), 2171-2178.

45. Lara, H.H.; Garza-Trevino, E.N.; Ixtepan-Turrent, L.; Singh, D.K. *J. Nanobiotechnology* **2011**, 9, 30-38.

46. Rai, M.; Yadav, A.; Gade, A. *Biotechnol. Adv.* **2009**, 27, 76-83.

47. Monte-Serrano, M.; Fernandez-Saiz, P.; Orti-Lucas, R.M.; Harnando, B. *J. Microb. Biochem. Technol.* **2015**, 7(*6*), 398-403.

48. Orti-Lucas, R.M.; Munoz-Miguel, J. *Antimicrob. Resist. Infect. Control.* **2017**, 6, 61-68.

49. Zan, X.; Kozlov, M.; McCarthy, T.J.; Su, Z. *Biomacromolecules* **2010**, 11, 1082-1088.

50. Chaudhari, A.A.; Ashmore, D.; deb Nath, S.; Kate, K.; Dennis, V.; Singh, S.R.; Owen, D.R.; Palazzo, C.; Arnold, R.D.; Miller, M.E.; Pillai, S.R. *J. Nanobiotechnol.* **2016**, 14, 58-73.

51. Liu, J.; Sonshine, D.A.; Shervani, S.; Hurt, R.H. *ACS Nano*, **2010**, 4(*11*), 6903-6913.

52. Brobbey, K.J.; Haapanen, J.; Gunell, M.; Toivakka, M.; Makela, J.M.; Eerola, E.; Ali, R.; Saleen, M.R.; Honkanen, S.; Bobacka, J.; Saarinen, J.J. *Thin Solid Films* **2018**, 645, 166-172.

53. Coad, B.R.; Griesser, H.J.; Peleg, A.Y.; Travern, A. *PLOS Pathog.* **2016**, 12, 6-13.

54. Vincent, M.; Hartemann, P.; Engels-Deutsch, M. *Int. J. Hyg. Environ. Health* **2016**, 219, 585-591.

55. Pasquet, J.; Chevalier, Y.; Pelletier, J.; Couval, E.; Bouvier, D.; Bolzinger, M. *Colloids Surf. A Physicochem. Eng. Asp.* **2014**, 457, 263-274.

56. Bahar, A.A.; Ren, D. *Pharmaceuticals* **2013**, 6, 1543-1575.

57. Kim, J.; Pitts, B.; Stewart, P.S.; Camper, A.; Yoon, J. *Antimicrob. Agents Chemother.* **2008**, 52(*4*), 1446-1453.

58. Fang, F.C. *J. Clin. Invest.* **1997**, 99(*12*), 2818-2825.

59. Ignarro, L.J.; Buga, G.M.; Wood, K.S.; Byrns, R.E.; Chaudhuri, G. *Proc. Natl. Acad. Sci.* **1987**, 84(*24*), 9265-9269.

60. SoRelle, R. *Circulation* **1998**, 98, 2365-2366.

61. Wink, D.A.; Mitchell, J.B. *Free Radic. Biol. Med.* **1998**, 25(*4*), 434-456.

62. Moncada, S.; Higgs, E.A. *Eur. J. Clin. Invest.* **1991**, 21(*4*), 361-374.

63. Luiking, Y.C.; Engelen, M.P.K.J.; Deutz, N.E.P. *Curr. Opin. Clin. Nutr. Metab. Care.* **2010**, 13(*1*), 97-104.

64. Yang, Z.; Yang, Y.; Xiong, K.; Li, X.; Qi, P.; Tu, Q.; Jing, F.; Weng, Y.; Wang, J.; Huang, N. *Biomaterials* **2015**, 63, 80-92.

65. Wu, B.; Gerlitz, G.; Grinnell, B.W.; Meyerhoff, M.E. *Biomaterials* **2007**, 28(*28*), 4047-4055.

66. Kahn, H.A.; Ahmad, A.; Mehboob, R. *Asian Pac. J. Trop. Biomed.* **2015**, 5(*7*), 509-514.

67. Gerberding, J.L. *Infect. Control Hosp. Epidemiol.* **1998**, 19(*8*), 575-577.

68. Riccio, D.A.; Schoenfisch, M.H. *Chem. Soc. Rev.* **2012**, 41(*10*), 3731-3741.

69. Williams, D.L.H. *Acc. Chem. Res.* **1999**, 32, 869-876.

70. Hogg, N. *Free Radic. Biol. Med.* **2000**, 28(10), 1478-1486.

71. Stamler, J.S.; Toone, E.J. *Curr. Opin. Chem. Biol.* **2002**, 6, 779-785.

72. Gu, J.; Lewis, R.S. *Ann. Biomed. Eng.* **2007**, 35(*9*), 1554-1560.

73. Gorssi, L.; Montevecchi, P.C. *Chemistry* **2002**, 8(*2*), 380-387.

74. Barnett, D.J.; Rios, A.; Williams, D.L.H. *J. Chem. Soc. Perkin Trans. 2* **1995**, 1279-1282.

75. Fox, S.; Wilkinson, T.S.; Wheatley, P.S.; Xiao, B.; Morris, R.E.; Sutherland, A.; Simpson, A.J.; Barlow, P.G.; Butler, A.R.; Megson, I.L.; Rossi, A.G. *Acta Biomater.***2010**, 6, 1515-1521.

76. Ho, K.K.K.; Ozcelik, B.; Willcox, M.D.P.; Thissen, H.; Kumar, N. *Chem. Commun.* **2017**, 53, 6488-6491.

77. Hetrick, E.M.; Shin, J.H.; Paul, H.S.; Schoenfisch, M.H. *Biomaterials* **2009**, 30, 2782-2789.

78. Heilman, B.J.; St. John, J.; Oliver, S.R.J.; Mascharak, P.K. *JACS* **2012**, 134, 11573-11582.

79. Worley, B.V.; Soto, R.J.; Kinsley, P.C.; Schoenfisch, M.H. *ACS Biomater. Sci. Eng.* **2016**, 2, 426-437.

80. Nablo, B.J.; Schoenfisch, M.H. *Biomacromolecules* **2004**, 5, 2034-2041.

81. Lu, Y.; Slomberg, D.L.; Schoenfisch, M.H. *Biomaterials* **2014**, 35, 1716-1724.

82. Lu, Y.; Shah, A.; Hunter, R.A.; Soto, R.J.; Schoenfisch, M.H. *Acta Biomater.* **2015**, 12, 62-69.

83. Kim, J.O.; Noh, J.; Thapa, R.K.; Hasan, N.; Choi, M.; Kim, J.H.; Lee, J.; Ku, S.K.; Yoo, J. *Int. J. Biol. Macromol.* **2015**, 79, 217-225.

84. Barraud, N.; Hassett, D.J.; Hwang, S.H.; Rice, S.A.; Kjelleberg, S.; Webb, J.S. *J. Bacteriol.* **2006**, 188(*21*), 7344-7353.

85. Barraud, N.; Storey, M.V.; Moore, Z.P.; Webb, J.S.; Rice, S.A.; Kjelleberg, S. *Microb. Biotechnol.* **2009**, 2(*3*), 370-378.

86. Colletta, A.; Wu, J.; Kappler, M.; Chen, H.; Xi, C.; Meyerhoff, M.E. *ACS Biomater. Sci. Eng.* **2015**, 1(*6*), 416-424.

87. Handa, H.; Major, T.C.; Brisbois, E.J.; Amoako, K.A.; Meyerhoff, M.E.; Bartlett, R.H. *J. Mater. Chem. B* **2014**, 2(*8*), 1059-1067.

88. Brisbois, E.J.; Bayliss, J.; Wu, J.; Major, T.C.; Xi, C.; Wang, S.C.; Bartlett, R.H.; Handa, H.; Meyerhoff, M.E. *Acta Biomater.* **2014**, 10, 4136-4142.

89. Brisbois, E.J.; Davis, R.P.; Jones, A.M.; Major, T.C.; Bartlett, R.H.; Meyerhoff, M.E.; Handa, H. *J. Mater. Chem. B. Mater. Biol. Med.* **2015**, 3(*8*), 1639-1645.

90. Carpenter, A.W.; Schoenfisch, M.H. *Chem. Soc. Rev.* **2012**, 41, 3742-3752.

91. Hughes, M.N. *Methods in Enzymology: Chemistry of Nitric Oxide and Related Species*, Vol. 436.; Elsevier: Amsterdam, 2008.

92. Feelisch, M.; Stamler, J.S. *Methods in Nitric Oxide Research*, John Wiley & Sons: New York, 1996.

93. Pacelli, R.; Wink, D.A.; Cook, J.A.; Krishna, M.C.; DeGradd, W.; Friedman, N.; Tsokos, M.; Samuni, A.; Mitchell, J.B. *J. Exp. Med.* **1995**, 182, 1469-1479.

94. Kaplan, S.S.; Lancaster, J.R.; Basford, R.E.; Simmons, R.L. *Infect. Immun.* **1996**, 64(*1*), 69-76.

95. Thomas, D.D.; Ridnour, L.A.; Isenberg, J.S.; Flores-Santana, W.; Switzer, C.H.; Donzelli, S.; Hussain, P.; Vecoli, C.; Paolocci, N.; Ambs, S.; Colton, C.A.; Harris, C.C.; Roberts, D.D., Wink, D.A. *Free Radic. Biol. Med.* **2008**, 45(1), 18-31.

96. Coneski, P.N.; Schoenfisch, M.H. *Chem. Soc. Rev.* **2012**, 41, 3753-3758.

97. Harding, J.L.; Reynolds, M.M. *Anal. Chem.* **2014**, 86(*4*), 2025-2032.

98. Neufeld, B.H.; Reynolds, M.M. *Biointerphases* **2016**, 11, e031012.

99. Hetrick, E.M.; Schoenfisch, M.H. *Annu. Rev. Anal. Chem.* **2009**, 2, 409-433.

100. Griess, J.P. *Philos. Trans. R. Soc*. **1864**, 154, 667-731.

101. Promega Corporation. *Technical Bulletin: Griess Reagent System*, 2009.

102. Giustarini, D.; Rossi, R.; Milzani, A.; Dalle-Donne, I. *Methods Enzymol.* **2008**, 440, 361-380.

103. Bates, J.N. *Neuroprotocols* **1992**, 1(*2*), 141-149.

104. Privett, B.J.; Shin, J.H.; Schoenfisch, M.H. *Chem. Soc. Rev.* **2010**, 39, 1925-1935.

105. Kitamura, Y.; Uzawa, T.; Oka, K.; Komai, Y.; Ogawa, H.; Takizawa, N.; Kobayashi, H.; Tanishita, K. *Anal. Chem.* **2000**, 72, 2957-2962.

106. Allen, B.W.; Piantadosi, C.A.; Coury, L.A. *Nitric Oxide* **2000**, 4(*1*), 75-84.

107. Mann, M.N.; Neufeld, B.H.; Hawker, M.J.; Pegalajar-Jurado, A.; Paricio, L.N.; Reynolds, M.M.; Fisher, E.R. *Biointerphases* **2016**, 11, e031005.

108. Green, J.D.; Fulghum, T.; Nordhaus, M.A. *Biointerphases* **2011**, 6(*4*), MR13-28.

109. Terada, A.; Okuyama, K.; Nishikawa, M.; Tsuneda, S.; Hosomi, M. *Biotechnol. Bioeng.* **2012**, 109(*7*), 1745-1754.

110. Gottenbos, B.; Grijpma, D.W.; van der Mei, H.C.; Feijen, J.; Busscher, H.J. *J. Antimicrob. Chemother.* **2001**, 48(*1*), 7-13.

111. McBain, A.J.; Ledder, R.G.; Moore, L.E.; Catrenich, C.E.; Gilbert, P. *Appl. Environ. Microbiol.* **2004**, 70(*6*), 3449-3456.

112. Chen, S.; Li, L.; Zhao, C.; Zheng, J. *Polymer* **2010**, 51, 5283-5293.

113. Banerjee, I.; Pangule, R.C.; Kane, R.S. *Adv. Mater.* **2011**, 23, 690-718.

114. Zhang, H.; Chiao, M. *J. Med. Biol. Eng.* **2015**, 35(2), 143-155.

115. Chapman, R.G.; Ostuni, E.; Takayama, S.; Holmlin, R.E.; Yan, L.; Whitesides, G.M. *JACS* **2000**, 122, 8303-8304.

116. Ostuni, E.; Chapman, R.G.; Holmlin, R.E.; Takayama, S.; Whitesides, G.M. *Langmuir* **2001**, 17, 5605-5620.

117. Tuson, H.H.; Weibel, D.B. *Soft Matter* **2013**, 9(*18*), 4368-4380.

118. Ceri, H.; Olson, M.E.; Stremick, C.; Read, R.R.; Morck, D.; Buret, A. *J. Clin. Micrbiol.* **1999**, 37(*6*), 1771-1776.

119. Aaron, S.D.; Ferris, W.; Ramotar, K.; Vandemheen, K.; Chan, F.; Saginur, R. *J. Clin. Microbiol.* **2002**, 40(*11*), 4172-4179.

120. Zhang, W.; Zhang, Y.; Ji, J.; Zhao, J.; Yan, Q.; Chu, P.K. *Polymer* **2006**, 47(*21*), 7441-7445.

121. Cometa, S.; Iatta, R.; Ricci, M.A.; Ferretti, C.; De Giglio, E. *J. Bioact. Compat. Polym.* **2013**, 28(*5*), 508-522.

122. Pishbin, F.; Mourino, V.; Gilchrist, J.B.; McComb, D.W.; Kreppel, S.; Salih, V.; Ryan, M.P.; Boccaccini, A.R. *Acta Biomater.* **2013**, 9, 7469-7479.

123. Kumar, V.; Jolivalt, C.; Pulpytel, J.; Jafari, R.; Arefi-Khonsari, F. *J. Biomed. Mater. Res. A.* **2013**, 101A, 1121-1132.

124. Stock, N.; Biswas, S. *Chem. Rev.* **2012**, 112, 933-969.

125. Butova, V.V.; Soldatov, M.A.; Guda, A.A.; Lomachenko, K.A.; Lamberti, C. *Russ. Chem. Rev.* **2016**, 85(*3*), 280-307.

126. Eddaoudi, M.; Moler, D.B.; Li, H.; Chen, B.; Reineke, T.M.; O'Keefe, M.; Yaghi, O.M. *Acc. Chem. Res.* **2001**, 34, 319-330.

127. Burtch, N.C.; Jasuja, H.; Walton, K.S. *Chem. Rev.* **2014**, 114, 10575-10612.

128. Berchel, M.; Gall, T.L.; Denis, C.; Hir, S.L.; Quentel, F.; Elleouet, C.; Montier, T.; Rueff, J.; Salaun, J.; Haelters, J.; Hix, G.B.; Lehn, P.; Jaffres, P. *New J. Chem.* **2011**, 35, 1000-1003.

129. Liu, Y.; Xu, X.; Xia, Q.; Yuan, G.; He, Q.; Cui, Y. *Chem. Commun.* **2010**, 46, 2608-2610.

130. Aguado, S.; Quiros, J.; Canivet, J.; Farrusseng, D.; Boltes, K.; Rosal, R. *Chemosphere* **2014**, 113, 188-192.

131. Tamames-Tabar, C.; Imbuluzqueta, E.; Guillou, N.; Serre, C.; Miller, S.R.; Elkaim, E.; Horcajada, P.; Blanco-Prieto, M.J. *Cryst. Eng. Comm.* **2015**, 17, 456-462.

132. Wyszogrodzka, G.; Marszalek, B.; Gil, B.; Dorozynski, P. *Drug Discov. Today* **2016**, 21(*6*), 1009-1017.

133. Sezginel, K.B.; Keskin, S.; Uzun, A. *Langmuir* **2016**, 32, 1139-1147.

134. Rubin, H.N.; Reynolds, M.M. *Inorg. Chem.* **2017**, 56, 5266-5274.

135. Rodriguez, H.S.; Hinestroza, J.P.; Ochoa-Puentes, C.; Sierra, C.A.; Soto, C.Y. *J. Appl. Polym. Sci.* **2014**, 131, 40815-40820.

136. Abbasi, A.R.; Akhbari, K.; Morsali, A. *Ultrason. Sonochem.* **2012**, 19, 846-852.

137. Neufeld, B.H.; Neufeld, M.J.; Lutzke, A.; Schweickart, S.M.; Reynolds, M.M. *Adv. Funct. Mater.* **2017**, 27, 1702255-1702264.

138. Vertes, A.; Hitchins, V.; Phillips, K.S. *Anal. Chem.* **2012**, 84(9), 3858-3866.

139. Welch, K.; Cai, Y.; Stromme, M. *J. Funct. Biomater.* **2012**, 3(*2*), 418-431.

140. Azeredo, J.; Azevedo, N.F.; Briandet, R.; Cerca, N.; Coenye, T.; Costa, A.R.; Desvauz, M.; Di Bonaventura, G.; Hebraud, M.; Jaglic, Z.; Kacaniova, M.; Knochel, S.; Lourenco, A.; Mergulhao, F.; Meyer, R.L.; Nychas, G.; Simoes, M.; Tresse, O.; Sternberg, C. *Crit. Rev. Microbiol.* **2017**, 43(*3*), 313-351.

141. Larimer, C.; Winder, E.; Jeters, R.; Prowant, M.; Nettleship, I.; Addleman, R.S.; Bonheyo, G.T. *Anal. Bioanal. Chem.* **2016**, 408, 999-1008.

142. Franklin, M.J.; Chang, C.; Akiyama, T.; Bothner, B. *Microbiol. Spectr.* **2015**, 3(4).

143. Johnson, M.B.; Criss, A.K. *J. Vis. Exp.* **2013**, 79, 50729-50738.

144. Stiefel, P.; Schmidt-Emrich, S.; Maniura-Weber, K.; Ren, Q. *BMC Microbiol.* **2015**, 15, 36-45.

145. Hawkins, K.R.; Yager, P. *Lab Chip* **2003**, 3, 248-252.

146. Pokhriyal, A.; Lu, M.; Chaudhery, V.; Huang, C.; Schulz, S.; Cunningham, B.T. *Opt. Express.* **2010,** 18(*24*), 24793-24808.

147. Riss, T.L.; Moravec, R.A.; Niles, A.L.; Duellman, S.; Benink, H.A.; Worzella, T.J.; Minor, L. *Cell Viability Assays*, Eli Lilly & Company: Bethesda, MD, 2013.

148. Ginouves, M.; Carme, B.; Couppie, P.; Prevot, G. *J. Clin. Microbiol.* **2014,** 52(*6*), 2131-2138.

149. Hamilton, M.A. *The log reduction (LR) measure of disinfectant efficacy,* MSU Center for Biofilm Engineering: Montana, 2010.

CHAPTER 2

PLANKTONIC REDUCTION USING NITRIC-OXIDE RELEASING TYGON® FILMS

2.1 BACKGROUND

This project represents an extension of a collaboration between the research groups of Prof. Melissa M. Reynolds and Prof. Ellen R. Fisher at Colorado State University. The first study published between the groups examined the effects of surface modification through water-plasma treatment of a nitrosated polymer substrate.[1] This project showed the surface wettability could be drastically enhanced after water-plasma treatment, without impeding the release of NO. In a subsequent publication (adapted below), the enhanced wettability and NO release of a different polymer system was developed and the bacterial response to the materials was evaluated. The components regarding implementation of water-plasma treatment, including extensive surface characterization via XPS, goniometry, and protein deposition studies, were performed by Michelle N. Mann, Morgan J. Hawker, and Adoracion Pegalajar-Jurado, colleagues in the Fisher group. The contributions by Bella H. Neufeld were solely dedicated to the RSNO synthesis, fabrication of the NO-releasing films, NO measurements, and bacteria studies. Michelle N. Mann, Adoracion Pegalajar-Jurado, and Lindsey N. Paricio also participated in the bacterial kill rate measurements. The following chapter contains the experiments and results related to the studies performed by Bella H. Neufeld. This project was originally published in Biointerphases (Mann, M.N.; Neufeld, B.H.; Hawker, M.J.; Pegalajar-Jurado, A.; Paricio, L.N.; Reynolds, M.M.; Fisher, E.R. Plasma-modified nitric oxide-releasing polymer films exhibit time-delayed 8-log reduction in growth of bacteria. *Biointerphases* **2016**, 11,

031005) and has been adapted with permission. Copyright 2016, American Vacuum Society. Prof. Melissa M. Reynolds and Prof. Ellen R. Fisher acted as the advisors on this project.

2.2 INTRODUCTION

While the use of indwelling medical devices is often associated with a host of adverse biological responses, it is not just indwelling materials that can elicit these effects, but rather any material that may encounter biological fluid.[2] In the case of extracorporeal circuitry (ECC), there is a substantial concern with both blood clot formation on the tubing itself and the likelihood for bloodstream infections related to the implementation of such tubing.[3,4] ECC relates to any procedure where blood is removed from the body, pumped through tubing, and then circulated back into the body. Therefore, any adverse implication that may happen while in the tubing portion of the device, such as bacterial colonization, has major impacts on the patient.[5-7] Additionally, the patients undergoing ECC are likely already in a compromised immune state (given the necessity to use ECC in the first place) and will be less likely to fight off any infection that might ensue from the procedure. Therefore, it is critical to develop a material that minimizes the likelihood for bacteria to colonize the surface of the material.[8] One such approach to this challenge is to target bacteria in their planktonic state, where they are considered more susceptible to antibacterial agents than once they have colonized a surface.[9,10]

ECCs can be comprised of multiple polymeric materials but the primary component is Tygon®, a proprietary blend of polyvinyl chloride (PVC). There are several approaches currently employed to kill bacteria (whether in the planktonic or biofilm state) and often the chosen method is dictated by the material substrate.[8] In the case of Tygon®, the relative stability of the polymer backbones lends itself to direct integration of therapeutic agents, rather than chemical alteration of the polymer itself. For example, methods have been used that impregnate

the Tygon® material with antibiotics or other known antimicrobial agents (such as metallic ions) to mitigate the interactions with bacteria.[11,12] While these methods have shown efficacy against multiple strains of bacteria, they come with inherent limitations such as toxicity, cost, and overall considerations of developed resistance.[13-15] Nitric oxide (NO) is a well-known antibacterial agent that can minimize some of the concerns associated with the other options and will be the therapeutic used in this study.

Since receiving the Nobel Prize in 1998 for its discovery as the natural endothelium-derived relaxing factor, research around NO has become increasingly prevalent.[16,17] Besides its role in vasodilation, NO has been widely established to be a potent antibacterial agent in discrete concentration ranges.[18] Due to its ability to effectively kill both Gram-positive and Gram-negative bacteria (representing a broad-spectrum agent) and its considered decreased likelihood for developed resistance, it has been utilized in an enormous amount of antibacterial studies.[19-24] This includes using NO as inhalation therapy (in its native gaseous form) or through the incorporation of NO and NO donor moieties into materials that may release NO under certain conditions. Currently the only FDA approved use of NO is through the inhalation of the gaseous form to treat respiratory failure. While this form of therapy has shown great efficacy to treat patients (particularly premature babies) the systemic approach is not ideal for mitigating infection associated with a medical device.[25,26] To administer a localized delivery of NO, it is first necessary to convert the NO gas into a substance that can ultimately be impregnated into the device. These come in the form of NO donors.

A variety of NO donor systems have been applied for medical applications, but the two most common are *S*-nitrosothiols (RSNOs) and *N*-diazeniumdiolates.[27] Early research using NO-releasing materials focused primarily on the latter, until cytotoxicity issues arose around the

decomposition products and the trajectory shifted to be more centered around the former.[28] In addition to the decreased concern around toxic byproducts, RSNOs represent an attractive NO donor system because they are known to release NO under physiological conditions (37 °C, pH 7.4).[29] It should be noted that, while RSNOs have many favorable attributes, they are also relatively unstable and promptly decompose in the presence of light. This is one reason that the incorporation of an RSNO within the stable and robust polymeric matrix of Tygon® is a logical blended material to utilize for relatively long-term studies of bacteria with decreased concern for donor leaching (as will be discussed further in the chapter).

The synthesis of RSNOs involves nitrosating a thiol residue, either in small molecule form or on a polymer backbone. In an aqueous solvent, the thiol substrate is mixed with sodium nitrite under acidic conditions until the development of the RSNO.[30] This study utilized glutathione as the starting compound, which was subsequently nitrosated to form *S*-nitrosoglutathione (GSNO). This particular RSNO was chosen due to its biological relevance (associated with decreased concern around toxicity) and its relative stability among other small molecule RSNOs.[31] Once the nitrosated product has been synthesized, these compounds can be readily characterized by UV-Vis spectroscopy. RSNOs are known to exhibit two fingerprint regions in the UV-Vis spectrum at ~335 nm (attributed to the $n_o \rightarrow \pi^*$ transition) and ~550 nm (arising from the $n_N \rightarrow \pi^*$ transition).[30] The prominent absorbance feature for GSNO occurs at 336 nm and can give insight into the extent of nitrosation from the RSNO synthesis.[32] Once glutathione has been successfully nitrosated to form GSNO, the NO donor can be loaded into the Tygon® substrate.

The study presented herein describes the incorporation of GSNO into a Tygon® substrate at two different quantities (5 and 20% w/w) to determine the amount of NO necessary to cause a

significant reduction in viable bacteria of two clinically relevant strains (*Escherichia coli* and *Staphylococcus aureus*). The GSNO was characterized using UV-Vis spectroscopy and the films were analyzed for NO release using a nitric oxide analyzer. The resulting antibacterial activity of the films was assessed after 2, 4, 24, and 72 h using an agar plating method. Eliciting the reduction in planktonic bacteria using NO-releasing films minimizes the risk associated with bloodstream infections surrounding ECC use.

2.3 MATERIALS AND METHODS

2.3.1 Materials

All reagents used to prepare GSNO are described elsewhere.[32] The model polymer in all studies was Tygon® (Formula R-3603, Saint-Gobain Performance Plastics, Akron, OH, USA). *Escherichia coli* (*E. coli*, ATCC 25922) and *Staphylococcus aureus* (*S. aureus,* ATCC 29213) were obtained from American Type Culture Collection (ATCC, USA). Oxoid™ nutrient broth media (NBM, OXCM0001B), Oxoid™ nutrient agar (NA, OXCM0003B), tetrahydrofuran (THF), and EPA vials were purchased from Fisher Scientific (Fair Lawn, NJ, USA). Glycerol (≥99.5%) was obtained from Sigma-Aldrich and a 30% v/v solution was prepared in ultrapure water (Millipore, 18 mΩ cm). A 0.85% w/v solution of sodium chloride (Teknova, Ultrapure grade) was prepared in ultrapure water and autoclaved. Tissue culture plates (6 well) were purchased from VWR (Arlington Heights, IL, USA).

2.3.2 Experimental Methods

GSNO synthesis. GSNO was used as the NO donor and was prepared by nitrosating the thiol residue of glutathione. GSNO was synthesized following the protocol published by Hart.[32] Briefly, glutathione (5 mmol) was added to a mixture of 8 mL of ice-cold water and 2.5 mL of 2 M hydrochloric acid. For the nitrosation step, sodium nitrate (5 mmol) was added to the

mixture to form nitrous acid as the nitrosating agent. The solution was then stirred on ice for 40 min. The GSNO product was precipitated by adding 10 mL of acetone, and the product was filtered and washed with water to remove any excess of nitrite. The GSNO was subsequently rinsed with acetone, dried under vacuum for 1.5 h protected from direct light, and stored in EPA vials at −20 °C until use to prevent any donor decomposition. Characterization of GSNO was performed by UV-Vis spectroscopy as previously reported.[33]

Film fabrication. To prepare the Tygon® solution, Tygon® was dissolved in THF at a concentration of 0.075 g mL^{-1}. Tygon® only films were prepared by delivering 750 μL of the Tygon®/THF solution to the bottom of a 20 mL glass beaker. GSNO-incorporated films were prepared by blending either 5% or 20% w/w GSNO in Tygon® solution before casting into the beaker. Films were dried overnight at room temperature and protected from light.

NO release analysis. To quantify the release of nitric oxide from both GSNO incorporated films, nitric oxide analyzers (NOAs, Sievers 280i, GE Analytical Instruments, Boulder, CO, USA) were used to measure NO release from polymer films. This technique is highly selective and sensitive for the direct chemiluminescent detection of NO.[33] Prior to data collection, NOAs were calibrated using zero gas (UHP N_2) and 45 ppm NO/N_2. Samples were introduced to the NOA cell containing NBM at 37 °C to mimic bacterial culture conditions and the sample intervals were 5 s and 1 min for 24 and 72 hours, respectively. NO released from the polymer samples was swept into the reaction cells by N_2 flow gas at 200 mL/min. Average concentration data collected over the sample interval were converted to moles of NO using a previously determined calibration constant. By calculating the theoretical amount of NO in each film the percentage of NO released from each film could be determined. Surface flux was calculated by dividing the amount of NO released by the film surface area as a function of time. All measurements were

performed in triplicate, and statistical analyses were completed using a two-tailed t-test with significance considered at $p \leq 0.05$.

Bacteria studies. 5 and 20% GSNO films were analyzed for biocidal performance. Lyophilized bacteria were reconstituted in warm NBM and grown overnight at 37 °C and 150 rpm. The overnight culture was diluted 1:1 using a glycerol solution (30% v/v) and stored at −80 °C. Prior to each assay, a tube of bacterial culture was thawed and centrifuged at 4700 rpm for 10 min to collect a pellet. The pellet was re-suspended in warm NBM and incubated overnight at 37 °C and 150 rpm. The overnight culture was diluted with fresh warm NBM to an optical density at 600 nm ($O.D._{600nm}$) of ~0.1 and incubated (37 ºC at 100 rpm) until it reached the logarithmic growth phase ($O.D._{600nm}$ ~0.3) prior to exposing the films to the bacteria solution.

The bactericidal activity of GSNO incorporated films was determined following a protocol based on the National Committee for Clinical Laboratory Standards guidelines.[35,36] All bactericidal activity assays were performed in 37 ºC NBM to closely mimic *in vivo* conditions and to ensure excess nutrients were available to allow for continuous growth of bacterium during the 72 h testing period.

Aliquots of the bacterial solution (2 mL) in logarithmic growth phase ($O.D._{600nm}$ ~0.3) were added to each well containing one of the three different films (Tygon®, 5% GSNO and 20% GSNO). Bacterial culture was also placed in empty wells as additional positive controls. All samples were placed in a static incubator at 37 ºC for the duration of the assay. To assess the number of colony forming units per mL (CFU/mL) over time, 100 µL aliquots were removed from each well at 2, 4, 24 and 72 h. Each aliquot underwent serial 10-fold dilutions using sterile 0.85% (w/v) NaCl to reach 10^6 or 10^7 dilution factor. Subsequently, 50 µL of diluted bacterial

solution were plated onto nutrient agar.[37] Plates were left overnight in a static incubator at 37 ºC, counted the following day, and CFU/mL of bacterial culture was calculated using equation 2.1.

$$\frac{\text{colony forming units (CFU)}}{\text{volume (mL)}} = \frac{\text{number of colonies}}{\text{dilution factor} \times \text{plated volume (mL)}} \qquad (2.1)$$

For the assay described above, a limit of detection (LOD) of 1 CFU/mL is applied, and the limit of quantification (LOQ) in estimated to be 25 CFU/mL by the American Society for Testing and Materials (ASTM) and Current Good Manufacturing Practice (CGMP) for the United States Food and Drug Administration (FDA).[37,38] Therefore, 1 CFU/mL was assigned to plates containing no colonies.

All biocidal activity experiments consisted of at least nine replicates ($n \geq 9$), and data are reported as mean ± standard deviation. Statistical analyses were performed using a one-tailed Student's t-test with significance considered at $p < 0.05$.

2.4 RESULTS AND DISCUSSION

There have been a number of reports on the antibacterial activity of NO-releasing polymer films due to their potent antimicrobial action.[39-42] Additionally, there is precedence for NO to be used in the place of antibiotics as studies have shown decreased likelihood for developed resistance to NO.[43] This is attributable to the production of NO by bacteria themselves, as well as the multiple mechanistic pathways of action associated with NO as an antibacterial agent.[44] One underlying concern with using blended NO-donor systems is the ability for the donor to leach out of the polymer matrix. In the case of GSNO, the issue is not necessarily around toxicity with donor leaching, but rather that the desired localized effect is no longer accessible. The particular model system utilized in this study was chosen in part because previous work has been done examining the extent of donor leaching under various conditions

and found it to be minimal.[45] Once the GSNO Tygon® films were fabricated, NOAs were utilized to quantify the NO release.

NO release analysis. Multiple methods can be employed to determine the release of NO from a system, but the most sensitive and selective for NO is through use of an NOA. This works by the chemiluminescent detection of a photon emitted from the reaction of NO with ozone to produce an excited state NO_2 (see reactions 2.1 and 2.2). This highly sensitive technique can obtain values of NO in the ppb region and the selectivity of the instrument comes from both the chemiluminescent based reaction and filters in place within the instrument.[34,46]

$$NO + O_3 \rightarrow NO_2^* + O_2 \qquad (2.1)$$

$$NO_2^* \rightarrow NO_2 + h\nu \qquad (2.2)$$

Use of the NOAs also enables NO quantification in conditions that mimic the desired experiments closely (in this case, bacteria viability assays). Therefore, all NOA measurements took place at 37 ºC, in NBM, covered from light. Total NO release (including flux) was acquired over a 24 h period (and later for 72 h), again to mimic the experimental conditions of the bacteria assays employed. Additionally, it is essential to perform the NO release studies in NBM, as previous work has shown that there is a significant suppression of the NO signal in the presence of cell media as opposed to phosphate buffered saline (PBS).[47] Figure 2.1 shows the results of the NO release studies for both 5 and 20% GSNO incorporated films over 24 h in mols of NO released versus time. The NO release plots for both types of films show fairly typical behavior, where there is a steady rise in the release out of the polymer system followed by a maintained steady-state release for the remainder of the period.[45] Based on the reaction set up, the likely factors influencing NO release from this system are the slightly elevated temperature (37 ºC) and pH of solvent (7.4).[30] The total mols released over the entire 24 h study period for 5% GSNO and

20% GSNO were 0.38 ± 0.04 x 10^{-5} mols (corresponding to 1.89 ± 0.21 μmol NO/mL media and 0.52 ± 0.07 nmol/cm^2*min) and 1.31 ± 0.13 x 10^{-5} mols (corresponding to 6.55 ± 0.66 μmol NO/mL media and 1.73 ± 0.38 nmol/cm^2*min), respectively. These values represent 44 ± 5% NO released for 5% GSNO and 39 ± 4% NO released for 20% GSNO (based on the total theoretical reservoir of available NO).

The representative NO release profiles presented in Figure 2.1 differ in the overall trace for real-time NO release between the 5 and 20% blended films. While the 5% film appears to reach a steady-state NO release (in pmols) within a few hours, the 20% blended film release profile over the tested 24 h seems to extinguish its NO reservoir at a faster rate. Indeed, between the NO release profiles from hours four to 24, the decrease in the 20% blended film is ~50%, while the 5% blended film shows little to no decrease in the rate of NO release. One possible explanation for this could be the increased availability of thiyl radicals in the higher donor concentration film that more easily lend themselves to disulfide formation. As the NO is cleaved from the RSNO, radical-radical bond formation is necessary through two thiyl radicals to form the disulfide (oxidized glutathione in this case), otherwise it is possible to reform the *S*-nitrosated moiety through radical-radical formation between NO and the thiyl radical. Thus, it is possible that the increased decomposition profile observed for the 20% GSNO blended film is due to the higher availability of thiyl radicals formed through the NO cleavage, ultimately increasing the rate of disulfide formation.

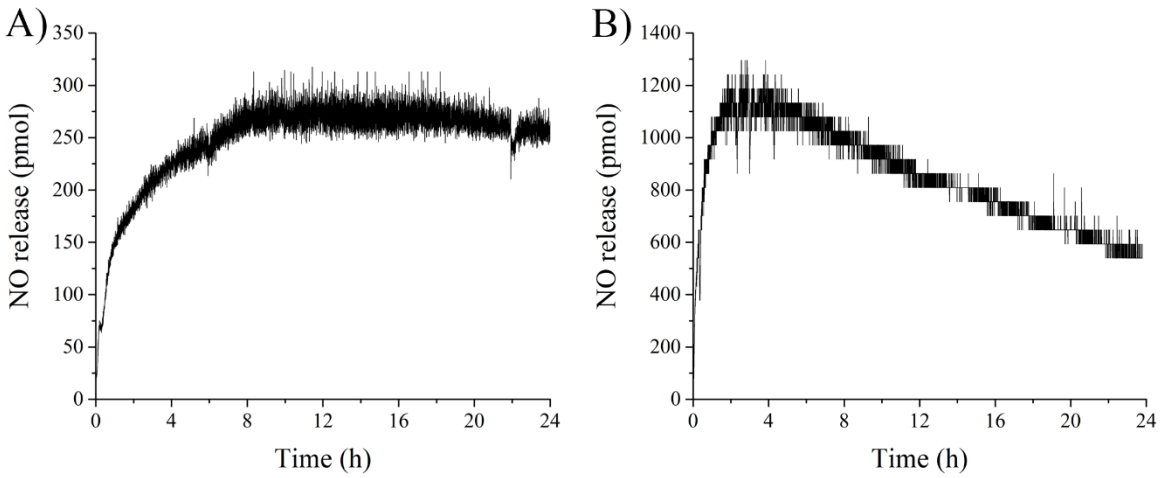

Figure 2.1 Representative NO release plot of A) 5% GSNO incorporation into Tygon® films and B) 20% GSNO incorporation into Tygon® films. Data collected via nitric oxide analyzers over a 24 h period where cell was maintained at 37 ºC, protected from light, and analysis was performed in media.

Bacteria kill rate studies. To study the effects of NO on planktonic bacteria, two clinically relevant strains were chosen for the model system. *E. coli* (Gram negative bacteria) is thought to be responsible for ~265,000 infections in the United States annually and *S. aureus* (Gram positive bacteria) is considered one of the most common strains associated with bloodstream infections, particularly those obtained in clinical settings.[48,49] A patient is considered most susceptible to acquiring an infection after the first 6 h of device incorporation, so the initial time points for antibacterial efficacy were selected based on this information (2 and 4 h exposure period).[50] It is essential to ensure there is no regrowth of the bacteria, therefore longer time points were also employed (24 and 72 h) to prove continued efficacy of the NO-releasing films. Additionally, the optimal experimental conditions for all bacterial assays are essential so as not to compromise the integrity of healthy cells by a factor other than the GSNO-Tygon® films. This includes maintaining the bacteria at elevated temperatures (37 ºC) and growing the bacteria in NBM (as opposed to PBS or other saline solutions). Lastly, two positive controls were tested against bacteria and both can be independently compared to the NO samples. The first control is

the bacterial solution in the absence of any films, which gives insight into the overall metabolic activity of the bacteria being tested. The second control is the Tygon® film that has not been impregnated with GSNO. This will ensure that any decrease in cellular viability is directly attributable to the GSNO (and subsequently NO) and not to the film itself being present in the bacterial solution.

The bacteria kill rate studies were conducted using an agar plating method.[36,37] After subsequent exposure to either the Tygon® film alone or the GSNO-Tygon® incorporated films (or simply the bacterial solution as the positive control), aliquots were removed from the well-plate and subsequently diluted using a sodium chloride solution. After the appropriate number of serial dilutions, an aliquot was plated on agar, incubated, and the number of CFUs were assessed the following morning. The implementation of this technique allows extreme sensitivity for assessing bacterial viability, with a LOD of 1 CFU/mL. Although there is increased inherent variability with the agar plating method, it was chosen in this study to elicit the largest effect on a bacterial population.

When testing the 5% GSNO-Tygon® films against both strains of bacteria, no reduction in cellular viability was observed at any time point tested. This would indicate that this level of NO release is not enough to elicit an antibacterial effect against strains of *E. coli* and *S. aureus*. The use of the 20% GSNO-Tygon® films, however, showed a dramatic decrease in cellular viability against both strains over a 24 h exposure period. As shown in Figure 2.2, in the first two and four hours of exposure of the *E. coli* solution to the 20% GSNO-Tygon® films, there is a slight decrease in viability (10^8 CFUs/mL for both controls versus 10^7 CFUs/mL for the 20% GSNO-Tygon® films). Although a slight decrease is observed, there remains a very large amount of bacteria present that could still pose a risk for causing bloodstream infections. The

results after 24 h exposure to the 20% GSNO-Tygon® films, however, is quite substantial. There is no detection of viable *E. coli* cells after this exposure period, resulting in an astounding log-8 reduction in viable bacteria (log-8 = 99.999999%). This also represents the LOD for this technique of 1 CFU/mL. A similar trend can be seen in the presence of *S. aureus* cells, where the initial two and four hours of exposure cause little to no reduction in viable bacteria (in fact in one case there is a slight increase), but after 24 h of exposure to the 20% GSNO-Tygon® films, there are no detectable cells. This again results in a log-8 reduction and the LOD for this technique. After determining the exposure period necessary for the observed reduction in bacteria, an additional extended time point was chosen to ensure no re-growth of the bacteria was possible (minimizing concern with developing infection at a later stage). The viability of both *E. coli* and *S. aureus* cells were tested again after 72 h of exposure and, indeed, no re-growth of bacteria was observed, indicating the maintenance of a log-8 reduction in the presence of the 20% GSNO-Tygon® films.

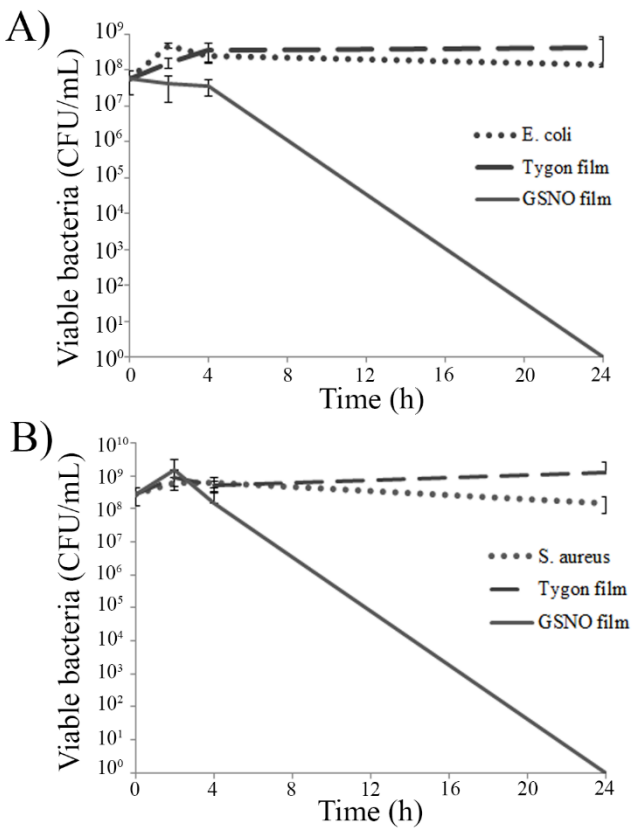

Figure 2.2 The concentration of viable bacteria versus time of A) *E. coli* and B) *S. aureus* in the presence of Tygon® and 20% GSNO-Tygon® films. Average and standard deviation displayed, (n≥9).

The difference in activity between the 5 and 20% GSNO-Tygon® films gives insight into the amount of NO necessary to elicit antibacterial efficacy. While a total concentration of 1.89 ± 0.21 µmol NO/mL media over 24 h did not have an effect, the somewhat modest increase to 6.55 ± 0.66 µmol NO/mL media demonstrated an incredibly large effect. This is likely related to the antibacterial mechanism of action by NO. Though still not fully understood, it is thought that both NO and NO byproducts are responsible for bacteria cellular damage. NO has the ability to permeate intact cell membranes and cause irreversible DNA damage, but species that arise from NO in cellular environments (namely peroxynitrite) are also thought to cause substantial oxidative and nitrosative damage both intracellularly and to the bacterial membrane itself.[43,50]

2.5 CONCLUSIONS

Tygon® films impregnated with two different amounts of GSNO were fabricated and characterized to study their antibacterial efficacy against *E. coli* and *S. aureus*. The significant difference in behavior between the two films tested (5 and 20% GSNO incorporation) gives insight into the amount of NO necessary to elicit antibacterial properties. Where the 5% blended film (corresponding to $0.38 \pm 0.04 \times 10^{-5}$ mols NO over a 24 h period) did not result in a reduction in cellular viability, increasing the donor content to 20% (corresponding to $1.31 \pm 0.13 \times 10^{-5}$ mols NO over a 24 h period) resulted in an astounding log-8 reduction in both tested bacteria strains. The ability to demonstrate the enhanced antibacterial effects using the 20% GSNO-Tygon® films provides precedence to incorporate these NO donors into standard Tygon® tubing currently used in ECC applications to mitigate the risk of bloodstream infections. The demonstration of the films utilized in this study to cause log-8 reductions of clinically relevant strains of bacteria associated with HAIs greatly advances the world of biomaterials.

CHAPTER 2 – REFERENCES

1. Pegalajar-Jurado, A.; Joslin, J.M.; Hawker, M.J.; Reynolds, M.M.; Fisher, E.R. *ACS Appl. Mater. Interfaces* **2016**, 6(*15*), 12307-12320.
2. Anderson, J.M.; Rodriguez, A.; Chang, D.T. *Semin. Immunol.* **2008**, 20(*2*), 86-100.
3. Peek, G.J.; Scott, R.; Killer, H.M.; Firmin, R.K. *Perfusion* **2002**, 17(*2*), 125-132.
4. Hong, J.; Larsson, A.; Ekdahl, K.N.; Elgue, G.; Larsson, R.; Nilsson, B. *J. Lab. Clin. Med.* **2001**, 138(*2*), 139-145.
5. Butt, W.; MacLaren, G. *F1000Prime Reports* **2013**, 5, 55-61.
6. Bisdas, T.; Beutel, G.; Warnecke, G.; Hoeper, M.M.; Kuehn, C.; Haverich, A.; Teebken, O.E. *Ann. Thorac. Surg.* **2011**, 92(*2*), 626-631.
7. Speranza, G.; Gottardi, G.; Pederzolli, C.; Lunelli, L.; Canteri, R.; Pasquardini, L.; Carli, E; Lui, A.; Maniglio, D.; Brugnara, M.; Anderle, M. *Biomaterials* **2004**, 25(*11*), 2029-2037.
8. Cloutier, M.; Mantovani, D.; Rosei, F. *Trends Biotechnol*., **2015**, *33***,** 637-652.
9. Gristina, A.G.; Hobgood, C.D.; Webb, L.X.; Myrvik, Q.N. *Biomaterials* **1987**, 8, 423-426.
10. Costerton, J.W.; Stewart, P.S.; Greenberg, E.P. *Science* **1999**, 284, 1318-1322.
11. Wassil, S.K.; Crill, C.M.; Phelps, S.J. *J. Pediatr. Pharmacol. Ther.* **2007**, 12(*2*), 77-90.
12. Li, X.H.; Xing, Y.G.; Jiang, Y.H.; Ding, Y.L. *Food Sci. Technol. Int.* **2010**, 16(*3*), 225-232.
13. Poon, V.K.M.; Burd, A. *Burns* **2004**, 30(*2*), 140-147.

14. Marr. A.K.; Gooderham, W.J.; Hancock, R.E.W. *Curr. Opin. Pharmacol* **2006**, 6, 468-472.

15. Rolain, J.M.; Canton, R.; Cornaglia, G. *Clin. Microbiol. Infect.* **2012**, 18(*7*), 615-616.

16. Ignarro, L.J. *Annu. Rev. Pharmacol. Toxicol.* **1990**, 30, 535-560.

17. Thomas, D.D. et al. *Free Radic. Biol. Med.* **2008**, 45(*1*), 18-31.

18. Coneski, P.N.; Schoenfisch, M.H. *Chem. Soc. Rev.* **2012**, 41, 3753-3758.

19. Singha, P.; Pant, J.; Goudie, M.J.; Workman, C.D.; Handa, H. *Biomater. Sci.* **2017**, 5, 1246-1255.

20. Ren, H.; Wu, J.; Colletta, A.; Meyerhoff, M.E.; Xi, C. *Front. Microbiol.* **2016**, 7, 1260-1268.

21. Wo, Y.; Xu, L.; Li, Z.; Matzger, A.J.; Meyerhoff, M.E.; Siedlecki, C.A. *Biomater. Sci.* **2017**, 5, 1265-1278.

22. Madariaga-Venegas, F.; Fernandez-Soto, R.; Duarte, L.F.; Suarez, N.; Delgadillo, D.; Jara, J.A.; Fernandez-Ramires, R.; Urzua, B.; Molina-Berrios, A. *PLOS One* **2017**, 12(*5*), e0176755.

23. Quinn, J.F.; Whittaker, M.R.; Davis, T.P. *J. Control. Release* **2015**, 205, 190-205.

24. Backlund, C.J.; Worley, B.V.; Schoenfisch, M.H. *Acta Biomater.* **2016**, 29, 198-205.

25. Akmal, A.H.; Hasan, M. *Ann. Thorac. Med.* **2008**, 3(*3*), 100-103.

26. Committee on Fetus and Newborn, American Academy of Pediatrics, *Pediatrics* **2000**, 106(*2*).

27. Riccio, D.A.; Schoenfisch, M.H. *Chem. Soc. Rev.* **2012**, 41(*10*), 3731-3741.

28. Keefer, L.K. *ACS Chem. Biol.* **2011**, 6(*11*), 1147-1155.

29. Hogg, N. *Free Radic. Biol. Med.* **2000**, 28(*10*), 1478-1486.

30. Williams, D.L.H. *Acc. Chem. Res.* **1999**, 32, 869-876.

31. Wang, W.; Ballatori, N. *Pharmacol. Rev.* **1998**, 50(*3*), 335-356.

32. Hart, T.W. *Tetrahedron Lett.* **1985**, 26(*16*), 2013-2016.

33. Damodaran, V.B.; Joslin, J.M.; Wold, K.A.; Lantvit, S.M.; Reynolds, M.M. *J. Mater. Chem.* **2012**, 22, 5990-6001.

34. Bates, J.N. *Neuroprotocols* **1992**, 1(*2*), 141-149.

35. Barry, A.L.; Craig, W.A.; Nadler, H.; Reller, L.B.; Sanders, C.C.; Swenson, J.M. *Methods for Determining Bactericidal Activity of Antimicrobial Agents; Approved Guidelines* **1999.**

36. Cavalieri, S.J. et al. American Society for Microbiology. *Manual of Antimicrobial Susceptibility Testing*. Coyle, M.B.: Seattle, 2005.

37. *Standard Practice for Determining Microbial Colony Counts from Water Analyzed by Plating Methods*. (ASTM International, West Conshohocken, Pennsylvania, 2012).

38. Sutton, S. J. *Validation Technol.* **2011**, 17(*3*), 42-46.

39. Seabra, A.B.; Martins, D.; Simoes, M.M.S.G.; Da Silva, R.; Brocchi, M.; De Oliveira, M.G. *Artif. Organs* **2010**, 34(*7*), E204-E214.

40. Jones, M.L.; Ganopolsky, J.G.; Labbe, A.; Wahl, C.; Prakash, S. *Appl. Microbiol. Biotechnol.* **2010**, 88, 401-407.

41. Nablo, B.J.; Schoenfisch, M.H. *J. Biomed. Mater. Res. A* **2003**, 67A, 1276-1283.

42. Coneski, PN.; Rao, K.S.; Schoenfisch, M.H. *Biomacromolecules* **2010**, 11(*11*), 3208-3215.

43. Privett, B.J.; Broadnax, A.D.; Bauman, S.J.; Riccio, D.A.; Schoenfisch, M.H. *Nitric Oxide* **2012**, 3(*31*), 169-173.

44. Fang, F.C. *J. Clin. Invest.* **1997**, 99(*12*), 2818-2825.

45. Joslin, J.M.; Lantvit, S.M.; Reynolds, M.M. *ACS Appl. Mater. Inter.* **2013**, 5(*19*), 9285-9294.

46. Fontijn, A.; Sabadell, A.J.; Ronco, R.J. *Anal. Chem.* **1970**, 42(*6*), 575-579.

47. Harding, J.L.; Reynolds, M.M. *Anal. Chem.* **2014**, 86, 2025-2032.

48. Centers for Disease Control and Prevention. E. coli. https://www.cdc.gov/ecoli/general/index.html.

49. Tong, S.Y.C.; Davis, J.S.; Eichenberger, E.; Holland, T.L.; Fowler, V.G. *Clin. Microbiol. Rev.* **2015**, 28(*3*), 603-661.

50. Poelstra, K.A.; Barekzi, N.A.; Rediske, A.M.; Felts, A.G.; Slunt, J.B.; Grainger, D.W. *J. Biomed. Mater. Res.* **2002**, 60(*1*), 206-215.

51. Carpenter, A.W.; Schoenfisch, M.H. *Chem. Soc. Rev.* **2012**, 41(*10*), 3742-3752.

CHAPTER 3

DETERMINATION OF CRITICAL AMOUNT OF NITRIC OXIDE TO KILL PRE-FORMED BIOFILM

3.1 BACKGROUND

While surveying the literature associated with the influence of NO on biofilms, mass inconsistencies emerged with regards to reporting the amount of NO utilized in the mentioned studies. In some cases, only the amount of the donor compound was reported (not of NO itself) and in other cases, there was never a quantitative value stated at all. When the amount of NO applied to the studied system was included, it became evident that there exist numerous reporting units. This is unfortunate as it becomes very difficult to compare studies that utilize NO in relation to biofilms and it also increases the knowledge gap in understanding the amount of NO necessary to elicit certain desired biological effects. Lastly, when working with complex biological systems such as biofilms, it became clear that multiple techniques are necessary to accurately measure the influence of a therapeutic on a biofilm system. This work aims to begin that discussion by 1) reporting NO amounts in several, useful formats, 2) demonstrating the discrepancy between the NO donor amount and that of NO itself, and finally 3) providing multiple cellular viability techniques to confirm the observed results. This work was originally published in Biointerphases (Neufeld, B.H.; Reynolds, M.M. Critical nitric oxide concentration for *Pseudomonas aeruginosa* biofilm reduction on polyurethane substrates. *Biointerphases* **2016**, 11, 031012) and has been adapted with permission. Copyright 2016, American Vacuum Society. The work was completed by Bella H. Neufeld and Prof. Melissa M. Reynolds acted as the advisor on this project.

3.2 INTRODUCTION

Healthcare-associated infections (HAIs) are considered the sixth leading cause of death in Western industrialized countries and affect ~5 out of every 100 patient hospital visits in the United States.[1-3] Some of the most common and costly clinical infections are related to indwelling medical devices, such as intravascular catheters made from polyurethane materials.[4,5] Biofilms, defined as microbial communities residing on a surface, are responsible for ~80% of all clinical infections.[2,6] These biofilms have intrinsic properties that make them extremely difficult to kill once formed. More specifically, the extracellular matrix secreted by biofilms provides a protective layer that traditional antibiotics cannot penetrate.[6,7] One particularly ubiquitous bacteria strain that forms robust biofilms is the Gram-negative *Pseudomonas aeruginosa* (*P. aeruginosa*). This opportunistic pathogen is often utilized for initial biofilm studies due to its inherent ability to become resistant to multiple antibiotics, prevalence in hospital settings, and association with critical illnesses (such as cystic fibrosis) along with catheter-related infections.[8-10] The need for non-traditional antibiotics and alternative approaches to kill Gram-negative biofilms composed of bacteria such as *P. aeruginosa* is urgent and remains elusive in this field.[3,11]

There are a number of synthetic strategies currently employed to combat biofilms, including drug releasing nanoparticles, synthetic proteins, peptides, enzymes, antibacterial essential oils, elemental metals and nonmetals (such as silver and iodine), cationic compounds (such as quaternary ammonium complexes), and polymers (such as chitosan).[3,12-18] The extensive focus on novel antibacterial approaches shows the importance and urgency of this growing problem associated with infection. Identification of a treatment strategy for biofilm destruction that is cost effective, reproducible, and non-toxic to mammalian cells remains a challenge.[3] In

addition, one of the most critical aspects of designing novel antibacterial materials is to ensure that resistance towards the agent will not be developed.[19] This ultimately means identifying an approach that leads to multiple bactericidal pathways to limit the likelihood of antibacterial resistance. Nitric oxide (NO) presents a promising opportunity to fulfill these requirements as a broad-spectrum antimicrobial agent.[20,21]

NO has been identified as a viable candidate to disrupt, disperse, and even inhibit *P. aeruginosa* biofilms due to its broad-range antimicrobial action and dual mechanistic activity against bacteria.[2,21,22] NO has been shown to have an effect on a wide variety of bacteria strains (from Gram positive to Gram negative and from food-borne strains to clinically relevant strains); however, most of the work reported has been on planktonic bacteria with minimal focus on biofilm destruction.[23-26] Treating planktonic bacteria is important, as planktonic bacteria can be responsible for infections in the bloodstream and elsewhere.[27] It is understood by the community, however, that the vast majority of bacteria exist in the biofilm state to allow bacteria to better exchange nutrients and provide overall protection due to the encapsulating extracellular matrix.[28,29] In addition, bacteria in biofilms are thought to be highly resistant to biocidal and antibiotic agents than bacteria in the planktonic form, thus identifying a critical concentration of NO that elicits a desired response on a robust *P. aeruginosa* biofilm is essential to combat these prevalent clinical infections.[2,31,32] Indeed, it is understood that the biological response of NO is concentration dependent; however only broad concentration ranges are understood at this time, as the desired effect is dependent on the NO donor, material platform, and intended application.[32]

There has been considerable work performed in the field of NO-releasing materials and their capabilities to elicit numerous biological responses, including but not limited to their antimicrobial properties. Some of these studies use NO-releasing platforms to determine the

ideal flux of NO to ultimately inhibit biofilm formation while others focus on the amount of NO needed to cause the dispersal of a pre-formed biofilm. For example, the Schoenfisch group demonstrated a 50-65% reduction in the bacterial attachment of *P. aeruginosa* for NO fluxes ranging from 0.06-1.30 nmol NO $cm^{-2}min^{-1}$, while Barraud et al. determined that NO donor concentrations ranging from 25 to 500 nM cause dispersal of *P. aeruginosa* biofilms.[33-35] These NO and NO donor amounts for inhibition and dispersal are useful as they can help dictate the ideal ranges for new drug-delivery systems. In addition, these inhibition and dispersal assays exploit discrete phases in the biofilm life cycle and, therefore, require different concentrations of NO to elicit the response. Likewise, the study employed here targets a pre-formed biofilm in the mature stages of the biofilm life cycle but attempts to identify the critical NO concentration for reduction of viable biofilm bacteria, rather than dispersal or inhibition of such bacteria.

While work has been done on NO for inhibition and dispersal, identification of the optimal concentration for reduction of viable bacteria in a pre-formed biofilm has yet to be determined. The approach taken in this work deviates from the current literature whereby inhibition and dispersal are studied, and instead considers significant reduction of a biofilm (>90%) on a medically relevant polymeric surface. The identification of this critical NO concentration is useful in this field, as it can be applied to new NO material platforms to elicit a similar biofilm response. This work uses a system whereby the bacteria strain *P. aeruginosa* is grown on polyurethane films for 24 h in order to form a robust biofilm followed by the addition of the small molecule NO donor, *S*-nitrosoglutathione, in aqueous solution for an additional 24 h in order to determine the critical amount of NO (Figure 3.1). Herein we report the identification of the critical concentration of NO needed to elicit >90% reduction of a *P. aeruginosa* biofilm grown on polyurethane films.

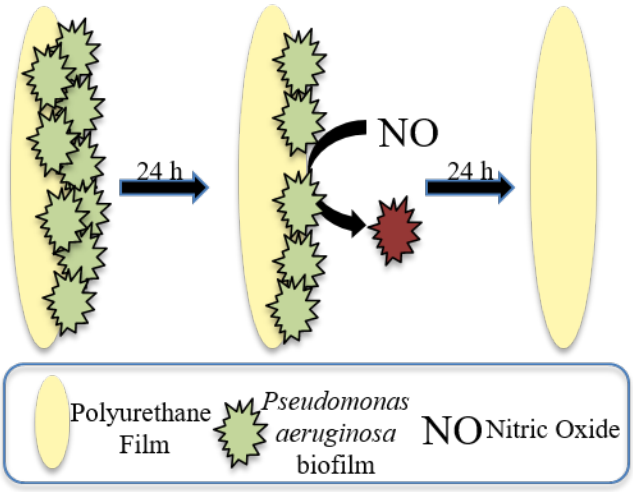

Figure 3.1 Schematic presented in this study to identify critical amount of NO needed to cause >90% reduction in viable bacteria of a pre-formed biofilm of *P. aeruginosa* on polyurethane films. (Reprinted with permission. Copyright 2016, American Vacuum Society)

3.3 MATERIALS AND METHODS

3.3.1 Materials

Reduced glutathione was purchased from Amresco (Solon, OH, USA). Sodium nitrite (99.999% pure) was purchased from Alfa Aesar (Ward Hill, MA, USA). Concentrated hydrochloric acid (HCl) was purchased from EMD (Darmstadt, Germany). Dichloromethane (DCM), acetone, and glycerol were purchased from Sigma Aldrich (St. Louis, USA). SG-80A medical grade polyurethane was obtained from Lubrizol (Wickliffe, OH, USA). *Pseudomonas aeruginosa* (PAO1, wild type) was provided by Dr. Brad Borlee at Colorado State University. Oxoid™ nutrient broth media (NBM, OXCM0001B), Oxoid™ nutrient agar (NA, OXCM0003B), sodium chloride, propidium iodide (PI), formaldehyde, phosphate buffered saline (PBS), and EPA vials were purchased from Fisher Scientific (Fair Lawn, NJ, USA). CellTiter Blue (CTB) was purchased from Promega (Madison, WI, USA). 24-well and 96-well tissue culture treated plates were obtained from Corning (Corning, NY, USA).

3.3.2 Experimental Methods

Polyurethane film preparation. Medical-grade, SG-80A polyurethane polymer (PU) was added to DCM (5% w/v) and allowed to stir overnight to solubilize. 100 μL aliquots of the polymer solution were cast onto a glass disk substrate (12 mm diameter) three times (allowing for each layer to dry in between each addition) for a total of three layers of polymer. Films were subsequently covered and allowed to cure overnight. The films were removed from the glass substrates before being placed in 24 well plates for further experiments.

S-nitrosoglutathione synthesis. *S*-nitrosoglutathione (GSNO) was synthesized following a previous method.[36] Briefly, an ice cold solution of 5 mmol reduced glutathione with 8 mL ultrapure water (Millipore, 18 MΩ) and 2.5 mL 2 M HCl was prepared in an EPA vial. Sodium nitrite (5 mmol) was added to this solution and allowed to stir for 40 min before the addition of 10 mL cold acetone. The product was filtered and washed with cold water and acetone before drying under vacuum for 4 h. Characterization of each batch of GSNO was performed using UV-Visible spectroscopy (Nicolet Evolution 300 spectrometer, Thermo Electron Corporation, Madison, WI, USA) by monitoring the absorbance feature at 336 nm (ε = 922 $M^{-1}cm^{-1}$) to ensure high purity.[37] GSNO was stored in an amber, copper-free, EPA vial to prevent light and copper initiated decomposition and at -20 °C until use to prevent further thermal decomposition of the donor.

3.3.3 Bacteria studies

Pseudomonas aeruginosa bacteria culture. Initial stock cultures of *Pseudomonas aeruginosa (P. aeruginosa)* were obtained by streaking agar plates and inoculating the bacterium in nutrient broth. This stock culture was grown overnight in NBM to an $O.D._{600nm}$ ~1.0. This bacterial solution was combined with glycerol (30% v/v) in a 1:1 fashion to obtain a final glycerol

concentration of 15% (v/v). These solutions were stored at -80 °C until use. Prior to each bacterial assay, a 10 mL frozen culture was allowed to thaw at room temperature and then centrifuged at 4700 rpm for 10 min. The supernatant was discarded and the pellet was resuspended in 5 mL NBM. This bacterial solution was transferred to an additional 45 mL NBM and allowed to grow overnight in a 37 °C incubator under stirring conditions until the $O.D_{600nm}$. ~1.0. The following day, the overnight culture was diluted to an $O.D._{600nm}$ ~0.35 using warmed NBM before the addition of the bacterial solution to tissue-cultured treated 24-well plates.

Biofilm growth. The PU films were removed from the glass substrates and placed into a well of a 24-well plate before the addition of 1 mL of bacterial solution. The bacteria were allowed to grow on the PU films for 24 h in a 37 °C incubator, at which point the media was removed and replaced by either fresh media (representing the positive control) or a solution of GSNO prepared in fresh media. The bacteria were allowed to grow for an additional 24 h in a 37 °C incubator before bacterial assays were performed.

Biofilm viability assays. In order to assess the bacterial viability of the biofilms, a CTB assay was performed.[38] Briefly, the NBM was removed from each well and washed once with PBS. To ensure that the biofilm assessed was only from the PU film only and not the surrounding well, the films were moved to a new well and 400 μL of CTB solution was added. The CTB solution was made by combining 20 μL CTB reagent with 100 μL NBM. The well plate was covered from light and incubated at 37 °C for 4 h before 100 μL aliquots were transferred to a 96-well plate and the absorbance of each well was measured at 570 and 600 nm (Synergy 2 Multi-Mode Reader, BioTek, Winooski, VT, USA). Reduction in bacteria viability was assessed by normalizing the sample wells to the positive control wells (containing NBM without GSNO present). All samples were tested in replicate ($n \geq 9$).

The number of colony forming-units (CFUs) was assessed by an agar plating technique that has been previously published in addition to the above-mentioned CTB method.[39] Prior to each experiment, the media was removed and the films were washed twice with fresh NBM. To ensure the biofilm assessed was from the PU film only and not the surrounding well, each film was transferred to a new well and fresh recovery NBM was added. The plate was covered from light and sonicated for 30 min in order to break up the biofilm into the planktonic form (power and frequency of ultrasonication bath were 100 W and 42 kHz, respectively). 100 µL aliquots were taken from each well post-sonication and 10-fold serial dilutions were performed in a sodium chloride solution (0.85% w/v). 50 µL aliquots of the dilute bacterial solutions were plated on agar and placed in a 37 °C incubator overnight. The agar plates were counted the following day and assessed for CFUs and ultimately converted to CFU/mL by equation 3.1.[40] All samples were tested in replicate (n≥9).

$$\frac{\boldsymbol{CFU}}{\boldsymbol{mL}} = \frac{\boldsymbol{Number\ of\ CFUs}}{(\boldsymbol{Vol\ Plated})*(\boldsymbol{Dilution\ Factor})} \qquad (3.1)$$

Fluorescence microscopy was utilized to observe the non-viable bacterial cells on the surface of the PU films using PI. Prior to film staining, the media was removed from the wells and washed three times with PBS. 500 µL formaldehyde (3.7% v/v in PBS) were added to fix the bacterial cells and allowed to incubate for 15 min. The formaldehyde was subsequently removed and washed three times with PBS. 300 µL of the PI solution were added to each well and the plate was placed incubated at 37 °C for 20 min. The PI solution was made by combining 3 µL PI per 1 mL PBS. The stain was removed after the incubation period and the samples were washed three times with PBS. The films were imaged using an Olympus IX73 fluorescence microscope

and analyzed by Olympus CellSens software. The excitation and emission wavelengths for PI are 533 nm and 617 nm, respectively. Images were collected in triplicate (n=3).

3.3.4 Nitric oxide release

The concentration of GSNO was assessed for NO release content over a 24 h period using a Nitric Oxide Analyzer (NOA, Sievers 280i, GE Analytical Instruments, Boulder, CO, USA). The NOA sample holder was under nitrogen, contained 4 mL NBM, maintained at 37 °C, and covered from light in order to mimic both experimental and physiological conditions. The collection interval was 1 min and sufficient baseline of the NBM was obtained before injection of GSNO. Prior to each experiment, the NOA was calibrated using UHP Nitrogen as zero gas and 45 PPM NO/Nitrogen, according to manufacturer standard operating procedures. Each experiment was allowed to run for 24 h before analyzing total moles released over that time period. This analysis was done using a previously obtained calibration constant for each individual NOA. All NO data points were collected in triplicate (n=3).

3.3.5 Statistical analysis

All studies were performed with at least three replicates with at least three samples for every replicate. The NOA studies, CTB assay, and agar plating method results are reported as the average and the standard error of the mean for all replicates. All data were analyzed for outliers using the Grubbs Outliers Test. The biofilm viability assays, time kill experiments, and contribution from non-nitrosated glutathione were measured for statistical significance using the student's t-test or a one-way ANOVA analysis followed by a Tukey Honestly Significant Difference *post-hoc* test ($p < 0.05$).

3.4 RESULTS AND DISCUSSION

In this study, *P. aeruginosa* biofilms were grown onto PU films to assess the efficacy of NO in biofilm reduction (Figure 3.1). In an attempt to identify the critical concentration of NO that would elicit >90% reduction in viable biofilm bacteria, various concentrations (5-25 mM) of the biologically relevant small molecule NO donor was added in solution to the pre-formed biofilm for a 24 h challenge period. After establishing the critical amount of NO needed to cause >90% reduction in *P. aeruginosa* biofilms, the relevant concentration was tested for total NO content by NOAs to identify the total NO amount over the 24 h challenge period. Finally, time-dependent studies were performed over the 24 h challenge period to determine when the biofilm viability reduction occurred.

3.4.1 Biofilm reduction with various NO concentrations

The system utilized in the study of biofilm reduction was comprised of a PU substrate for biofilm growth and *S*-nitrosothiol NO donor for biofilm reduction. *S*-nitrosothiols are one of the most common classes of NO donor and were chosen for this study as they are endogenous NO species, release NO under physiological conditions, and do not contain some of the harmful byproducts sometimes associated with other donors.[41-43] GSNO, specifically, was chosen due to its relative stability compared with other small molecule donors and physiological relevance.[43] Each batch of GSNO that was synthesized was characterized for purity by UV-Vis spectroscopy by a previously determined method.[37] The reaction of GSNO to yield NO is shown in reaction 3.1, where GSSG represents oxidized glutathione (disulfide).

$$2GSNO \rightarrow 2NO + GSSG \qquad (3.1)$$

NO has been shown to have antibacterial properties towards a broad-spectrum of bacteria strains.[44] The antibacterial action of NO is thought to originate from both NO itself, as the small

diatomic molecule has the ability to cross the cell membrane and cause irreversible DNA damage, as well as reactions between NO and reactive nitrogen and oxygen species present to produce other potent antibacterial molecules, namely peroxynitrite and dinitrogen trioxide.[22] This has been shown throughout the literature for predominantly planktonic species, but more recently, work has been done to show similar affects towards biofilm bacteria, though the exact concentrations are still unknown.[45-47]

Concentrations of NO in the millimolar range have been shown to have cytotoxic antibacterial effects such as cell apoptosis or programmed death.[32,48] This led to initial NO concentrations ranging from ~1-10 mM (corresponding to GSNO concentrations ranges of 5-25 mM) for biofilm viability assays. These ranges may cause damage to both bacterial cells and mammalian cells, therefore the desired NO concentration needs to be delivered in a localized fashion rather than a systemic approach to fully utilize towards pre-existing biofilms. The bacteria were allowed to grow on the PU films for 24 h in NBM and in a 37 °C incubator before the addition of NO, which was critical to ensure a healthy and robust biofilm present on the films. Additionally, the bacteria were exposed to the challenge material (in this case, NO) for an additional 24 h in an attempt to mimic the overall 48 h biofilm (for positive control) that may be relevant for catheter-related infections.[49] The NO donor was introduced to the biofilm in NBM and maintained at 37 °C to ensure that the bacteria had available nutrients to allow further bacterial growth and that the reduction in biofilm viability was not due to improper experimental conditions. This method differs from other biofilm studies where the challenge material is introduced in PBS, possibly compromising the optimal growing conditions of viable bacteria.[18,24,50] After 24 h exposure to solution phase NO introduced via variable GSNO concentrations, biofilm reduction was determined by three assays: (1) agar plating method, (2)

cellular viability by CTB assay, and (3) fluorescence imaging of the PU films using PI. All three assays were used to assess the critical concentration of NO needed to elicit >90% reduction in viable biofilm, as each assay provides different information.

Utilizing the CTB assay gives insight into the biofilm bacteria metabolic capacity that remains after 24 h exposure to NO. This assay relies on the metabolic activity of healthy cells to reduce the compound resazurin to the compound resorufin, both of which can be measured for their absorbance properties in order to identify percent conversion of these compounds as compared to a positive control (PU films without the addition of challenge material). GSNO concentrations ranging from 5-25 mM (~1-10 mM NO) were assessed for biofilm reduction using this assay, and the critical amount of GSNO was determined to be 10 mM (Figure 3.2). This GSNO concentration resulted in only 9 ± 2% viable bacteria remaining in the biofilm after exposure to NO for 24 h. No increased reduction was found using higher GSNO concentrations (>10 mM) and decreasing the GSNO concentration (<10 mM) led to a higher amount of viable bacteria (7 mM GSNO resulted in a reduction of only ~48%). It should be noted that for all CTB experiments, the positive control wells were highly fluorescent due to the resorufin compound, indicating the presence of high metabolic activity and viable bacteria in the absence of NO. As a further control, the non-nitrosated reduced glutathione was also tested at the same concentration. This concentration of reduced glutathione was found to have no statistically significant difference to the cellular viability of the positive control.

In order to quantitatively assess the viable bacteria in the absence and presence of NO as a complimentary technique to the CTB assay results, an agar plating method was employed. This technique involves breaking apart the biofilm and resuspending the viable bacteria back to the planktonic form in the recovery media via 30 min sonication period.[39] This allows for

comparison of the positive control PU films versus films exposed to NO for the challenge period. The assumption is that the same relative amount of biofilm will be removed from both the control and sample films during the sonication period, such that a reduction in biofilm between the control and sample can be assessed. The method of re-suspending biofilm bacteria has been established to show that the sonication itself does not disturb the viable bacteria (ultimately leading to artificially increased bacteria reduction).[39] This can also be seen by the positive controls presented in this study, where the PU films in media have a bacteria concentration ~10^6 CFU/mL. This technique was also performed using varying concentrations of GSNO (ranging from 5-25 mM) in order to determine the critical threshold that resulted in the largest bacteria reduction. Similar to the CTB assay, this critical GSNO concentration was found to be 10 mM (Figure 3.2), with only 2.0 ± 0.3% viable bacteria present after 24 h exposure to NO when compared to the positive control. Increased reduction was not seen when increasing the GSNO concentration and decreasing the concentration of GSNO did indeed show increased viability of biofilm (7 mM GSNO resulted in a reduction of only 33%). The results between the CTB and agar plating methods were not statistically different at the 95% confidence interval, indicating that these methods and overall results are in agreement with one another providing further insight into the true critical concentration of NO.

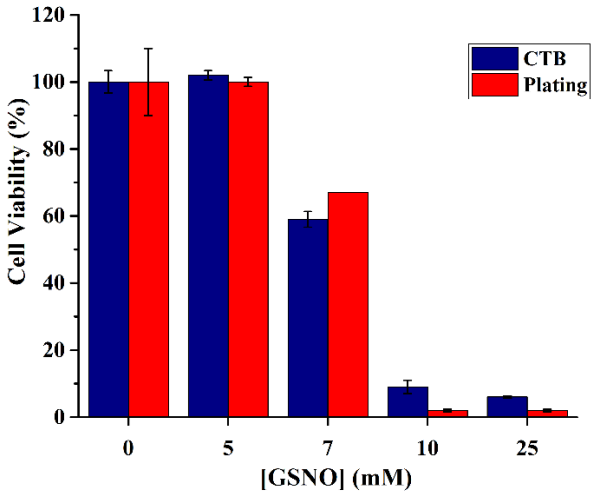

Figure 3.2 Bacteria cellular viability of 24 h biofilm versus concentrations of GSNO in NBM for 24 h (0 mM GSNO represents positive control). Blue bars represent the CellTiter Blue (CTB) assay and red bars represent the agar plating method. All data are n≥9, with average and standard error of the mean shown. (Reprinted with permission. Copyright 2016, American Vacuum Society)

Final determination of the response of biofilms exposed to NO was conducted using fluorescence microscopy. In this analysis, PI was utilized to image the amount of viable bacteria on the films themselves. PI binds to cellular DNA and is a good indicator of non-viable bacteria cells, as it does not have the ability to permeate live cells. Therefore, those that appear red are considered dead. For this assay, only 10 mM GSNO was run against the positive control after determining the critical GSNO concentration from CTB and agar plating method. Figure 3.3 shows the results of PI staining of (a) PU film positive controls, and (b) PU films exposed to 10 mM GSNO in NBM. It can be seen in this figure that the positive control films show few red (dead) cells while the films exposed to GSNO have very large areas covered in red (dead) cells. The large red areas on the PU films exposed to NO indicate that, although the biofilm remains on the PU films after 24 h exposure, almost the entirety of such biofilm is comprised of dead cells. Although this method does not indicate viable cells, the previous CTB and agar plating results

demonstrated that viable cells are indeed present on the surface of the positive control films (~10^6 CFU/mL). These images, therefore, give further evidence of the reduction in biofilm viability by NO. A live staining method could not be used, as the polyurethane substrate itself absorbs green stains.

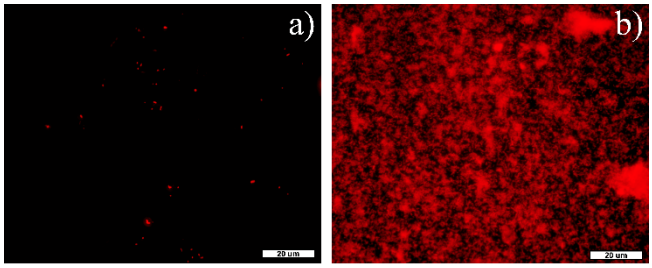

Figure 3.3 Representative fluorescence microscopy images of PU films using PI to stain dead bacteria cells in a 48 h biofilm. (a) Positive control for 48 h biofilm where the media was replaced after 24 h, and (b) PU films after exposure to 10 mM GSNO in NBM for 24 h (n≥3). A DEAD stain only was used, as common LIVE stains are absorbed into the polyurethane material. (Reprinted with permission. Copyright 2016, American Vacuum Society)

3.4.2 Biofilm reduction at varying time points.

Following the determination of critical NO concentration for reduction in viable biofilm, time-dependent experiments were performed to assess when the 90% reduction of the biofilm occurred. The CTB assay was utilized for this study and the cellular viability of the 24 h biofilm was evaluated after 4, 8, 12, and 16 h time points. The results of this study can be seen in Figure 3.4 and Table 3.1, where the 90% reduction occurs at the 12 h mark. There is no statistical difference between the cellular viabilities found at 12, 16, and 24 h. Although the biofilm viability reduction occurred at the 12 h time point, it is essential to continue the study out to 24 h at a minimum to determine if there is regrowth of the bacteria given optimal growing conditions (in NBM at 37 °C). Indeed, as shown in the previous sections, the viability of the biofilm does

not increase and remains at ~10% relative to the positive control for the entire 24 h challenge period.

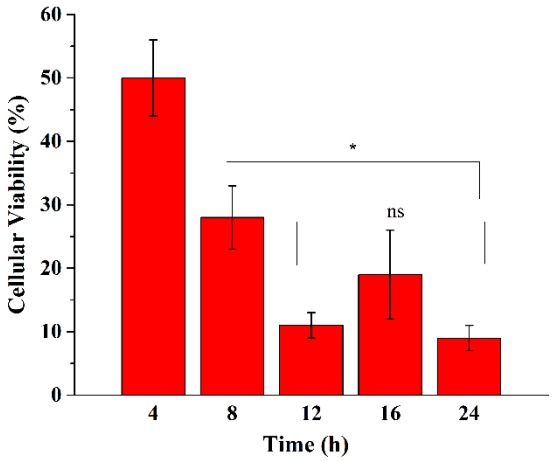

Figure 3.4 Bacteria cellular viability of 24 h biofilm determined by the CTB assay at varying time points of exposure to 10 mM GSNO in NBM at 37 °C. Data are presented as average and standard error of the mean (n≥9). Statistically significant differences in cellular viability are indicated (*) and no statistically significant differences in cellular viabilities are indicated (ns). (Reprinted with permission. Copyright 2016, American Vacuum Society)

Table 3.1 Reduction in viable biofilm bacteria given by CTB assay after varying exposure times to 10 mM GSNO in NBM at 37 °C. Data are presented as average and standard error of the mean (n≥9). The viability reduction between 12, 16, and 24 h are statistically similar.

Time (h)	Biofilm Bacteria Reduction (%)
4	50 ± 6
8	72 ± 5
12	89 ± 2
16	81 ± 7
24	91 ± 2

3.4.3 Determination of NO Concentration

It is critical to report not only the NO donor concentration needed to cause a significant reduction in a pre-existing *P. aeruginosa* biofilm, but also to identify the amount of NO itself

delivered over the biofilm challenge period. The use of NOAs for NO detection will allow for complete determination of the total amount of NO over the challenge period, which can then be converted to concentration for aqueous donor systems or to flux for NO-releasing materials. NO detection via NOAs allows for both extremely sensitive as well as selective detection based on the instrumental setup and the chemiluminescent reaction between NO and ozone, whereby excited state NO_2 is formed and releases a photon upon relaxation from the excited state.[51] For these NOA experiments the NO release measurement was made in NBM, which is essential as our group previously demonstrated that scavenging agents can exist within media that may significantly diminish the total NO released as compared to using PBS or water for total NO content.[52]

Once the critical NO concentration was determined via the biofilm reduction assays mentioned above, the 10 mM GSNO solution was ultimately tested for total NO release over the 24 h challenge period. The NBM added to the NOA cells was sufficiently purged with nitrogen to remove any oxygen before data collection began and continuous nitrogen flow was maintained throughout collection period at 200 mL min^{-1}, allowing the released NO to be swept from the NOA sample holder into the reaction chamber. Figure 3.5a shows a representative real-time NO release profile (in μM), where there is an initial small burst of NO followed by a steady-state release for the remainder of the collection period, and Figure 3.5b shows a representative cumulative NO release over the collection period (in mM). This type of profile has been shown previously for small molecule *S*-nitrosothiols, where the NO decomposition pathway is triggered by heat and pH conditions (37 °C and pH 7.4).[53,54] The near immediate steady-state release of GSNO upon injection into the NOA port is an additional reason why GSNO was chosen as the small molecule NO donor, as this NO donor is stable compared to many small molecule *S*-

nitrosothiols and the release remains relatively constant for the entire 24 h biofilm challenge period.[40] The total moles of NO released over 24 h was found to be 1.09 ± 0.12 x 10^{-5} mol NO, which corresponds to 2.73 ± 0.31 μmol NO/mL NBM. The total NO released over the 24 h period corresponds to 27 ± 3% of the total theoretical NO reservoir based on the starting concentration as determined by UV-Vis spectroscopy.

After determination of the biofilm exposure time to NO corresponding to a 90% reduction, the total moles over the 12 h period was also assessed in NBM. The total moles of NO released over 12 h was found to be 5.97 ± 0.66 x 10^{-6} mol NO, which corresponds to 1.49 ± 0.17 μmol NO/mL NBM, representing roughly 55% of the total amount released over the 24 h challenge period. Interestingly, this critical NO concentration falls within the upper range of the NO flux found by the Schoenfisch group necessary to cause a reduction in bacterial attachment of *P. aeruginosa* on a surface.[33,34] As a point of comparison, the Schoenfisch group has determined the minimum bactericidal concentrations for varying NO systems that achieve a 3-log reduction on planktonic *P. aeruginosa*, ranging from 0.10 - 0.45 μmol/mL.[18] This concentration range is significantly lower than the found NO concentration in this work (~3 μmol/mL), where the reduction is not nearly as substantial as 3-log, illustrating the enhanced antimicrobial susceptibility of *P. aeruginosa* in the planktonic form.

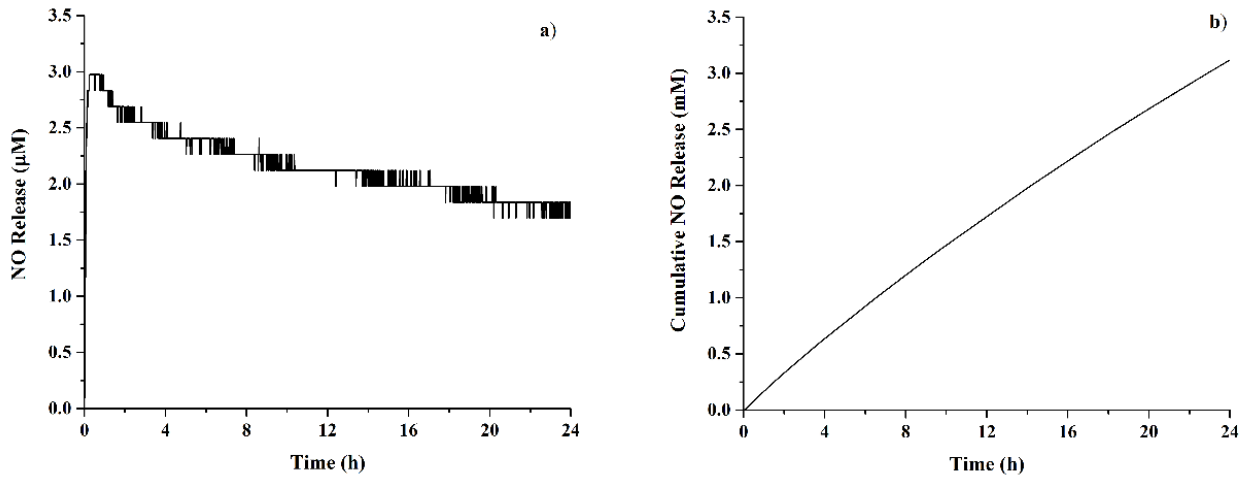

Figure 3.5 NO release of critical NO concentration. (a) Representative NO release profile collected via NOA of 10 mM GSNO in bacteria media at 37 °C and covered from light. (b) Representative cumulative NO release of 10 mM GSNO under same conditions. Data were collected over 24 h with a 1 min collection interval (n=3). (Reprinted with permission. Copyright 2016, American Vacuum Society)

One of the current challenges in the NO field is the abundance and variability of NO reporting parameters, including units (total flux versus steady-state flux, total concentration versus maximum burst concentration, half-life associated with NO release, percent NO recovery), time periods measured, normalizing to surface area of material, donor versus NO concentration, and NO detection methods. This wide range of parameters makes it difficult to compare or utilize the concentration from one study to another, in which a similar biological response is desired. The ultimate goal for this study was to identify the critical concentration of NO such that this amount can be applied for varying applications where *P. aeruginosa* is prevalent on a PU surface. The identification of this critical NO concentration can ultimately be engineered into new material platforms to elicit a similar biological response. Overall, this method of NO determination and critical concentration reporting can be applied to many systems, where a single or multi-species biofilm is grown on a medically-relevant polymer substrate.

3.5 CONCLUSIONS

A system composed on *P. aeruginosa* biofilms grown on PU substrates was utilized to determine the critical amount of NO needed to cause >90% reduction of viable biofilm bacteria. These types of biofilms are prevalent in hospital settings and are of particular concern with regard to indwelling medical devices, such as catheters. Identifying the key concentration of NO that can elicit the desired response in such a biofilm is necessary for translation across biofilm studies. A range of NO concentrations were assessed and the critical concentration found in this work was 10 mM GSNO or 1.49 ± 0.17 μmol NO/mL NBM. The concentration found can be employed in future studies where *P. aeruginosa* is grown on PU substrates. Ultimately, this method can be applied further to determine critical NO amounts associated with biofilm inhibition and dispersal based on a similar model system.

CHAPTER 3 – REFERENCES

1. Scott, R.D. The Direct Medical Costs of Healthcare-Associated Infections in U.S. Hospitals and the Benefits of Prevention. Centers for Disease Control and Prevention (2009).
2. Barraud, N.; Storey, M.V.; Moore, Z.P.; Webb, J.S.; Rice, S.A.; Kjelleberg, S. *Microbial. Biotech.* **2009**, 2(*3*), 370-378.
3. Cloutier, M.; Mantovani, D.; Rosei, F. *Trends Biotechnol.* **2015**, 33, 637-652.
4. Fu, W.; Forster, T.; Mayer, O.; Curtin, J.J.; Lehman, S.M.; Donlan, R.D. *Antimicrob. Agents Chemother.* **2010**, 54, 397-404.
5. Colleta, A.; Wu, J.; Wo, Y.; Kappler, M.; Chen, H.; Xi, C.; Meyerhoff, M.E. *ACS Biomater. Sci. Eng.* **2015**, 1, 416-424.
6. Hall-Stoodley, L.; Costerton, J.W.; Stoodley, P. *Nature Rev. Microbiol.* **2004**, 2, 95-108.
7. Hernandez-Jimenez, E.; del Campo, R.; Toledano, V.; Vallejo-Cremades, M.T.; Munoz, A.; Largo, C.; Arnalich, F.; Garcia-Rio, F.; Cubillos-Zapata, C.; Lopez-Collazo, E. *Biochem. Biophys. Res. Comm.* **2013**, 441(*4*), 947-952.
8. Irie, Y.; Borlee, B.R.; O'Connor, J.R.; Hill, P.J.; Harwood, C.S.; Wozniak, D.J.; Parsek, M.R. *PNAS* **2012**, 109(*50*), 20632-20636.
9. Falagas, M.E.; Kopterides, P. *J. Hosp. Infect.* **2006**, 64, 7-15.
10. Wright, G.D. *Nat. Rev. Microb.* **2007**, 5, 175-186.
11. Bazaka, O.; Bazaka, K. *Antibacterial Surfaces: Cytotoxic Effects and Biocompatibility of Antimicrobial Surfaces*. (Springer Int, Switzerland, 2005).

12. Duong, H.T.T.; Adnan, N.N.M.; Barraud, N.; Basuki, J.S.; Kutty, S.K.; Jung, K.; Kumar, N.; Davis, T.P.; Boyer, C. *J. Mater. Chem. B.* **2014**, 2, 5003-5011.

13. Vreuls, C.; Zocchi, G.; Thierry, B.; Garitte, G.; Griesser, S.S.; Archambeau, C.; Van de Weerdt, C.; Martial, J.; Griesser, H. *J. Mater. Chem.* **2010**, 20, 8092-8098.

14. Bazaka, K.; Jacob, M.V.; Truong, V.K.; Wang, F.; Pushpamali, W.A.A.; Wang, J.Y.; Ellis, A.V.; Berndt, C.C.; Crawford, R.J.; Ivanova, E.P. *Biomacromolecules* **2010**, 11(*8*), 2016-2026.

15. Chaloupka, K.; Malam, Y.; Seifalian, A.M. *Trends Biotechnol.* **2010**, 28, 580-588.

16. Shirai, T.; Shimizu, T.; Ohtani, K.; Zen, Y.; Takaya, M.; Tsuchiya, H. *Acta Biomater.* **2011**, 7, 1928-1933.

17. Camona-Ribeiro, A.M.; Dias de Melo Carrasco, L. *Int. J. Mol. Sci.* **2013**, 14, 9906-9946.

18. Lu, Y.; Slomberg, D.L.; Schoenfisch, M.H. *Biomaterials* **2014**, 35, 1716-1724.

19. Chatterjee, M.; Anju, C.P.; Biswas, L.; Kumar, V.A.; Mohan, C.G. *Int. J. Med. Microb.* **2016**, 306, 48-58.

20. Privett, B.J.; Broadnax, A.D.; Bauman, S.J.; Riccio, D.A.; Schoenfisch, M.H. *Nitric Oxide* **2012**, 26, 169-173.

21. Barraud, N.; Kelso, M.J.; Rice, S.A.; Kjelleberg, S. *Curr. Pharm. Des.* **2015**, 21, 31-42.

22. Fang, F.C. *J. Clin. Invest.* **1997**, 99, 2818-2825.

23. Jones, M.L.; Ganopolsky, J.G.; Labbe, A.; Prakash, S. *Appl. Microbiol. Biotechnol.* **2010**, 87(*2*), 509-516.

24. Hetrick, E.M.; Shin, J.H.; Stasko, N.A.; Johnson, C.B.; Wespe, D.A.; Holmuhamedov, E.; Schoenfisch, M.H. *ACS Nano* **2008**, 2, 235-246.

25. Sun, B.; Slomberg, D.L.; Chudasama, S.L.; Lu, Y.; Schoenfisch, M.H. *Biomacromolecules* **2012**, 13, 3343-3354.

26. Bogdan, C. *Nat. Immun.* **2001**, 2, 907-916.

27. Von Eiff, C.; Jansen, B.; Kohnen, W.; Becker, K. *Drugs* **2005**, 65, 179-214.

28. Hall-Stoodley, L.; Costerton, J.W.; Stoodley, P. *Nature Rev. Microbiol.* **2004**, 2, 95-108.

29. Stoodley, P.; Sauer, K.; Davies, D.G.; Costerton, J.W. *Annu. Rev. Microbiol.* **2002**, 56, 187-209.

30. Buckingham-Meyer, K.; Goeres, D.M.; Hamilton, M.A. *J. Microbiol. Methods* **2007**, 70(*2*), 236-244.

31. Spoering, A.L.; Lewis, K. *J. Bacteriol.* **2001**, 183(*23*), 6746-6751.

32. Coneski, P.N.; Schoenfisch, M.H. *Chem. Soc. Rev.* **2012**, 41, 3753-3758.

33. Dobmeier, K.P.; Schoenfisch, M.H. *Biomacromolecules* **2004**, 5, 2493-2495.

34. Hetrick, E.M.; Schoenfisch, M.H. *Biomaterials* **2007**, 28, 1948-1956.

35. Barraud, N.; Hassett, D.J.; Hwang, S.; Rice, S.A.; Kjelleberg, S.; Webb, J.S. *J. Bacteriol.* **2006**, 182(*21*), 7344-7353.

36. Hart, T.W. *Tetrahedron Lett.* **1985**, 26, 2013-2016.

37. Damodaran, V.B.; Joslin, J.M.; Wold, K.A.; Lantvit, S.M.; Reynolds, M.M. *J. Mater. Chem.* **2012**, 22, 5990-6001.

38. Promega Corporation. "CellTiter-Blue Cell Viability Assay". Promega Corporation, Madison, WI (2013).

39. Ceri, H.; Olson, M.E.; Stremick, C.; Read, R.R.; Morck, D.; Buret, A. *J. Clin. Microbiol.* **1999**, 37, 1771-1776.

40. Hamilton, M.A. "The log reduction (LR) measure of disinfectant efficacy". MSU Center for Biofilm Engineering, 2010.

41. Butler, A.R.; Rhodes, P. *Anal. Biochem.* **1997**, 249, 1-9.

42. Wang, P.G.; Xian, M.; Tang, X.; Wu, X.; Wen, Z.; Cai, T.; Janczuk, A.J. *Chem. Rev.* **2002**, 102, 1091-1134.

43. Williams, D.L.H. *Acc. Chem. Res.* **1999**, 32, 869-876.

44. Carpenter, A.W.; Schoenfisch, M.H. *Chem. Soc. Rev.* **2012**, 41, 3742-3752.

45. Kim, J.O.; Noh, J.; Thapa, R.K.; Hasan, N.; Choi, M.; Kim, J.H.; Lee, J.; Ku, S.K.; Yoo, J. *Int. J. Biol. Macromol.* **2015**, 79, 217-225.

46. Lu, Y.; Shah, A.; Hunter, R.A.; Soto, R.J.; Schoenfisch, M.H. *Acta Biomater.* **2015**, 12, 62-69.

47. Pegalajar-Jurado, A.; Wold, K.A.; Joslin, J.M.; Neufeld, B.H.; Arabea, K.A.; Suazo, L.A.; McDaniel, S.L.; Bowen, R.A.; Reynolds, M.M. *J. Control. Release* **2015**, 217, 228-234.

48. Ridnour, L.A.; Thomas, D.D.; Mancardi, D.; Espey, M.G.; Miranda, K.M.; Paolocci, N.; Feelisch, M.; Fukuto, J.; Wink, D.A. *Biol. Chem.* **2004**, 385, 1-10.

49. Shah, H.; Bosch, W.; Thompson, K.M.; Hellinger, W.C. *Neurohospitalist* **2013**, 3(*3*), 144-151.

50. Worley, B.V.; Schilly, K.M.; Schoenfisch, M.H. *Mol. Pharmaceutics* **2015**, 12, 1573-1583.

51. Fontijn, A.; Sabadell, A.J.; Ronco, R.J. *Anal. Chem.* **1970**, 42(*6*), 575-579.

52. Harding, J.L.; Reynolds, M.M. *Anal. Chem.* **2014**, 86, 2025-2032.

53. Joslin, J.M.; Lantvit, S.M.; Reynolds, M.M. *ACS Appl. Mater. Interfaces* **2013**, 5, 9285-9294.

54. Joslin, J.M.; Reynolds, M.M. *ACS Appl. Mater. Interfaces* **2012**, 4, 1126-1133.

CHAPTER 4

ANTIBACTERIAL SURFACE OF METAL–ORGANIC FRAMEWORK-CHITOSAN COMPOSITE FILMS

4.1 BACKGROUND

The application of metal–organic frameworks (MOFs) embedded into polymer substrates has been used primarily in Prof. Melissa M. Reynolds research group to catalytically produce NO from endogenous RSNOs (a reaction possible through copper sites). The particular MOF described in this study has been widely used in the Reynolds group, as it has shown to be robust and stable in aqueous environments (a challenging property to identify with MOFs). The preliminary idea for the work presented in this chapter was to use the catalytic NO production from the MOF-polymer films to kill and inhibit present bacteria. As an initial control study, an experiment was performed with only the bacterial solution and the MOF-polymer films (no RSNO present). The results were rather remarkable (as will be shown in this chapter) in that we identified a surface that could inhibit *P. aeruginosa* without the need for NO. Interestingly, the addition of RSNOs to the system did not enhance the ability to impede bacterial attachment. This work was originally published in Advanced Functional Materials (Neufeld, B.H.; Neufeld, M.J.; Lutzke, A.; Schweickart, S.M.; Reynolds, M.M Metal-Organic Framework Material Inhibits Biofilm Formation of *Pseudomonas aeruginosa*. *Adv. Funct. Mater*. **2017**, 27, 1702255-1702264) and an inside cover image was accepted for this manuscript (see below). The work has been adapted with permission from Wiley-VCH Verlag GmbH & Co. KGaA. Film fabrication (including MOF synthesis) was performed by Alec Lutzke. Film characterization using pXRD and SEM was conducted by Megan J. Neufeld. Film characterization using ATR-IR was done by

Sarah M. Schweickart. Copper leaching studies and all bacterial assessment was performed by Bella H. Neufeld. Prof. Melissa M. Reynolds acted as the advisor on this project.

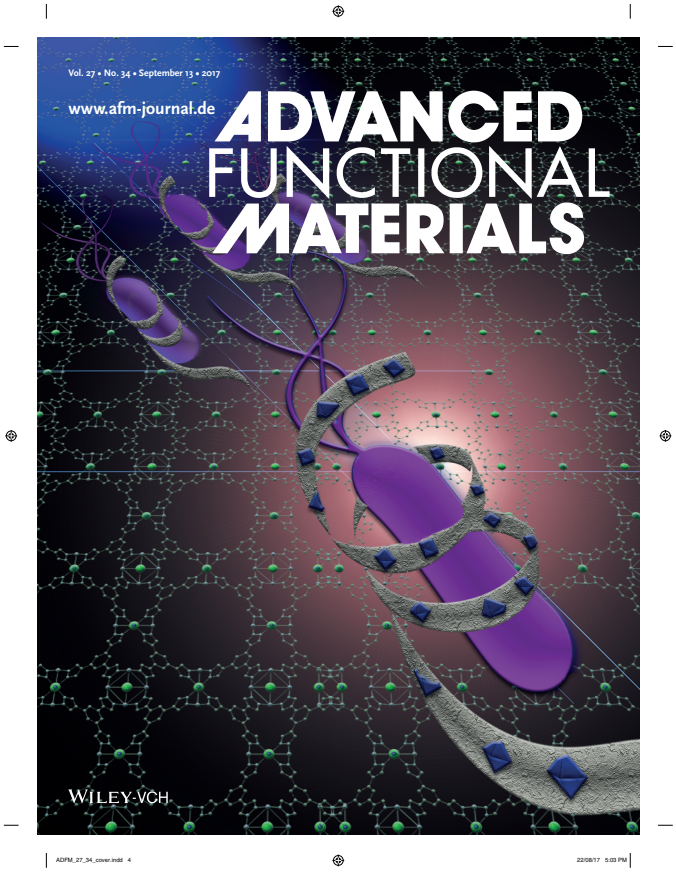

4.2 INTRODUCTION

The prevalence of antibiotic resistant bacteria poses a serious threat to human health, leading to increased and prolonged bacterial infections.[1,2] While bacteria in the free-floating, planktonic state remain susceptible to traditional antibiotics, the vast majority of bacteria exist in the biofilm state, where many antimicrobial agents are less effective.[3-5] The Gram-negative bacterium *Pseudomonas aeruginosa* (*P. aeruginosa*) is one particularly concerning bacterial strain due to its capacity to rapidly and efficiently form biofilms as well as its inherent ability to develop resistance to antibiotics.[6,7] The biofilm life cycle is considered to occur in three stages,

with the first two steps consisting of reversible and irreversible attachment of planktonic bacteria onto a surface.[3,8] Therefore, identifying a material with the inherent properties to ultimately repel or reduce the bacterial adhesion of harmful pathogens represents a promising direction for controlling biofilm formation.[9,10]

Chitosan is a polysaccharide derived from the biopolymer chitin and has been utilized in multiple biological studies due to its overall biocompatibility and biodegradability.[11] It is composed of β-(1,4)-linked glucosamine and *N*-acetyl glucosamine units and has been shown to have little to no toxic byproducts.[12,13] Although there has been emphasis on the antibacterial nature of chitosan in solution against planktonic bacteria, another common use of chitosan as a biomaterial is in the form of wound dressings where it functions as a hemostatic agent.[14] Thrombus formation arising from this type of hemostatic effect may increase the likelihood of biofilm formation, as the adhered proteins onto the chitosan wound dressing provide an ideal area for bacteria to attach.[15,16] Therefore, embedding the chitosan matrix with a compound that may improve the material's ability to resist bacterial attachment is one approach to this challenge.

Metal–organic frameworks (MOFs) are a unique class of hybrid materials combining metal centers with organic linkers to produce materials with high porosity. Variation of the metal and ligand has large effects on the overall properties and, therefore, applications of MOFs.[17,18] While these materials have been widely exploited in gas storage and catalysis, there are fewer studies utilizing MOFs in biological settings.[19-21] The known biocidal activity of copper has led to some investigation of copper-based MOFs in biological settings for use as potential antibacterial agents. For example, a small number of initial bacteria studies have been carried out using the copper-based MOF copper(II) benzene-1,3,5-tricarboxylate (also known as Cu-BTC or

HKUST-1) as an antibacterial agent. The observed biocidal effects have been attributed to metal sites and the slow, continuous leaching of copper ions, as this MOF undergoes substantial and immediate degradation in aqueous systems.[22-25] These particular studies did not evaluate bacterial attachment onto MOF-containing surfaces, but rather the biocidal activity of the MOF against planktonic bacteria in solution by copper ions released from the framework. Although copper leaching into bacterial solution has significant antibacterial effects, in the study presented herein, the aim was to develop a material that intrinsically prevents the attachment of bacteria without the need for a biocide-eluting surface.

Unlike Cu-BTC, one copper-based MOF that has been shown to exhibit high stability under aqueous conditions is Cu-BTTri ($H_3[(Cu_4Cl)_3{-}(BTTri)_8]$ (H_3BTTri = 1,3,5-tris(1H-1,2,3-triazol-5-yl)benzene)) and was originally reported by Demessence *et al*.[26] Due to the underlying water stability of Cu-BTTri and the presence of copper centers, this MOF is a particularly attractive potential candidate for biological applications.[26,27] Although the antibacterial activity of copper-based MOFs has been studied with regards to the leaching of copper ions by unstable MOFs, the identification of new antibacterial activity achieved using a water-stable, copper-based MOF would present an interesting and unique development that permits a more passive approach to a MOF-polymer antibacterial surface. The goal of this work was to determine if the observed antibacterial effect seen using the unstable Cu-BTC could be distinguished from the antibacterial activity using a stable system (Cu-BTTri), in which the effect cannot be attributed to copper in solution (see Figure 4.1). Ultimately, this identification of an antibacterial surface to inhibit bacterial attachment has far-reaching implications, as planktonic bacteria are far more susceptible to antimicrobials and, therefore, less of a concern than biofilm formation.

Herein we report the first antibacterial use of the water-stable MOF Cu-BTTri in a chitosan matrix (denoted as chitosan/Cu-BTTri throughout the text). This represents one of the first accounts of utilizing MOFs as antimicrobials, without the concern of degradation in aqueous environments. The chitosan and chitosan/Cu-BTTri films (at various MOF percent compositions) were assessed for their bacterial inhibition properties using cellular viability assays after 6 and 24 h exposure times to *P. aeruginosa*. The films were saved after initial bacteria studies and attachment experiments were performed again using the same films to demonstrate reusability of the material, suggesting the films maintain their function as an antibacterial surface. This is the first demonstration of chitosan/Cu-BTTri material films for use in biological studies and one of the first accounts of achieving ~85% reduction of *P. aeruginosa* onto a biomaterial within 24 h.

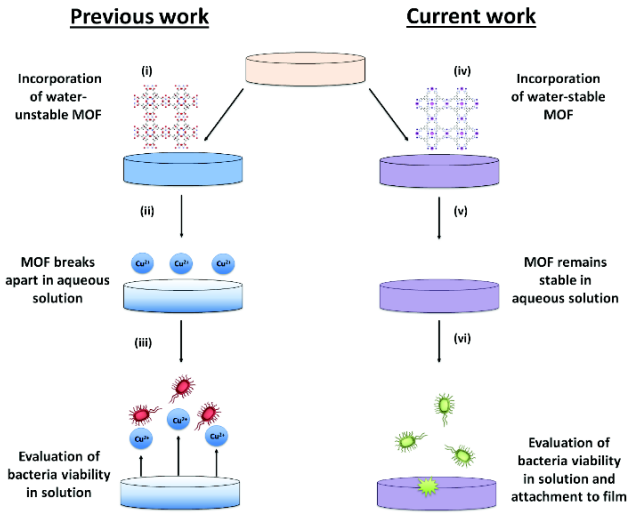

Figure 4.1 General schematic for bacteria study: left image displays the previous work published on MOF antibacterial literature (with a representative Cu-BTC structure shown), where the MOF breaks down to release copper ions that act as an antibacterial agent; right image displays the current study presented in this manuscript (with a representative Cu-BTTri structure shown), where a water-stable MOF is incorporated into a film to study bacterial attachment. (Reprinted with permission. Copyright 2017, Wiley-VCH Verlag GmbH & Co. KGaA)

4.3 MATERIALS AND METHODS

4.3.1 Materials

Low molecular weight chitosan (96% deacetylated) and copper(I) iodide (99.5%) were purchased from Sigma-Aldrich (St. Louis, MO, USA). Phosphate buffered saline (PBS) tablets and copper(II) chloride dihydrate were obtained from EMD Chemicals (Gibbstown, NJ, USA). 1,3,5-tribromobenzene (98%), trimethylsilylacetylene (98%), trimethylsilyl azide (94%), diethylamine (99%), were purchased from Alfa Aesar (Ward Hill, MA, USA). Deionized water (18.2 MΩ·cm) was prepared using a Millipore Direct-Q water purification system. Bis(triphenylphosphine)palladium(II) dichloride (98%) was obtained from TCI America (Portland, OR, USA). Chelex-100 Resin was purchased from Bio-Rad (Hercules, CA, USA). *Pseudomonas aeruginosa* (PAO1) was provided by Dr. Brad Borlee at Colorado State University. Oxoid™ nutrient broth media (NBM, OXCM0001B), Oxoid™ nutrient agar (NA, OXCM0003B), and sodium chloride were purchased from Fisher Scientific (Fair Lawn, NJ, USA). CellTiter Blue was purchased from Promega (Madison, WI, USA). Ethanol was purchased from Pharmco-AAPER (Brookfield, CT, USA). 24-well and 96-well tissue culture nontreated plates were obtained from Corning (Corning, NY, USA).

4.3.2 Experimental Methods

Synthesis of Cu-BTTri-H_2O ($H_3[(Cu_4Cl)_3(BTTri)_8(H_2O)_{12}]\cdot 72H_2O$), chitosan films and chitosan/Cu-BTTri films: Synthesis of ligand and MOF were conducted as previously reported.[26] Preparation of chitosan/Cu-BTTri followed identical protocol to previous publication.[28] In brief, chitosan acetate (in water, 3% w v-1) was cast into PTFE molds for 48 h. The films were removed and placed in PBS (100 mL) for 15 min. 13 mm diameter films were cut from the films

and used for further experiments. The chitosan/Cu-BTTri films were made in a similar fashion, with the addition of 1, 5, 10, or 20% MOF incorporation before casting into PTFE molds.

Chitosan and chitosan/Cu-BTTri Cu content and soaking studies: The average copper content of chitosan/Cu-BTTri films was determined by ICP-AES analysis where dissolution of films (n = 3) in 1% acetic acid was performed, followed by addition of 37% hydrochloric acid to decompose Cu-BTTri. The 10% w w^{-1} films were found to contain 295 ± 8 μmol Cu g^{-1}. Additional formulations with 1, 5, and 20% Cu-BTTri w w^{-1} contained 31 ± 15, 156 ± 12, and 527 ± 97 μmol Cu g^{-1}, respectively. Chitosan films dissolved under identical conditions were found to contain 0.320 ± 0.025 μmol Cu g^{-1}. Based on the formula unit of Cu-BTTri-H_2O ($H_3(Cu_4Cl)_3(BTTri)_8(H_2O)_{12} \cdot 72H_2O$), the Cu-BTTri content of the final deprotonated 10% films was estimated at 11% w w^{-1} using the copper content determined by ICP-AES. In the case of 1, 5, and 20% w w^{-1} films, the estimated Cu-BTTri content was 1, 6, and 20% w w^{-1}, respectively.

In addition, films were analyzed for residual copper content from synthetic procedure by soaking in NBM at 37 °C for 24, 48, and 72 h. These solutions were analyzed for elemental analysis using ICP-AES. The resulting copper in solution from the chitosan and chitosan/Cu-BTTri films were determined after subtracting the copper content from the NBM itself under the same conditions. The average copper in solution (mg L^{-1}) was normalized for each film by the volume of added NBM (mL) and mass of each film (mg). The percent copper in solution was found by comparing the mass of copper from the soaking solutions over the given soaking periods and the average mass of the total copper content of the films.

Pseudomonas aeruginosa bacteria culture: An initial stock culture of *P. aeruginosa* (PAO1) was obtained by streaking onto agar plates and inoculating a colony in NBM and grown overnight at

37 °C until an $O.D._{600nm}$ ~1.0 was reached. This bacterial solution was combined with glycerol (30% v v^{-1}) in a 1:1 fashion to obtain a final glycerol concentration of 15% (v v^{-1}). These solutions were stored at -80 °C until use. Prior to each bacterial assay, a frozen culture was allowed to thaw and then centrifuged at 4700 rpm for 10 min. The supernatant was discarded and the pellet was resuspended using 5 mL NBM. This was transferred to an additional NBM (45 mL) and allowed to grow overnight under stirring conditions until the $O.D._{600nm}$ ~1.0. The following day, the overnight culture was diluted to an $O.D._{600nm}$ ~0.35 using warmed NBM prior to beginning the attachment assays.

Bacteria attachment assays: Prior to bacteria attachment assays, all films were hydrated overnight using sterile DI water before being transferred to vials containing a mass normalized amount of NBM (1 mL NBM/3.05 mg film) as determined by the leaching assays. The films were stored in NBM at 37 °C for 72 h. Before being exposed to the bacterial solution, the films were removed from the NBM and placed in a 24-well non-tissue culture treated plate. An aliquot of *P. aeruginosa* bacterial solution (1 mL) was placed into wells containing the films, with empty wells used as the positive control. The wells were placed in an incubator at 37 °C for either 6 or 24 h before quantifying the attached bacteria.

A bacteria cellular viability assay was utilized to determine the amount of viable cells on the surface of the films or wells after the exposure period. This was done by removing the bacteria solution from all wells, washing the wells one time with sterilized PBS, moving the films to a new well such that only the bacteria attached to the films and not the surrounding well was assayed, and CellTiter Blue solution (400 µL) was added. The CellTiter Blue solution consisted of 1:5 ratio of CellTiter Blue reagent with NBM. The plate was placed back in the 37 °C incubator for 1-2 h before 100 µL aliquots were transferred to a 96-well plate and the

absorbance was measured at 570 and 600 nm (Synergy 2 Multi-Mode Reader, BioTek, Winooski, VT, USA). The cellular viability obtained by these absorbance values was normalized for film and well area ($n \geq 6$).

In addition, the number of colony-forming units (CFUs) that remained on each 10% film or well after the exposure period was determined using a sonication and plating method. The bacteria solution was removed from all wells, the wells were washed one time with warmed NBM, films were transferred to new wells, and fresh NBM was added to all wells. The plate was then sonicated for 30 min to remove the viable bacteria from the films or wells and 100 μL aliquots were serial diluted and 50 μL was plated on agar. The agar plates were placed in a static 37 °C incubator overnight and CFUs were counted the following morning. The amount of attached bacteria identified using this method was normalized by the area of the films or wells ($n=6$).

Reusability of chitosan and chitosan/Cu-BTTri films: The chitosan and 10% chitosan/Cu-BTTri films were saved after completing the initial round of attachment studies to determine if a similar reduction in attachment could be seen with the sterilized films. This was done by sterilizing the films in ethanol overnight and then allowing them to rehydrate in water before performing the CellTiter Blue assay again. This assay was performed in an identical fashion to initial bacterial attachment studies using CellTiter Blue and a 6 and 24 h exposure period ($n=6$).

Bacteria control studies (10% chitosan/Cu-BTTri films): The bactericidal activity of the bacterial attachment solution was determined by removing an aliquot of the bacteria solution after the exposure period and tested for bacteria cellular viability using the CellTiter Blue assay ($n=6$). The bactericidal activity of the average amount of copper in solution from the chitosan/Cu-BTTri films (as found by ICP-AES) was determined by exposing that amount of copper (in the form of

copper chloride) to the *P. aeruginosa* bacterial solution for 24 h. The mass of copper chloride was added to the bacteria solution in NBM and stored at 37 °C. After 24 h, 100 μL aliquots of the control wells (equal volume of NBM without added copper chloride) and the copper sample wells were combined with 300 μL CellTiter Blue solution. The wells were analyzed in a similar fashion to the CellTiter Blue attachment assay for bacteria cellular viability (n=3).

The average amount of triazole present in the chitosan/Cu-BTTri films was exposed to *P. aeruginosa* bacteria solution in a similar fashion to the copper chloride solution to test for antibacterial activity. Briefly, the average mass of triazole powder was introduced to the bacteria solution in NBM for a 24 h exposure period. Aliquots of the remaining bacterial solution were combined with CellTiter Blue solution and the cellular viability was assessed by comparing the wells containing triazole to the wells containing NBM only. The triazole powder in the absence of bacteria was also tested using the CellTiter Blue solution as a negative control to ensure the triazole did not adversely affect the CellTiter Blue reagent (n=3).

Control studies were also performed using chitosan films with copper chelated to the chitosan. These films were soaked for either 24 or 72 h in NBM at 37 °C and the resulting soaking solution was exposed to *P. aeruginosa* bacteria solution. The CellTiter Blue assay was performed on the bacteria solution after 24 h exposure time and the copper-chitosan soaking solutions were compared to a positive control of bacteria solution only (n=4).

The metal chelator Chelex-100 Resin (1-2 mg) was added to wells containing the 10% chitosan/Cu-BTTri films before performing the 6 and 24 h attachment studies. An equivalent amount of Chelex-100 Resin was also added the bacterial solution in the absence of the films as an additional control study (n=3).

Statistical analysis: All biological assays were performed using at least 6 samples and assayed in replicate form. Viability assays are reported as the mean and 95% confidence interval. All data was evaluated for potential outliers using the Grubbs Test. The statistical differences in data were evaluated using either the Student's t test or a one-way ANOVA test with a Tukey Honestly Significant Difference *post-hoc* test ($p < 0.05$) at the 95% confidence level.

4.4 RESULTS AND DISCUSSION

4.4.1 Synthesis and Characterization

Synthesis and characterization of Cu-BTTri and chitosan/Cu-BTTri films. All materials used in this study were prepared following previously reported protocols.[26,28] Characterization by SEM-EDS, ATR-IR, and pXRD confirmed the MOF assembly, MOF incorporation into the chitosan films, and structural integrity of MOF after bacteria experiments were performed (not shown). These analyses confirmed stability of Cu-BTTri before and after bacteria studies. Finally, soaking studies in NBM were performed to remove any copper sites not directly coordinated within the framework.[29]

4.4.2 Bacteria Studies

Currently, there are multiple methods employed to decrease or halt the adhesion step of bacteria onto a surface. The two main approaches are materials that release antibacterial agents and materials with bacteria killing or repelling surfaces.[9,30,31] The first method is considered an active approach, where the healthy bacteria are ultimately compromised by exposure to a biocidal agent being released from a material. Conversely, the second approach is considered passive, as there is not a need for a drug-releasing agent, but rather the material contains inherent properties that reduce the amount of adhered bacteria onto that surface (either through contact killing or repelling surfaces). These passive surfaces are particularly attractive for use in

biomedical applications because they do not require a reservoir of antibacterial agents and can theoretically be used multiple times.[30,31] Thus, the goal in this work was to determine if the chitosan/Cu-BTTri materials have the inherent properties to behave as a passive antibacterial surface.

Additionally, the antibacterial nature of copper-based MOFs has been primarily investigated by exploiting the slow and steady release of copper ions into solution caused by the breakdown of water unstable MOFs.[22] For example, it was previously observed that Cu-BTC grown on silk fibers exhibited high antibacterial action against both *Escherichia coli* (*E. coli*) and *Staphylococcus aureus* (*S. aureus*) planktonic bacteria. In general, copper ions have long been identified as an antibacterial agent, making it evident that copper-based MOFs are breaking down in solution over time and the copper ions are interacting with planktonic bacteria.[32] In contrast, Cu-BTTri, has been shown to be stable in aqueous environments, such as PBS and blood.[27] Thus, the utilization of Cu-BTTri allows for the investigation of the potential antibacterial nature of the MOF, while eliminating or minimizing activity due to byproducts and possible leachates that could be causing the observed activity on planktonic bacteria.

Bacterial attachment studies. The ability of chitosan and chitosan/Cu-BTTri films to inhibit bacterial attachment of *P. aeruginosa* over 6 and 24 h exposure periods was assessed using two bacterial viability assays. This particular bacteria strain is associated with a high level of antibiotic resistance and is one of the most common strains associated with biofilm formation.[6,7] Due to its ability to quickly form robust biofilms at wound sites, the critical goal is to find a material with the capabilities to inhibit the initial attachment of *P. aeruginosa* onto a surface, ultimately preventing the formation of a biofilm.[9,10] This discovery could have significant impacts on the overall length and severity of bacterial infections. Initial attachment experiments

are performed after 6 h of exposure to a surface, as this is considered the most critical time period after material implantation for biofilm formation to occur.[33] However, it is imperative to ensure that inhibition is maintained over the entire 24 h challenge period.

Viable bacteria cells remaining on the films were analyzed using a spectroscopic assay (CellTiter Blue) that exploits the ability of healthy bacteria to convert the blue colored compound resazurin (λ_{max} = 600 nm) to the highly pink compound resorufin (λ_{max} = 570 nm).[34] By monitoring the absorbance features of both compounds, an overall increase or decrease in metabolic activity of viable bacteria can be assessed by comparison to a positive control. In this case, the positive control (PC) represents non-tissue culture treated polystyrene wells. Throughout the text, however, the chitosan films without the incorporation of Cu-BTTri will also be utilized and discussed as a positive control, as a further point of comparison. Regardless of the assignment of control wells, bacterial viability was assessed after either 6 or 24 h and normalized by the given area available for bacteria attachment. Figure 4.2a displays the results of this assay, with the polystyrene well as the positive control. After 6 h of exposure to bacteria, a 55-65% (displayed as the confidence interval) reduction in attachment is seen for the chitosan films, while chitosan/Cu-BTTri films display an even greater reduction of 81-87% in attachment of viable bacteria. Given the established antibacterial properties of chitosan, it is useful to consider the reduction in viable bacteria onto the chitosan/Cu-BTTri when compared to the chitosan itself as a positive control. This results in a 50-68% reduction in attachment after the 6 h period. This is a significant reduction to achieve in a 6 h exposure period, however it is essential to ensure that the adherence of bacteria does not increase over 24 h.

As shown in Figure 4.2a, the ultimate reduction of attachment onto the chitosan/Cu-BTTri films is retained over the 24 h period, with an 82-86% reduction observed. Indeed, this is

a substantial reduction to achieve given the bacteria strain of *P. aeruginosa*. In contrast, the reduction was not maintained for the chitosan films, with only 33-43% reduction of attachment remaining after 24 h. If the chitosan/Cu-BTTri films are again compared to the chitosan films themselves as the positive control, a 75-79% reduction in bacterial attachment onto chitosan/Cu-BTTri films is observed. All results determined by the CellTiter Blue assay were supported by enumerating the number of bacterial colonies on the films or wells using a sonication and plating assay. This technique removes the viable bacteria from the surface by sonicating for 30 min to liberate the attached bacteria as the planktonic form, which can then be serial diluted and agar plated to ultimately determine the number of colony-forming units (CFUs).[35] Again, the determined CFUs were normalized by the given attachment area of the wells or films.

All chitosan/Cu-BTTri films utilized in the attachment assays were saved and sterilized to determine if the observed reduction in bacterial attachment could be shown again using the same films. The assays were performed in an identical fashion to initial studies, without the need for the 72 h NBM soaking period. Figure 4.2b shows the results of this study, where it is seen that a similar reduction in attachment is observed for all samples and both time points for the CellTiter Blue assay. Indeed, the bacteria cellular viabilities found for chitosan and chitosan/Cu-BTTri in the second round of assays is not statistically different from those determined from the first round of assays at a 95% confidence level. This observed continued function of the films demonstrates the usefulness and potential reusability of these novel materials to be used as biomaterials for antibacterial applications. This also suggests that the films may indeed be considered as passive antibacterial surfaces, as there is no loss of functionality after initial exposure to bacteria.

Previous reports of *P. aeruginosa* bacterial adhesion onto a surface vary widely with regards to the percent reduction observed. An example of an approach where an antimicrobial agent is released (in this case, nitric oxide) has been shown to inhibit *P. aeruginosa* attachment by 50-65% depending on the nitric oxide flux from the material.[36] Another approach where contact killing is employed through the use of cationic peptides immobilized on a surface achieved up to 80% inhibition of *P. aeruginosa*.[37] Finally, Hook et al. employed a passive approach for bacterial adhesion by implementing a novel material containing a combination of polymers to ultimately achieve ~80% reduction in *P. aeruginosa* attachment.[38] These examples highlight the significant reduction achieved in this work using the chitosan/Cu-BTTri materials, where an ~85% reduction in achieved within the first 6 h, maintained over 24 h, and have the capabilities to achieve the same reduction again after the initial round of experiments.

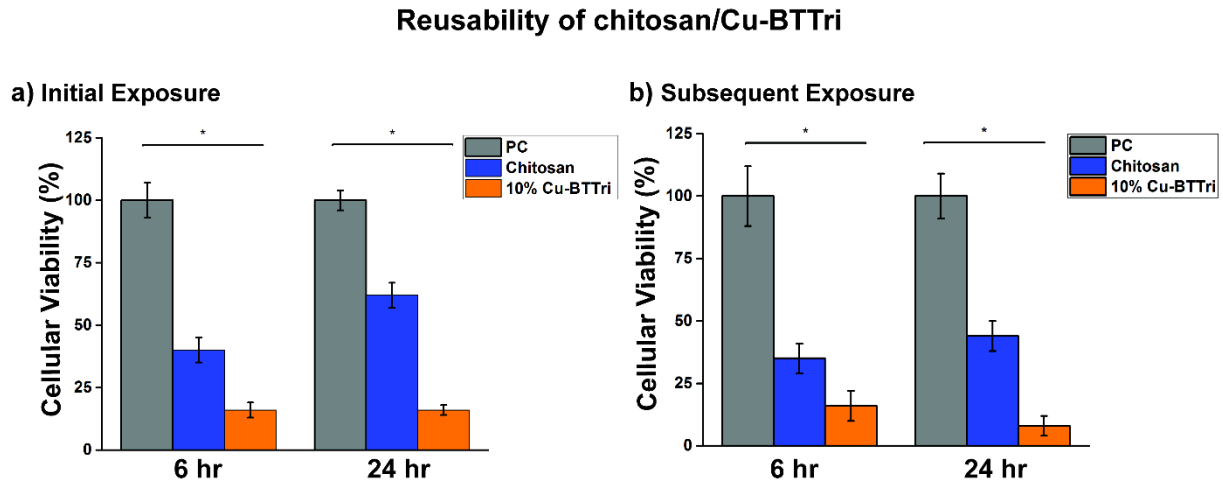

Figure 4.2 Cellular viability of attached *P. aeruginosa* bacteria onto polystyrene wells (PC=positive control), chitosan, and chitosan/Cu-BTTri films after (a) initial exposure and (b) subsequent exposure to bacteria for 6 and 24 h as determined by CTB assay. Average and 95% confidence interval displayed, n=6. Statistically significant differences between cellular viabilities are indicted (*) as determined by a one-way ANOVA. (Reprinted with permission. Copyright 2017, Wiley-VCH Verlag GmbH & Co. KGaA)

Bacteria control studies. Due to potential antimicrobial effects from possible leachates from the chitosan/Cu-BTTri films (namely copper ions), a number of control studies were performed using *P. aeruginosa* both in solution and on the films themselves. Results from ICP-AES revealed that, for the 10% w w^{-1} films, 0.0725 ± 0.0024 mg Cu L^{-1} NBM was present in the solutions after 72 h of soaking in NBM at 37 °C, representing ~2.5% of the total theoretical amount of copper in each film. To determine if this amount had any bactericidal effects on *P. aeruginosa*, an equivalent amount was introduced to the bacteria in NBM and exposed for 24 h. The results indicated that there was no statistical difference between the cellular viability of the bacteria exposed to this concentration of copper and that of the control wells. Future attachment experiments were performed only after the requisite 72 h soaking period to ensure this amount of copper was not present during attachment assays, however this still provides insight into the mechanism of action for Cu-BTTri, indicating that these levels of copper would not explain the observed effect. This concept was also tested using triazole ligand (1,3,5-tris(1H-1,2,3-triazol-5-yl)benzene) in powder form at the same amount that would be present in the chitosan/Cu-BTTri films (0.055 mg triazole mg^{-1} chitosan/Cu-BTTri film). This amount of ligand was exposed to *P. aeruginosa* for 24 h and the resulting bacteria solution was tested for cellular viability using the CellTiter Blue assay. Results from this were similar to the copper ion experiment, where there was no observed decrease in bacteria viability after exposure to triazole compared to the positive control. Finally, a metal ion chelator that displays selectivity for copper ions (Chelex-100 Resin) was added to the bacterial solution in the presence of the chitosan/Cu-BTTri films to remove any labile or weakly associated copper ions that may be contributing to the observed effect. There was no statistical difference in the amount of viable bacteria attached to the films in the absence or presence of the metal ion chelator, further giving insight into the mechanism of inhibition

arising from the intact Cu-BTTri within the chitosan matrix. An initial control experiment was also conducted using the metal chelator in the presence of bacteria only to ensure the Chelex-100 did not compromise the integrity of healthy bacteria cells.

In addition to testing the individual components of the MOF for antibacterial activity, the surrounding bacterial solution can also be tested for cellular viability in addition to quantifying the attached bacteria onto the films. This does not test individual components of potential leachates (as was the case for copper ions and triazole powder), but rather assesses the entire film solution for presence of any antibacterial agents. For this assay, aliquots of the bacteria solution surrounding the films (both chitosan and chitosan/Cu-BTTri) were mixed with the CellTiter Blue reagent to determine cellular viability. Likewise to the copper ion and triazole assays, there was no decrease in bacteria viability observed for either film (chitosan or chitosan/Cu-BTTri) when compared to the positive control. This ensures that leachates do not occur at sufficient concentration to compromise the integrity of healthy bacteria, further demonstrating the localized effect of the film on bacteria rather than the release of antibacterial agents. A summary of the control experiments and subsequent results can be found in Table 4.1.

Table 4.1 Bacteria control experiments using *P. aeruginosa* with chitosan and 10% w w^{-1} chitosan/Cu-BTTri film components tested for cellular viability by CellTiter Blue assay to isolate effects seen with bacterial attachment onto films (Y = yes; N = no) (n≥3).

Sample	> 80% Reduction in Viable Bacteria in 6 h	> 80% Reduction in Viable Bacteria in 24 h
Chitosan/Cu-BTTri	Y	Y
Chitosan	N	N
Copper ions[a]	N	N

Triazole powder	N	N
Bacterial solution	N	N

[a]Copper ions introduced in the form of copper(II) chloride

Impact of varying Cu-BTTri concentration. In order to determine the threshold for the observed reduction in bacterial attachment, a range of MOF compositions were tested, yielding 1%, 5%, 10%, and 20% w w^{-1} Cu-BTTri incorporation. Figure 4.3 displays the results of this assay for all film compositions, with the polystyrene well again used as the positive control. After 6 h of exposure to bacteria, the reduction in attachment observed between the chitosan films and the 1% chitosan/Cu-BTTri films are not statistically different. Similarly, the films containing additional incorporation of the MOF (5% and 20% w w^{-1}) display no statistical difference observed for all values of cellular viability when compared to the 10% films. After 24 h exposure to bacteria, the chitosan and the 1% Cu-BTTri films show no statistical difference in reduction, while the 5% and 20% films are comparable to what was observed for the original 10% films. Based on these findings using a variety of MOF compositions, the threshold for biofilm inhibition begins with the 5% w w^{-1} incorporation, and the desired function does not increase as more Cu-BTTri is incorporated into the chitosan matrix (as seen with both 10% and 20% w w^{-1}).

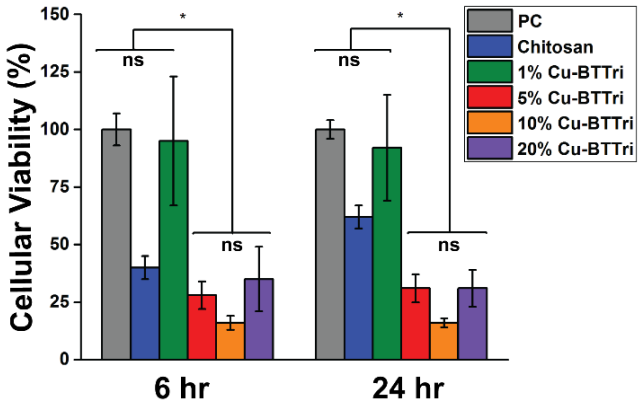

Figure 4.3 Cellular viability of attached *P. aeruginosa* bacteria onto polystyrene wells (PC=positive control), chitosan, and chitosan/Cu-BTTri films (at 1%, 5%, 10%, and 20% w w^{-1}

MOF incorporation) after exposure for 6 and 24 h as determined by CTB assay. Average and 95% confidence interval displayed, n=6. Statistically significant differences between cellular viabilities are indicted (*) and not statistically significant differences are indicated by (ns) as determined by a one-way ANOVA. (Reprinted with permission. Copyright 2017, Wiley-VCH Verlag GmbH & Co. KGaA)

While the exact mechanism of antibacterial action remains unclear, the extensive control studies performed using the 10% w w^{-1} chitosan/Cu-BTTri films gives insight into the factors that *do not* influence the observed antibacterial nature of the films. By ensuring that the bacterial solution above the films is not adversely affected compared to the positive control, it can be concluded that leachates from the films are not acting in an antibacterial fashion. Additionally, it would appear that any labile copper ions not directly coordinated within the material framework are not responsible for the inhibition of bacterial attachment, as the chelator control experiment would have removed those copper ions from solution. Lastly, demonstrating the observed effect for the incorporated Cu-BTTri at different weight percentages would indicate that there is an upper and lower limit to the amount of incorporated MOF necessary to elicit the desired response. When adding only 1% w w^{-1} Cu-BTTri, there was no statistical difference observed between the chitosan and chitosan/Cu-BTTri with regard to their inhibition properties. Conversely, increasing the incorporated Cu-BTTri from 5% to 10% and 20% w w^{-1} did not increase the observed antibacterial nature, suggesting a saturation point to the activity imparted onto the bacteria.

4.5 CONCLUSIONS

A significant reduction (~85%) in bacterial attachment was demonstrated using a water-stable MOF blended with chitosan. This inhibition is considered substantial in the field of novel antibacterial surfaces, particularly noteworthy for the bacteria strain *P. aeruginosa* which is known to be a robust biofilm former. Chitosan/Cu-BTTri blended

films were utilized for bacterial attachment inhibition properties by testing the activity against *P. aeruginosa* over 6 and 24 h periods. The biofilm inhibition of *P. aeruginosa* was observed for the 5, 10, and 20% w w^{-1} blended films after 6 h and was maintained for the entire 24 h challenge period. This functionality was retained after a second round of bacterial attachment studies, suggesting reusability of these materials as antibacterial surfaces. Finally, extensive control assays were performed to differentiate this observed antibacterial effect to the previous antibacterial publications for copper-based MOFs where the proposed mechanism is the slow, continuous release of copper ions. These control studies allow us to isolate the observed biological effects to the chitosan/Cu-BTTri film itself and not to possible leachates from films during experiments. This noteworthy finding presents an opportunity for a novel biomaterial to be utilized as a passive antibacterial surface in settings with prevalent bacterial infections to serve as a biofilm inhibitor.

CHAPTER 4 – REFERENCES

1. Wright, G.D. *Nature Rev. Microbiol.* **2007**, 5, 175-186.
2. Taubes, G. *Science* **2008**, 321, 356-361.
3. Hall-Stoodley, L.; Costerton, J.W.; Stoodley, P. *Nature Rev. Microbiol.* **2004**, 2, 95-108.
4. Stoodley, P.; Sauer, K.; Davies, D.G.; Costerton, J.W. *Annu. Rev. Microbiol.* **2002**, 56, 187-209.
5. Costerton, J.W.; Stewart, P.S.; Greenberg, E.P. *Science* **1999**, 284, 1318-1322.
6. Chatterjee, M.; Anju, C.P.; Biswas, L.; Kumar, V.A.; Mohan, C.G.; Biswas, R. *Int. J. Med. Microbiol.* **2016**, 306, 48-58.
7. Stover, C.K.; Pham, X.Q.; Erwin, A.L.; Mizoguchi, S.D.; Warrener, P.; Hickey, M.J.; Brinkman, F.S.L.; Hufnagle, W.O.; Kowalik, D.J.; Lagrou, M.; Garber, R.L.; Goltry, L.; Tolentino, E.; Westbrock-Wadman, S.; Yuan, Y.; Brody, L.L.; Coulter, S.N.; Folger, K.R.; Kas, A.; Larbig, K.; Lim, R.; Smith, K.; Spencer, D.; Wong, G.K.S.; Wu, Z.; Paulsen, I.T.; Reizer, J.; Saier, M.H.; Hancock, R.E.W.; Lory, S.; Olson, M.V. *Nature* **2000**, 406, 959-964.
8. O'Toole, G.; Kaplan, H.B.; Kolter, R. *Annu. Rev. Microbiol.* **2000**, 54, 49-79.
9. Cloutier, M.; Mantovani, D.; Rosei, F. *Trends Biotechnol*. **2015**, 33**,** 637-652.
10. Epa, V.C.; Hook, A.L.; Chang, C.; Yang, J.; Langer, R.; Anderson, D.G.; Williams, P.; Davies, M.C.; Alexander, M.R.; Winkler, D.A. *Adv. Funct. Mater.* **2014**, 24, 2085-2093.
11. Lu, Y.; Slomberg, D.L.; Schoenfisch, M.H. *Biomaterials* **2013**, 35, 1716-1724.
12. Kumar, M.N.V.R. *React. Funct. Polym.* **2000**, 46, 1-27.

13. Dash, M.; Chiellini, F.; Ottenbrite, R.M.; Chiellini, E. *Prog. Polym. Sci.* **2011**, 36, 981-1098.

14. Dai, T.; Tanaka, M.; Huang, Y.; Hamblin, M.R. *Expert Rev. Anti Infect. Ther.* **2011**, 9, 857-879.

15. Jain, G.; Allon, M.; Saddekni, S.; Barker, J.-F.; Maya, I.D. *Clin. J. Am. Soc. Nephrol*. **2009**, 4, 1787-1790.

16. Baumgartner, J.N.; Cooper, S.L. *ASAIO J*. **1996**, 42, M476-M479.

17. Eddaoudi, M.; Moler, D.B.; Li, H.; Chen, B.; Reineke, T.M.; O'Keefe, M.; Yaghi, O.M. *Acc. Chem. Res.* **2001**, 34, 319-330.

18. Stock, N.; Biswas, S. *Chem. Rev.* **2012**, 112, 933-969.

19. Furukawa, H.; Cordova, K.E.; O'Keefe, M.; Yaghi, O.M. *Science* **2013**, 341, 1230444.

20. Keskin, S.; Kizilel, S. *Ind. Eng. Chem. Res*. **2011**, 50, 1799-1812.

21. ul Qadir, N.; Said, S.A.M.; Bahaidarah, H.M. *Microporous Mesoporous Mater*. **2015**, 201, 61-90.

22. Wyszogradozka, G.; Marszalek, B.; Gil, B.; Dorozynski, P. *Drug Discov. Today* **2016,** 21, 1009-1018.

23. Gul-E-Noor, F.; Jee, B.; Poppl, A.; Hartmann, M.; Himsl, D.; Bertmer, M. *Phys. Chem. Chem. Phys*. **2011**, 13, 7783-7788.

24. Chiericatti, C.; Basilico, J.C.; Basilico, M.L.Z.; Zamaro, J.M. *Microporous Mesoporous Mater.* **2012**, 162, 60-63.

25. Abbasi, A.R.; Akhbari, K.; Morsali, A. *Ultrason. Sonochem.* **2011**, 19, 846-852.

26. Demessence, A.; D'Alessandro, D.M.; Foo, M.L.; Long, J.R. *J. Am. Chem. Soc.* **2009**, 131, 8784-8786.

27. Harding, J.L.; Metz, J.M.; Reynolds, M.M. *Adv. Funct. Mater*. **2014**, 24, 7503-7509.

28. Neufeld, M.J.; Lutzke, A.; Tapia, J.B.; Reynolds, M.M. *ACS Appl. Mater. Interfaces* **2017**, 9, 5139-5148.

29. Poppl, A.; Kunz, S.; Himsl, D.; Hartmann, M. *J. Phys. Chem. C* **2008**, 112, 2678-2684.

30. Hasan, J.; Crawford, R.J.; Ivanova, E.P. *Trends Biotechnol*. **2013**, 31, 295-304.

31. Pham, V.T.H.; Bhadra, C.M.; Truong, V.K.; Crawford, R.J.; Ivanova, E.P. *Antibacterial Surfaces*, Springer International Publishing, Switzerland **2015**, Ch. 6.

32. Dollwet, H.H.A.; Sorenson, J.R.J. *Trace Elem. Med*. **1985,** 2**,** 80-87.

33. Poelstra, K.A.; Barekzi, N.A.; Rediske, A.M.; Felts, A.G.; Slunt, J.B.; Grainger, D.W. *J. Biomed. Mater. Res.* **2002**, 60, 206-215.

34. Promega Corporation, Cell Titer-Blue Cell Viability Assay (Promega Corporation, Madison, WI, **2013**).

35. Ceri, H.; Olson, M.E.; Stremick, C.; Read, R.R.; Morck, D.; Buret, A. *J. Clin. Microbiol*. **1999**, 37, 1771-1776.

36. a) Dobmeier, K.P.; Schoenfisch, M.H. *Biomacromolecules* **2004**, 5**,** 2493-2495; b) Hetrick, E.M.; Schoenfisch, M.H. *Biomaterials* **2007**, 28, 1948-1956.

37. Dosler, S.; Karaaslan, E. *Peptides* **2014**, 62, 32-37.

38. Hook, A.L.; Chang, C.; Yang, J.; Atkinson, S.; Langer, R.; Anderson, D.G.; Davies, M.C.; Williams, P.; Alexander, M.R. *Adv. Mater*. **2013**, 25, 2542-2547.

CHAPTER 5

SMALL MOLECULE INTERFERENCES IN RESAZURIN AND MTT-BASED METABOLIC ASSAYS IN THE ABSENCE OF CELLS

5.1 BACKGROUND

The combination of thiol-containing moieties within the systems evaluated in Prof. Melissa Reynolds laboratory, along with the implementation of *in vitro* cytotoxicity assays for bacteria studies, led to the discovery that some commonly used spectroscopic assays can produce false positives or negatives. For example, it was noted that the addition of non-nitrosated glutathione to a solution of 3-(4,5-dimethylthiazol-2-yl)-2,5-diphenyl-tetrazolium bromide (the MTT starting reagent) will cause the solution to turn from yellow to purple, suggesting a chemical transformation from MTT to its formazan counterpart. This is a critical observation, as this spectroscopic transformation is often used to determine cytotoxicity of a tested therapeutic in the presence of viable cells (both mammalian and bacteria). The ability to cause this transition without cellular activity indicates that false responses may be prevalent with the use of some *in vitro* assays. Therefore, an in-depth study of several small molecules and their effect on two common spectroscopic cytotoxicity assays in the absence of viable cells was investigated to highlight the need for proper control studies to be performed. Alec Lutzke provided much of the guidance and support for this manuscript, including identifying the small molecules to be tested and some analysis of the data. Jesus B. Tapia performed LC-MS studies in an attempt to elucidate some of the chemical transformations that were taking place under these conditions. Bella H. Neufeld performed the experiments related to absorbance measurements of the two assays (96-well plate and UV-Vis experiments) and provided much of the analysis of the data.

This manuscript is currently under review in Analytical Chemistry. Prof. Melissa M. Reynolds acted as the advisor on this project.

5.2 INTRODUCTION

The use of *in vitro* assays has truly revolutionized the world of pharmaceuticals and therapeutic agents in their ability to rapidly and efficiently evaluate cytotoxicity of novel compounds without the need for expensive and sometimes controversial *in vivo* testing. Beginning in the 1980s, the use of these assays has become widespread and developed to be applicable in many types of systems, highlighting their importance in medicinal and biological chemistry.[1,2] The frequent use of *in vitro* assays (particularly those that utilize spectroscopic detection) in multiple scientific fields does, however, requires rigorous understanding of the chemistry involved in the spectroscopic transition in order to provide accurate accounts of cytotoxicity.

Many of the spectroscopic *in vitro* assays (including those discussed herein) rely on the ability of metabolically active cells to transform one compound to another (typically through reduction of the starting reagent). The initial or final compound (or both) can be evaluated based on their spectroscopic properties to determine cellular viability relative to a control sample.[3] This type of experimental method allows for high-throughput and simplicity in obtaining large datasets quickly. Two very common *in vitro* cytotoxicity assays are the resazurin-resorufin dye complexes (which is sold by multiple names including CellTiter Blue and Alamar Blue) and the MTT assay (3-(4,5-dimethylthiazol-2-yl)-2,5-diphenyl-tetrazolium bromide).[4,5] These assays rely on the cellular conversion of the starting compound (either resazurin or MTT) to the final compound (resorufin or MTT formazan) and represent a practical method based on cost, analysis time, and simplicity.[6,7] The chemical transformations and their spectroscopic effects, however,

can be produced via functional groups and moieties that may be present within the therapeutic sample without the need for cellular metabolic activity.[8]

Potential interferences for both the resazurin and MTT assays were identified as early as 1977 and 1995, respectively, and continue to be discussed in the literature today.[4,9] Goegan et al. noted the effect of protein concentration in media on the reduction of resazurin to resorufin, while Shoemaker et al. discuss the effect of MTT reduction to its formazan counterpart in the presence of certain herbal extracts.[10,11] While these interferences have been mentioned in previous literature, there has yet to be a rigorous study examining the effect and extent of such interferences for these two specific assays in the presence of various small molecules without the presence of cellular activity. Herein, we report the deviations from controls for 19 potentially interfering species at six concentrations in the presence of resazurin and MTT assays without cells present. This is in an effort to delineate the key structural features that give rise to false responses and highlight the importance of implementing proper control samples as a standard operating procedure of the assays. This is intended to be a fundamental study of the interactions between various functional groups (thiol, acid, amine, amide) and their resulting effect on the assay starting reagents. We were specifically interested in probing potential redox active species to determine their role in providing false responses and, therefore, the studied molecules were chosen based on their chemical moieties and are not necessarily biological in nature.

5.3 MATERIALS AND METHODS

5.3.1 Materials

Glutathione and LC-MS grade methanol were purchased from VWR (Solon, OH, USA). Oxidized glutathione, *N*-acetyl-D-penicillamine, cystamine dihydrochloride, D-penicillamine, DL-homocysteine, diethyl disulfide, 2-methyl-2-propanethiol, thioglycerol, and dimethyl

sulfoxide (DMSO) were purchased from Sigma Aldrich (St. Louis, MO, USA). L-Cysteine, mercaptosuccinic acid, *N*-acetyl-L-cysteine, diethylamine, and 2-propanethiol were purchased from Alfa Aesar (Ward Hill, MA, USA). Triethylamine and phosphate buffered saline (PBS) were purchased from EMD (Gibbstown, NJ, USA). Pyridine, potassium iodide (KI), ascorbic acid, and Oxoid Nutrient Broth Media (OXCM0001B) were purchased from Fisher Scientific (Fair Lawn, NJ, USA). Glycerol was purchased from Mallinckrodt Chemicals (Phillipsburg, NJ, USA). CellTiter Blue (resazurin-resorufin) was purchased from Promega (Madison, WI, USA). 24-well and 96-well tissue culture treated plates were obtained from Corning (Corning, NY, USA). Ethyl alcohol, 200 proof, was purchased from Pharmco-AAPER (Brookfield, CT, USA). *Escherichia coli* (*E. coli*, ATCC 25922) was purchased from the American Type Culture Collection (ATCC, USA).

5.3.2 Experimental Methods

Resazurin assay. The deviations from the negative control (resazurin with PBS) were determined by monitoring the absorbance values associated with the formation of the resorufin complex at 570 nm using a 96-well plate assay. Stock solutions (100 mM) of all 19 species were made in PBS and subsequently diluted five times to obtain six different concentrations. 100 µL aliquots of each concentration were added to a 96-well plate followed by the addition of 20 µL of the resazurin dye (already in solution at a fixed concentration as prepared by the manufacturer). The 96-well plate was placed in a plate reader and allowed to shake for 10 s before measuring the absorbance at 570 nm every hour for a total of four hours (Synergy 2 Multi-Mode Reader, BioTek, Winooski, VT, USA). The plate reader was maintained at 37 °C to mimic experimental conditions. The data are represented as the average percent deviation from the negative control.

This was calculated by the difference between the sample and control value, divided by the control value, and multiplied to obtain a percent value ($n \geq 3$).

To further elucidate the chemical transformations occurring between the sample analyte and resazurin, four representative species at 10 mM concentration (glutathione, oxidized glutathione, D-penicillamine, and mercaptosuccinic acid) were chosen as candidates that showed substantial deviations to perform further analysis. Both full UV-Visible (UV-Vis) spectra and mass spectrometric (MS) data were collected during the four-hour reaction period. The UV-Vis spectra were obtained by combining the interfering species with the resazurin dye in a 5:1 (species:resazurin dye) fashion and incubated at 37 °C. At each hour time point, aliquots were removed from the incubator and, if necessary, diluted using PBS before obtaining a UV-Vis spectrum from 200-800 nm (Nicolet Evolution 300, Thermo Electron Corporation, Madison, WI, USA). As a means of comparison, UV-Vis spectra were also obtained during the transformation of resazurin to resorufin in the presence of *E. coli* bacteria cells (representing a positive control for this assay). This was performed by growing a stock solution of *E. coli* until reaching an $O.D._{600}$~1.0. The stock culture was diluted using media to a working $O.D._{600}$~0.35 before combining the bacterial culture with the resazurin solution in an identical fashion as the interfering species. Sample preparation for MS analysis was performed using the same method as the UV-Vis spectra, using water as the aqueous solvent in place of PBS to minimize interfering ions and ion suppression in the mass spectrometer.

MTT assay. Similar to the resazurin assay analysis, the deviations from the control for the MTT assay (MTT with PBS) were monitored via the absorbance values associated with the formation of the formazan complex at 540 nm. The same 19 species at six concentrations were tested against the control wells, but these experiments were performed in a 24-well plate (instead of a

96-well plate) to minimize experimental variability. All sample solutions were made in PBS and 500 μL of each were added to a 24-well plate followed by the addition of 50 μL MTT solution (12 mM made in PBS). The plates were allowed to incubate at 37 °C and analyzed every hour by removing 425 μL of the solution followed by the addition of 250 μL DMSO. The plate was then incubated at 37 °C for an additional 10 min to allow the formazan complex to fully dissolve in the DMSO solvent before 100 μL aliquots were transferred to a 96-well plate and the absorbance measured at 540 nm. The data are represented as the average percent deviation from the negative control. This was calculated by the difference between the sample and control value, divided by the control value, and multiplied to obtain a percent value ($n \geq 3$).

Of the 19 sample species that were tested, five that showed substantial deviations from the control were chosen for further analysis by UV-Vis and MS. These five interfering species (glutathione, D-penicillamine, L-cysteine, *N*-acetyl-D-penicillamine, and mercaptosuccinic acid) were tested at 10 mM concentration. To obtain full UV-Vis spectra of the compounds, a similar protocol to the 24-well plate assay was employed before obtaining the UV-Vis measurement from 200-800 nm. These spectra were compared to a positive control of MTT in the presence of *E. coli* cells grown in an identical fashion to the description for the resazurin assay. To facilitate MS analysis, the sample mixture containing both PBS and DMSO was diluted in ethanol (0.1%) before injection into the instrument.

5.3.3 Statistical Analysis

All assays were performed at least three times with replicate samples. Statistical differences pertaining to the percent deviation from controls were determined by a two-tailed Student's *t*-test at the 95% confidence interval ($p < 0.05$). The data was further evaluated for outliers using the Grubbs test.

5.4 RESULTS AND DISCUSSION

Both the MTT and resazurin assays work by reduction of the compounds to their counterparts (formazan and resorufin, respectively) in the presence of metabolically active cells. Therefore, the relative conversion of the compounds can be directly correlated to the number of healthy cells present.[3] Although the exact mechanistic pathways for either assay are not entirely understood, it is thought that the resazurin is reduced either in chemically reduced media produced by cellular growth or enzymatic reduction within the mitochondria, while MTT reduction is likely to occur exclusively intracellularly by mitochondrial enzymes.[9,12] The resazurin assay (first discussed in 1977) represents a unique alternative to the popular MTT assay as it is non-toxic to cells and can be used for extended incubation or growth experiments, while the MTT assay (originally cited by Mosmann in 1983) is generally thought to be more sensitive in its ability to detect small changes within a viable cell population. Both assays were tested for interferences in this study due to their prevalence in the field of determining cytotoxicity or cell viability in the presence of novel therapeutic agents.[13-20]

The 19 potentially interfering species (see Figure 5.1) were chosen based on their biological relevance (i.e. glutathione, cysteine, penicillamine) and/or the functional groups present on the compounds to delineate the potential sources of interference (i.e. diethylamine, diethyl disulfide, 2-propanethiol).[21] The chosen species are not intended to be necessarily representative of the components of cell media, for example, but rather an array of molecules that may help decipher the sources of interference. The concentrations tested represent a large range (1 μM – 100 mM) intended to encompass the quantities that may be present under experimental conditions for a variety of analytes and substrates. Because researchers may analyze the data at any point during the four-hour incubation period (the recommended guideline

for both assays is anywhere between 1-4 hours after exposure to the assay reagent), these experiments were performed at each hour time point within the incubation period to mimic any experimental conditions that may be performed in a real laboratory setting. Both the MTT and resazurin assay experiments were performed as closely to protocols provided by the manufacturer to illustrate the interferences that can occur in real laboratory experiments.[6,7]

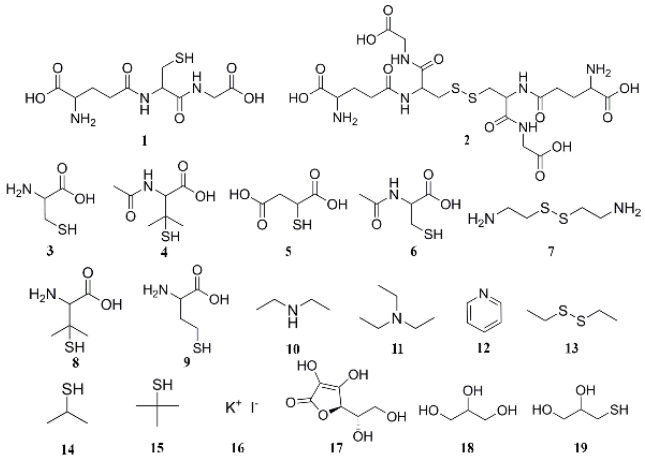

Figure 5.1 Potentially interfering species tested at 6 concentrations (1 μM- 100 mM) against resazurin and MTT assays to examine deviations from control in the absence of cells. 1 – glutathione; 2 – oxidized glutathione; 3 – L-Cysteine; 4 – *N*-Acetyl-D-penicillamine; 5 – mercaptosuccinic acid; 6 – *N*-Acetyl-L-cysteine; 7 – cystamine; 8 – D-Penicillamine; 9 – DL-Homocysteine; 10 – diethylamine; 11 – triethylamine; 12 – pyridine; 13 – diethyl disulfide; 14 – 2-Propanethiol; 15 – 2-Methyl-2-propanethiol; 16 – potassium iodide; 17 – ascorbic acid; 18 – glycerol; 19 – thioglycerol.

Table 5.1 displays the overall results related to the species that give rise to deviations that contain statistically significant differences from the control as determined by the corresponding absorbance values associated with either resorufin (570 nm) or formazan (540 nm). The quantitative values represent the largest deviations that occurred during the four-hour assay period. Of the 19 species that were tested against both assays, there is some overlap observed in terms of assay interferences, however there are more interferences at a greater magnitude noted

for the MTT assay. This may be related to the sensitivity of the assay relative to the resazurin assay or the increased potential required to transform resazurin to resorufin.[22,23] Based on the results displayed in Table 5.1, deviations occur throughout the tested concentrations but increase substantially with the higher tested concentrations (1, 10, and 100 mM).

It has been previously noted that species such as cysteine and dithiothreitol have shown interferences for the resazurin assay, suggesting that it may be thiol functional groups causing the reduction of resazurin to resorufin in the absence of cells.[12] Given the known reactivity of thiol redox chemistry in biological systems, it is a reasonable conclusion that these same principles may apply within *in vitro* systems. Therefore, a range of thiol-containing species were tested in this study to understand their effects on both assays, in combination with various other functional groups (as shown in column 2 of Table 5.1).

Initial studies were performed using glutathione (**1**) because it is a highly abundant biological molecule that is often utilized or mimicked for biological applications. Results from this experiment show that, indeed, there are strong deviations in the presence of resazurin at 10 and 100 mM. Deviations in the presence of MTT occur at every tested concentration and are even larger than anything observed with resazurin (>2000% in some cases). To isolate the effect of the thiol chemistry in species **1**, an oxidized form of glutathione (**2**) was subsequently tested, eliminating the ability for thiol functional groups to participate in the observed reduction reaction. Interestingly, both assays exhibited deviations from the control for the same concentrations as the reduced form of glutathione. To continue to delineate the effects observed between the two assays, a host of molecules were tested that contained primary, secondary, and tertiary thiols, amides, acids, primary, secondary, and tertiary amines, disulfides, and chemical analogues of starting materials. These species were chosen to identify the chemical sources of

interferences, but also represent an encompassing list for many functional groups that may be present in laboratory experiments, signifying chemical functional groups to be aware of in future studies that utilize these *in vitro* assays.

The results displayed in Table 5.1 give insight into which functional groups have an effect on both the resazurin and MTT assays. For example, it appears that the combination of thiols, carboxylic acids, and either amines or amides lead to rather substantial false responses for both assays (species **3**, **4**, **6**, **8**, and **9**). Of these, those that contain amines exhibit exaggerated effects when compared to their acetylated analogues. Notably, the interferences that were observed with **5**, which does not contain any amine or amide functionality but does have thiol and acidic groups, results in substantial deviations, similar to **3**, **4**, **6**, **8**, and **9**. This potentially indicates that those amine and amide functionalities are not directly involved in the reagent conversion, but may instead contribute to the overall solubility of the parent species. Additionally, species containing thiol or amines only (**10-15**) have little to no effective interference for either assay. To understand the role that redox chemistry may be contributing to the observed effects (as this has been suggested in previous research), KI, ascorbic acid, glycerol, and thioglycerol were tested (**16-19**). Both KI and glycerol showed minimal effects, while ascorbic acid and thioglycerol had rather substantial effects. This would suggest that perhaps it is truly the acidic and thiol functional groups playing a distinct role in either direct conversion or breakdown of the starting materials (as will be shown in the UV-Vis and MS analyses in following sections). The above analysis is true for both resazurin and MTT assays, however in many cases, resazurin is only affected at the highest tested concentration and the MTT results show consistently higher quantitative deviations.

Overall, quantitative results from Table 5.1 indicate that thiols and acids play the largest role in the conversion of resazurin and MTT, though they do not necessarily follow the same path for conversion as will be seen in the further analyses. The addition of amines and amides do not seem to directly contribute substantially to the interferences and may be more related to increasing the overall solubility of the interfering species. Finally, assessment of additional reducing agents does not cause an extreme effect, suggesting it may be specific to thiol chemistry and not simply the availability of redox active species.

Once the initial screening was complete using well-plate assays to identify which species at what concentrations were giving rise to these interferences (Table 5.1), four or five representative molecules that demonstrated substantial deviations (in some cases, >100% deviation from control) were utilized for more in-depth studies using UV-Vis and MS analyses.

Table 5.1 Results from resazurin (R) and MTT (M) assays in the presence of the 19 species listed at six tested concentrations. The value displayed is the either the largest average deviation that occurred at some point during the four-hour reaction period or a statistically significant difference was not present when compared to the controls, as denoted by "ns" ($n \geq 3$). Functional groups on each species are also displayed (T=thiol, An=amine, Ad=amide, A=acid, D=disulphide, Oh=alcohol).

		R	M	R	M	R	M	R	M	R	M	R	M
Sample	**Functional Groups Present**	**1 µM**		**10 µM**		**100 µM**		**1 mM**		**10 mM**		**100 mM**	
1	T, An, Am, A	ns	-19	ns	23	ns	113	ns	2336	-50	2378	-91	234
2	An, Ad, D, A	ns	23	ns	25	ns	30	ns	37	-69	-16	-71	-16
3	T, An, A	ns	-22	ns	18	ns	20	ns	170	23	3670	51	1897
4	T, ad, ac	ns	-26	ns	16	ns	34	ns	130	ns	273	-83	221
5	T, a	ns	-26	ns	-25	ns	117	ns	585	-90	609	-97	296

6	T, ad, a	ns	-28	ns	-23	ns	45	ns	1113	ns	894	-95	130
7	An, d	ns	-28	ns	-27	ns	-25	ns	-22	ns	ns	ns	52
8	T, an, a	ns	-24	ns	-20	ns	108	13	861	59	3010	-47	1878
9	T, an, a	ns	ns	ns	ns	ns	94	ns	1699	ns	3558	161	3049
10	An	ns	ns	ns	-18	ns	-13	ns	20	25	57	ns	132
11	An	ns	ns	ns	ns	ns	14	7	ns	9	20	ns	43
12	An	ns	ns	ns	14	ns	13	9	11	ns	13	ns	14
13	D	ns	13	ns	12	ns	14	ns	13	ns	13	ns	13
14	T	ns	ns	ns	ns	ns	ns	6	ns	ns	27	ns	247
15	T	ns	19	ns	18	ns	15	ns	12	ns	17	ns	28
16	-	-11	ns	ns	9	-24	9	-23	ns	-24	12	ns	39
17	A, oh	ns	ns	ns	41	ns	249	45	3718	-83	4535	-96	1984
18	Oh	ns	ns	ns	ns	8	ns	11	ns	ns	15	ns	103
19	T, oh	ns	ns	ns	ns	ns	119	ns	2045	ns	4487	47	1838

5.4.1 Resazurin assay

Figure 5.2 provides additional quantitative deviations for four representative species in the presence of the resazurin assay (**1**, **2**, **5**, and **8**) for all six tested concentrations occurring at each hour time point. It is clear that the deviations giving rise to false positives or negatives occur predominantly at the higher concentrations tested (10 and 100 mM) for all four species and are often present within the first hour of incubation with the starting material. This suggests that shorter incubation periods do not necessarily alleviate or minimize these interferences. Additionally, the deviations observed at 10 and 100 mM are substantial, often representing >60% deviation from the control samples. It is unclear from Figure 5.2 alone whether there is a direct transformation of resazurin to resorufin in the presence of these species, or whether a more convoluted chemical transformation is occurring that simply shifts the spectroscopic transitions.

In order to further understand this chemistry, UV-Vis spectra were obtained for all four species at 10 mM and compared to a spectrum of a positive control (resazurin in the presence of viable *E. coli* cells). The results of this study are shown in Figures 5.3 and 5.4.

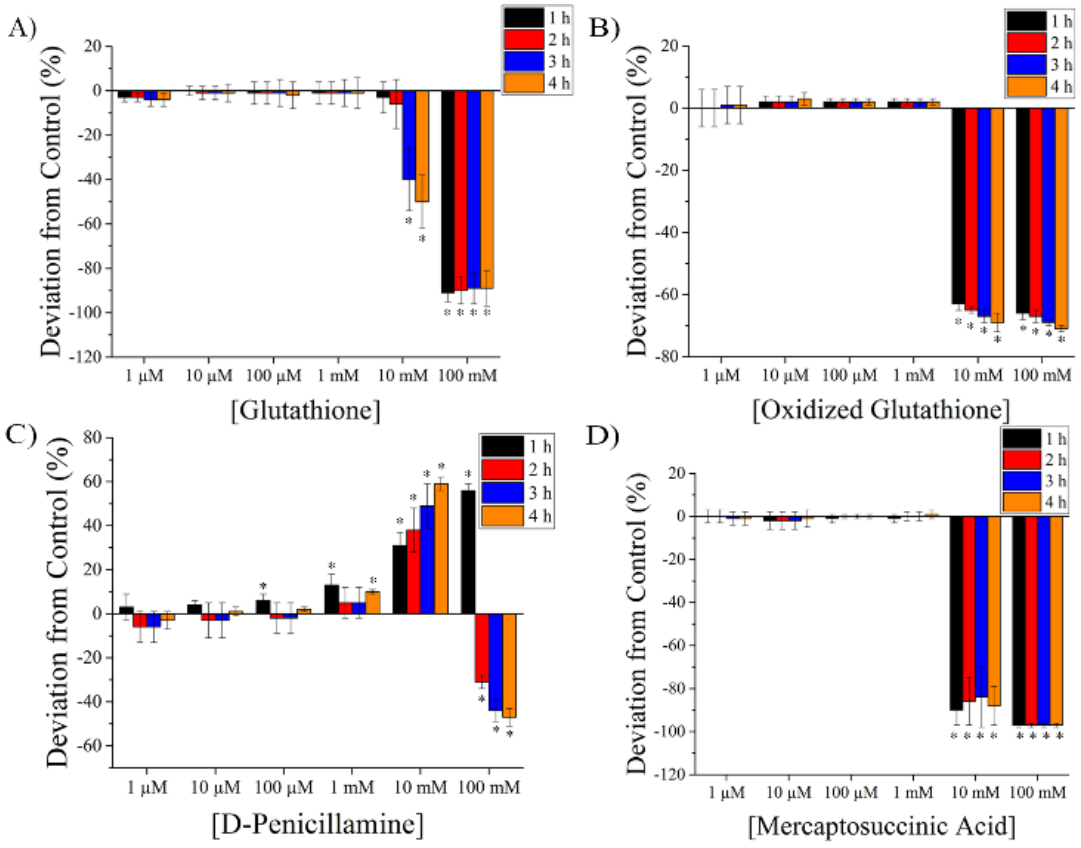

Figure 5.2 Representative interfering species that showed substantial deviations from control in the presence of the resazurin assay, with the percent deviation from control versus concentration of the molecule displayed as average and standard deviation. Data with (*) indicates statistically significant differences between control and sample value as determined by Student's t-test. The deviation at each hour time point (up to four hours) is also shown (n≥3).

Figure 5.3 shows the expected chemical transformation between the resazurin compound (λ_{max} ~600 nm) to the resorufin compound (λ_{max} ~570 nm) that would occur in the presence of metabolically active cells (in this case, *E. coli*). The analysis for this assay is to either monitor the fluorescence signal at 570 nm or monitor the absorbance values at both 570 and 600 nm.[6] It

should also be noted that there is an absorbance feature between 300-400 nm that is present in the starting material (resazurin) but disappears in the final compound (resorufin). These UV-Vis spectra can be used as a point of comparison between the expected assay behavior (before and after the introduction of viable cells) and what is observed in the presence of the four representative species in the absence of cells.

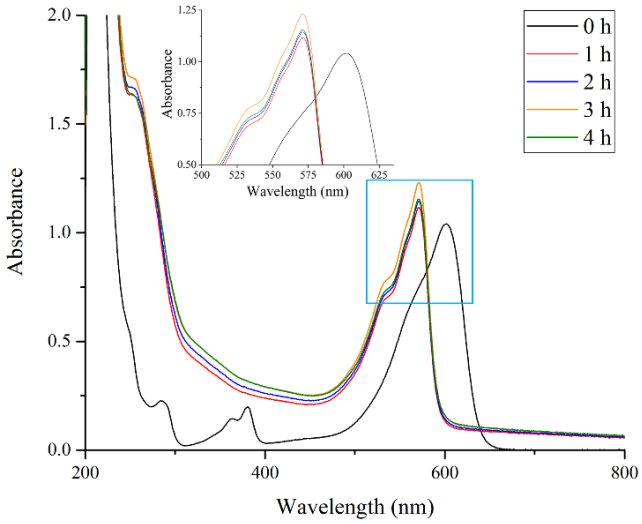

Figure 5.3 UV-Vis spectra obtained every hour after the introduction of *E. coli* cells with resazurin assay. There is a clear transition between ~600 nm (at time=0) and ~570 nm (after 1 h of incubation). Inset shows the zoomed in region of this shift.

Figure 5.4A shows the UV-Vis results from 10 mM glutathione (**1**) in the presence of resazurin taken after each hour of incubation. It is noteworthy that this spectrum looks remarkably similar to the positive control seen in Figure 5.3, where there is an initial peak at ~600 nm that shifts to the predominant absorbance feature ~570 nm. It is also apparent that the absorbance feature between 300-400 nm that was noted in the positive control is present in Figure 5.4A. This is also the case for D-penicillamine (**8**), as shown in Figure 5.4C, where there is an initial peak at 600 nm, that shifts to the predominant peak at ~570 nm. Again, the smaller absorbance feature between 300-400 nm that was present in the positive control spectrum

(Figure 5.3) can also be observed in Figure 5.4C. These spectra (Figures 5.4A and 5.4C) would suggest that the molecules **1** and **8** follow a similar mechanistic pathway to that of metabolically active cells, where there is a clear shift from the starting resazurin compound to the final resorufin compound. Structural similarities between these two molecules are the presence of thiol, amine, and acid functionalities.

Observing the UV-Vis spectra obtained for species **2** and **5** illustrate a more convoluted path to the interferences observed. Figure 5.4B shows the full UV-Vis spectrum for molecule **2** (oxidized glutathione), where there is no obvious peak associated with either resazurin (~600 nm) or resorufin (~570) but rather a multitude of overlapping peaks between 250-600 nm. Even though a direct absorbance feature is not observed for the resorufin compound, Figure 5.2B demonstrates that this still gives rise to a massive deviation from the control when monitoring the absorbance associated with resorufin formation (≥60%). This would suggest that, while interferences are occurring in the presence of resazurin and molecule **2**, there is not obvious chemical functionality that is directly reducing the resazurin to resorufin, as appears to be the case with molecules **1** and **8**. Likewise to molecule **2**, the UV-Vis spectra obtained for **5** (mercaptosuccinic acid) do not give rise to absorbance features at either wavelength associated with resazurin or resorufin. Instead, there is a slight peak at ~250 nm that increases over time, with the rest of the spectrum showing no deviation from the baseline. This suggests extreme signal suppression if monitoring the absorbance associated with resorufin, leading to false negatives and implicating that there is little to no cellular viability present. Based on the structure of **5**, these results would suggest that simply having a thiol group present is not enough to reduce the resazurin to resorufin in the absence of cells, but the addition of the acid groups appear to cause significant breakdown of the starting material.

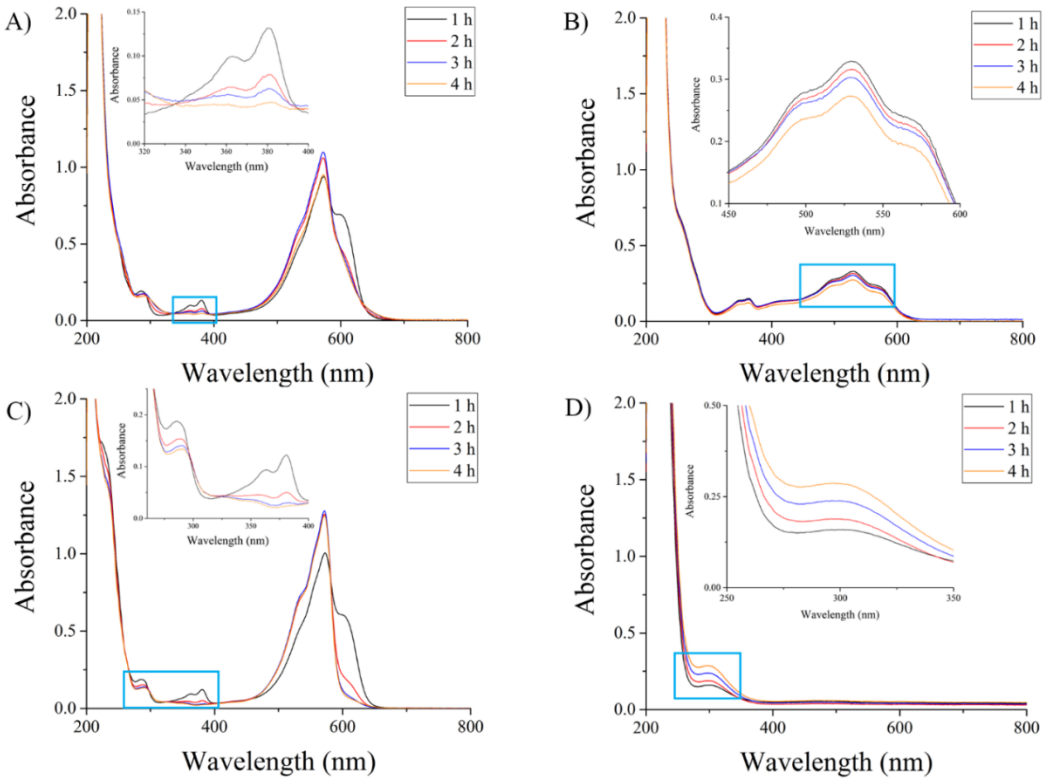

Figure 5.4 UV-Vis spectra obtained for the four representative interfering species at 10 mM (A – glutathione (**1**); B – oxidized glutathione (**2**); C – D-Penicillamine (**8**); D – mercaptosuccinic acid (**5**)) in the presence of resazurin assay after each hour of incubation. Inset in each spectra shows zoomed in regions of initial spectra obtained from 200-800 nm.

To track the reduction of resazurin to resorufin in the presence of molecules **1**, **2**, **5**, and **8**, mass spectra were also collected at each time interval consistent with the intervals for UV-Vis spectroscopic analysis (not shown). The results for species **1** shows an increased prevalence of resorufin (as compared to resazurin) within the first hour of exposure, which verifies the results observed with UV-Vis. MS data for species **2** does not show any appreciable signal from resorufin formation but does display a signal associated with resazurin. This would indicate that the overlapping peaks between 250-600 nm seen in Figure 5.4B are indeed partially from resazurin, but also include secondary species forming under these conditions. This is critical as merely taking absorbance values associated with resorufin formation (at 570 nm) would give rise to substantial false positives (as shown in Figure 5.2B), even though MS analysis shows no

substantial contribution from the reduced product. The same analysis for species **8** shows both initial and final compounds present throughout the entire reaction period. Results for species **5** are most interesting, where there is near full conversion of the resazurin to resorufin within the first hour of exposure, resulting in the greatest deviation from that observed with UV-Vis. This could indicate that a more complicated compound is forming within these reaction conditions that causes spectroscopic signal suppression at 570 nm.

5.4.2 MTT assay

Likewise to the resazurin assay, after screening the initial 19 species to determine if and to what extent deviation from controls exist in the presence of the MTT reagent, five molecules (**1**, **3**, **4**, **5**, and **8)** were chosen that showed substantial deviations to further study the interaction between the chosen molecule and MTT. Figure 5.5 shows the quantitative results from the well-plate assays between the MTT reagent and the selected interfering species at all six different concentrations over the four-hour reaction period. Although there are more deviations occurring at the lower tested concentrations when compared to the resazurin assay data, the largest deviations still exist at the higher concentrations of 10 and 100 mM. It would also appear that the majority of the observed deviations occur within the first hour of incubation (with the exception of **1**), suggesting that regardless of reaction time, the interferences are still substantial. Figure 5.5 also highlights the extent to which these interferences occur for the tested molecules. The deviations are significantly higher than any observed using the resazurin assay, with the most extreme cases being upwards of 3000% deviation from the control. This indicates that not only does the MTT assay exhibit more interferences given the 19 molecules tested, but also that these interferences are even more substantial than anything observed under the resazurin assay conditions (many of them >>100%). This point was also determined by van Tonder et al., where

they found that MTT produced significantly more interferences in the presence of glycolysis inhibitors than the resazurin assay.[24]

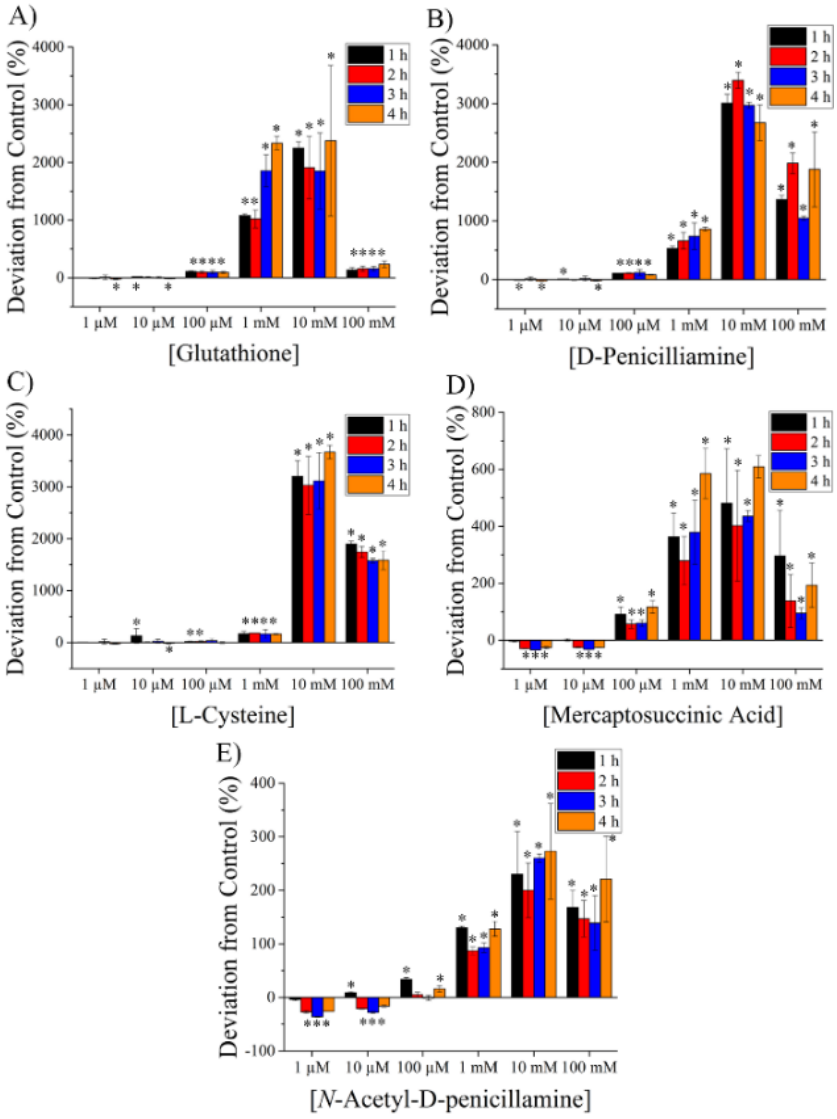

Figure 5.5 Representative interfering species that showed substantial deviations from control in the presence of the MTT assay, with the percent deviation from control versus concentration of the molecule displayed as average and standard deviation. Data with (*) indicates statistically significant differences between control and sample value as determined by Student's t-test. The deviation at each hour time point (up to four hours) is also shown (n≥3).

Both UV-Vis and MS analyses were conducted on the five representative species to better understand how these interferences are occurring. Similar to the resazurin assay data, all

five species were studied at a concentration of 10 mM. Figure 5.6 shows the UV-Vis spectra of the MTT reagent in the presence of metabolically active *E. coli* cells taken at each hour time point over a four-hour period. These spectra show a clear shift, where there is a decrease in the initial peak associated with the MTT reagent at ~380 nm and an increase in the peak associated with the formation of the formazan complex at ~540 nm. Generally the implementation of this assays works by monitoring the absorbance associated with the formazan complex, either at 570 nm (if using sodium dodecyl sulfate to solubilize the formazan) or at 540 nm (if using DMSO, as is this case in this study).[7] It should also be noted that there is a substantial absorbance peak ~270 nm after the transformation from MTT to formazan, that is blue shifted in the MTT reagent spectrum (~240 nm).

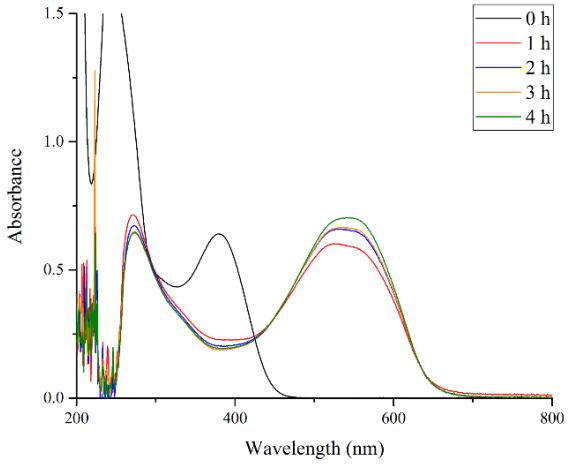

Figure 5.6 UV-Vis spectrum obtained every hour after the introduction of *E. coli* cells with MTT assay. There is a clear transition between absorbance features from ~380 nm (at time=0) and ~540 nm (after 1 h of incubation).

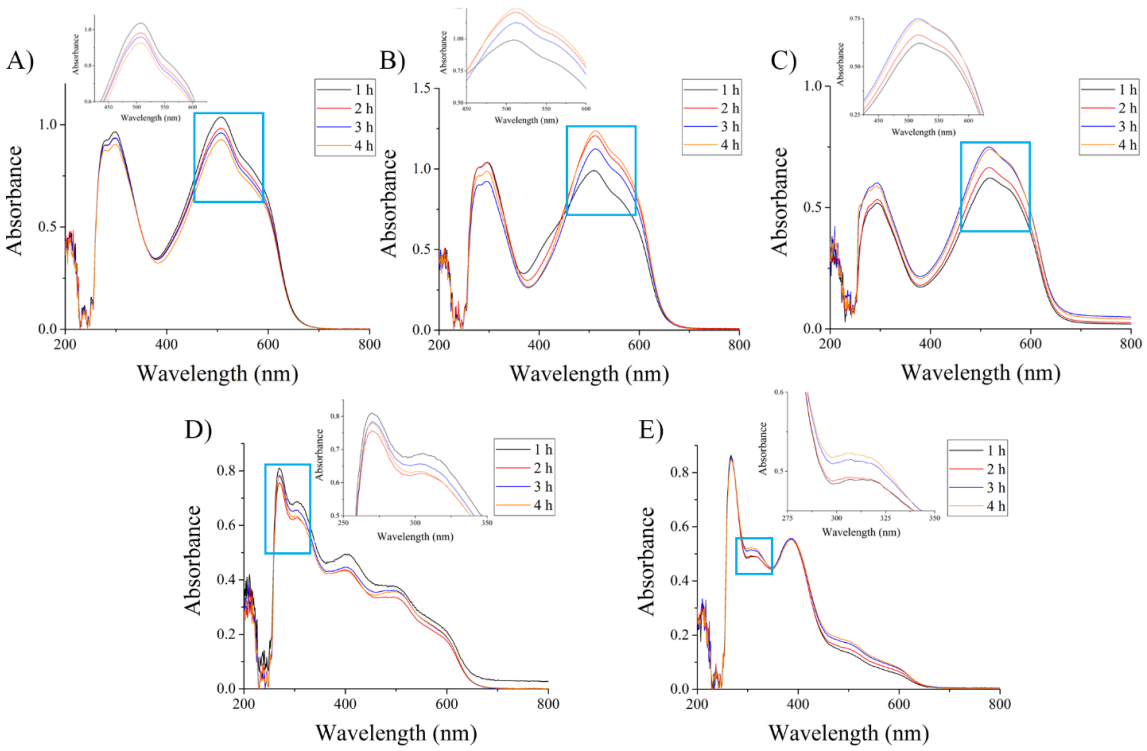

Figure 5.7 UV-Vis spectra obtained for the five representative interfering species at 10 mM (A – glutathione (**1**); B – D-Penicillamine (**8**); C – L-Cysteine (**3**); D – mercaptosuccinic acid (**5**); E – *N*-Acetyl-D-penicillamine (**4**)) in the presence of MTT assay after each hour of incubation. Inset in each spectra shows zoomed in regions of initial spectra obtained from 200-800 nm.

Figure 5.7 displays the UV-Vis spectra obtained for each of the five representative species at 10 mM in the presence of the MTT reagent. Figure 5.7A shows two dominant absorbance features at ~275-315 nm and ~500 nm with a shoulder at ~540 nm. These spectra look similar to that obtained in the presence of healthy, viable cells (with peaks around 270 and 540 nm), with no observed peak associated with the starting MTT reagent (though a small absorbance feature existing at ~380 nm could be hidden under the more dominant absorbance features). Interestingly, very similar spectra are obtained for both **8** and **3** (representing D-penicillamine and L-cysteine, respectively). Both of these molecules have dominant absorbance peaks at ~275-315 nm and ~500 nm, with the same shoulder observed for molecule **1**. All three studied interfering species share the same basic chemical functionalities of thiols, carboxylic

acidic groups, and primary amines. This would suggest that this combination of chemical moieties have the ability to transform the MTT reagent to its formazan counterpart in a relatively comparable manner as metabolically active cells do in the presence of MTT.

Similar to what was observed for molecule **5** in the presence of resazurin, the UV-Vis spectra obtained for **5** in the presence of MTT does not give rise to straightforward conversion of the MTT to the formazan complex. Instead, there are a multitude of peaks, beginning at ~270 nm, that diminish in intensity as the wavelength increases, and continues until ~600 nm. Again, it is difficult to say what chemical transformations are occurring in the presence of MTT and mercaptosuccinic acid (**5**) but suffice to say that the results obtained in the presence of this molecule could lead to false positives and potentially additional interferences given the complexity of the spectra. Lastly, molecule **4** displays spectra that look most similar to the starting spectra of MTT, but interestingly, still gives rise to deviations of ~200% relative to the control. This is attributable to the increase from baseline in the spectra at 540 nm, representing some transformation to the formazan complex. The only substantial difference in the chemical functionalities of **4** compared with the others tested is the absence of an amine group replaced by an amide, suggesting that amines are greater reducing agents than amides, and therefore, more likely to assist in the reduction described in this assay.

To track the conversion of MTT to formazan in the presence of species **1**, **3**, **4**, **5**, and **8**, mass spectra were also collected at each hour time interval (not shown). Results for species 1 show equal intensities associated with both MTT and its formazan counterpart, until hour 4 where there is a slight excess of formazan. This may suggest that the absorbance features for any residual MTT may be hidden under the dominant features for formazan, shown in the UV-Vis spectra. Results for both species **3** and **8** show nearly full conversion of MTT to its formazan

counterpart within the first hour of exposure, consistent findings with the UV-Vis spectra. The MS results for species **4** and **5** show a strong presence of MTT, and no appreciable amount of formazan. This was expected based on the UV-Vis analysis for these compounds, where there does not appear to be an obvious conversion of MTT to formazan. This was particularly true for **4**, where the UV-Vis spectrum looked most similar to the spectrum of MTT before conversion to formazan.

As previously mentioned, both assays have been investigated to some degree in an attempt to highlight the components that can cause potential interferences during *in vitro* studies. It should be noted, however, that the vast majority of work in this area is still in the presence of viable cells.[4,10,12,23,24] The first account of using the resazurin assay was in 1977, when De Jong et al. studied the activity of dehydrogenases in tobacco leaves.[4] In this initial report, they noticed substantial increases or decreases in the fluorescence signal produced by resorufin in the presence of certain plant extracts. They attributed this effect to the presence of primary amines (such as ethylenediamine), which they hypothesized interfered with the enzyme-substrate reaction involved in the cellular reduction of resazurin to resorufin. Interestingly, they did not observe this effect in the presence of diethylamine, which corroborates the work presented here, where diethylamine has no interference at low concentrations and minimal effects even at the highest tested concentrations. The authors also note that certain antioxidants can readily reduce resazurin to resorufin and specifically note the ability for cysteine to efficiently perform this reduction. Although De Jong et al. do not directly attribute this phenomenon to thiol residues, they continue to provide further examples of thiol-containing compounds that give rise to similar interferences.

Specific to MTT, both Shoemaker et al. and Natarajan et al. have reported on interferences associated with aqueous herbal extracts and antioxidant compounds, respectively, and both groups point directly to the availability of reactive thiol residues to be the responsible agent for these effects.[11,25] This was corroborated by noting the effects of vitamin E isomers in the presence of MTT, where extreme reduction was observed and attributed to the antioxidant properties of the samples.[26] Natarajan et al. also note that, while certain acids do seem to have an effect on this particular reaction, it is not as straightforward as the thiol containing residues in terms of direct conversion of MTT to formazan.[25] Another paper examined the ability for certain amino acids to reduce nitroblue tetrazolium (another biological assay based on the conversion of a tetrazolium salt to its formazan counterpart) and found the reaction would readily occur in the presence of folic acid without the need for cellular activity.[27] A review of the previous work done on these assays substantiates many of the findings presented in this work. Indeed, the presence of amine and thiol functionalities do seem to play a role in the reduction for both resazurin and MTT, while acidic groups interfere in a more convoluted manner. Finally, both resazurin and MTT assays have been noted to behave differently depending on the media employed in the study, and specifically to the protein concentration within the media.[10,23] Although not directly stated in these findings, this change in protein concentration could be related to available thiol, amine, and acidic residues that impart interferences in the presence of these two starting reagents.

5.5 CONCLUSIONS

Taken together, the substantial interferences and deviations observed with both the resazurin and MTT assays in the presence of a multitude of sample molecules highlights the need for particular care when performing these *in vitro* studies. Without the implementation of proper

control studies, collected data could lead to a significant amount of false positives or false negatives, minimizing the usefulness of the acquired information. There is no doubt that the use and application of these *in vitro* assays is critical to understanding the effects of novel compounds in the presence of cellular activity, but it is just as critical to ensure that the assays are truly representative of the interaction between the analyte and cells and not the analyte and assay reagents. By improving upon the accuracy of these methods, a better transition between *in vitro* to *in vivo* studies can be attained.

CHAPTER 5 – REFERENCES

1. Goh, J-Y.; Weaver, R.J.; Dixon, L.; Platt, N.J.; Roberts, R.A. Toxicol. Res. **2015**, 4, 1297-1307.
2. U.S. Department of Health and Human Services, National Institutes of Health, National Toxicology Program. (2006). In Vitro Cytotoxicity Test Methods: Background Review Document (NIH Publication No – 07-4518).
3. Riss, T.L.; Moravec, R.A.; Niles, A.L. et al. Cell Viability Assays. Eli Lilly & Company and the National Center for Advancing Translation Science: Bethesda, 2004.
4. De Jong, D.W.; Woodlief, W.G. Biochim. Biophys. Acta. **1977**, 484(*2*), 249-259.
5. Mosmann, T. J. Immunol. Methods **1983**, 65, 55-63.
6. Promega Corporation. "CellTiter-Blue Cell Viability Assay". Promega Corporation, Madison, WI (2013).
7. Sigma Aldrich Roche. "Cell Proliferation Kit I (MTT)". Sigma Aldrich, St. Louis, MO (2016).
8. Riss, T.L.; Moravec, R.A.; Niles, A.L.; Duellman, S.; Benink, H.A.; Worzella, T.J.; Minor, L. Assay Guidance Manual: Cell Viability Assays; Sittampalam, G.S.; Coussens, N.P.; Brimacombe, K. et al. Ed.; Eli Lilly & Company and the National Center for Advancing Translational Sciences: Bethesda, 2004.
9. Marshall, N.J.; Goodwin, C.J.; Holt, S.J. Growth Regul. **1995**, 5(*2*), 69-84.
10. Goegan, P.; Johnson, G.; Vincent, R. Toxic. in Vitro **1995**, 9(*3*), 257-266.
11. Shoemaker, M.; Cohen, I.; Campbell, M. J. Ethnopharmacol. **2004**, 93, 381-384.
12. O'Brien, J.; Wilson, I.; Orton, T.; Pognan, F. Eur. J. Biochem. **2000**, 267, 5421-5426.

13. Kosmala, A.; Fitzgerald, M.; Moore, E.; Stam, F. Anal. Lett. **2017**, 50(*1*), 219-232.

14. Kaushik, A.M.; Hsieh, K.W.; Chen, L.B.; Shin, D.J.; Liao, J.C.; Wang, T.H. Biosens. Bioelectron. **2017**, 97, 260-266.

15. Jayme, C.C.; de Paula, L.B.; Rezende, N.; Calori, I.R.; Franchi, L.P.; Tedesco, A.C. Exp. Cell Res. **2017**, 360(*2*), 404-412.

16. Ijaz, M.; Prantl, M.; Lupo, N.; Laffleur, F.; Asim, M.H.; Matuszczak, B.; Bernkop-Schnurch, A. Int. J. Pharm. **2017**, 534(*1-2*), 339-347.

17. Siu, J.T.; Liu, G.X.; Song, Y.; Li, D.; Dong, X.T.; Wang, J.X.; Yu, W.S. J. Colloid Interface Sci. **2018**, 510, 292-301.

18. Ghosh, P.; Bhoumik, A.; Saha, S.; Mukherjee, S.; Azmi, S.; Ghosh, J.K.; Dungdung, S.R. Cell Physiol. Biochem. **2018**, 233(*2*), 1041-1050.

19. Zamani, M.; Rostami, M.; Aghajanzadeh, M.; Manjili, H.K.; Rostamizadeh, K.; Danafar, H. J. Mater. Sci. **2018**, 53(*3*), 1634-1645.

20. Pourjavadi, A.; Tavakoli, E.; Motamedi, A.; Salimi, H. J. Appl. Polym. Sci. **2018**, 135(*7*).

21. Poole, L.B. Free Radical Biol. Med. **2015**, 80, 148-157.

22. Fotakis, G.; Timbrell, J.A. Toxicol. Lett. **2006**, 160, 171-177.

23. Grela, E.; Zabek, A.; Grabowiecka, A. Avicenna J. Med. Biotechnol. **2015**, 7(*4*), 159-167.

24. Tonder, A.v.; Joubert, A.M.; Cromarty, A.D. BMC Res. Notes. **2015**, 8(*47*), 1-10.

25. Natarajan, M.; Mohan, S.; Martinez, B.R.; Meltz, M.L.; Herman, T.S. Cancer Detect Prev. **2000**, 24(*5*), 405-414.

26. Lim, S.; Loh, H.; Ting, K.; Bradshaw, T.D.; Allaudin, Z.N. Trop. Life Sci. Res. **2015**, 26(*1*), 111-120.

27. Achilli, C.; Grandi, S.; Ciana, A.; Balduini, C.; Minetti, G. Chem. Pap. **2014**, 68(*5*), 662-667.

CHAPTER 6

CONCLUSIONS AND FUTURE DIRECTIONS

6.1 CONCLUSIONS

This dissertation has made significant contributions to the advancement of understanding bacteria, both in their planktonic and biofilm forms, and sets a foundation for future research to continue to mitigate the likelihood of hospital acquired bacterial infections. By probing three of the life stages associated with bacteria and surfaces (planktonic, attachment, mature biofilm), there is new insight into the ability to cause significant reductions of viable bacteria using the systems described throughout this dissertation. The experiments described throughout confirm that, indeed, each bacterial stage is distinct, and therefore, requires focused and specific therapeutic agents, both in their method of administration and overall dosages. The studies show multiple methods to fabricate biomaterials (including impregnating a therapeutic into a polymer matrix and adding a therapeutic in solution) and techniques employed to assess the efficacy of the given substrate (bacterial growth conditions and analytical tools). The multiple polymer substrates presented throughout the dissertation also provide opportunities to examine different intended medical applications (catheter, extracorporeal circuitry, wound dressing). The impact of this work within the fields of bioanalytical chemistry, materials science, and microbiology lies in the enhanced understanding of the susceptibility of bacteria within their distinct life stages, such that we can better target, address, and ultimately affect cellular interactions with biomaterials in a more comprehensive and purposeful manner. The vast concern associated with clinical infections and superbugs will not be solved overnight or in the time of one graduate career, however the

findings presented throughout this dissertation move the field one step closer to overcoming these deadly infections that are truly a worldwide problem.

6.2 FUTURE DIRECTIONS

Next steps with NO – attachment impediment and outright death. With the growing interest in impeding bacterial attachment, NO-releasing materials could play a large role in tailoring current biomaterials to aid in this challenge. While Chapter 2 described an NO-releasing system to evaluate antibacterial efficacy on planktonic bacteria, an immediate next study would be to examine the effects on bacterial attachment. Toward this end, work is currently being conducted investigating the critical loading of NO into a Tygon® substrate to impede bacterial attachment of different bacteria strains. The dual nature of the original manuscript (*Biointerphases* **2016,** 11, 031005) could be investigated further, with additional therapeutic agents or surface modification to determine the minimal threshold of NO needed to elicit the desired antibacterial effects. Additionally, the described NO-releasing material could be investigated for multi-purpose action, killing bacteria while simultaneously inhibiting platelet adhesion and activation, thereby exploiting more biological properties associated with NO. Using the NO-releasing Tygon® substrate is an excellent model system to probe such a question, as it is stable with regards to donor leaching and can easily be tuned for NO release.

Even with the vast number of publications describing the antibacterial action of novel NO-releasing materials, there remains a need to thoroughly characterize and report the amounts of NO used in these studies, especially those directly related to biofilms. This would assist in translating NO amounts across the literature to determine true quantities of NO necessary to elicit a desired biological effect. This concept was addressed in Chapter 3 and the method employed could ultimately be used for reporting values for any given system. Although that

particular study (*Biointerphases* **2016**, 11, 031012) addressed a pre-formed biofilm grown on polyurethane substrates, it is still unknown whether the polymer itself plays a role into the amount of NO needed to cause a reduction in biofilm bacteria. It would also be of interest to use the different biofilm growth methods (described in Chapter 1) and compare the amount of NO necessary under each environment. Finally, an examination of the NO donor employed would be a useful analysis for the NO community. This could be a comparison of small molecule NO donors versus macromolecular donors and RSNOs versus *N*-diazeniumdiolates, as these have different associated NO release profiles.

Probing bacteria life stages – biofilm dispersal. The understanding that the majority of bacteria exist in the biofilm state (as opposed to in the planktonic state) indicates that bacteria studies must focus on eradicating biofilms or inhibiting the ability for them to form in the first place. Therefore, a shift from planktonic to biofilm studies is necessary to make progress in this field. If planktonic studies are to be performed, then it is critical to show an extreme reduction in the cellular viability in the presence of a therapeutic over a significant time period (as demonstrated in Chapter 2). As for the biofilm studies, one area of research that is rather understudied is the final, dispersal stage of the biofilm life cycle. This is considered the most complicated step (appearing to vary from one bacteria strain to another) and the analytical methods used to determine biofilm dispersal are severely underdeveloped.

The final stage in the biofilm life cycle is marked by the release of planktonic bacteria from a mature biofilm, such that the newly released bacteria will colonize a new area and start the biofilm process over again. This is thought to occur when resources become scarce within the mature biofilm. Interestingly, some bacteria strains appear to produce endogenous NO to induce the dispersal phase. It has been noted that low doses of NO (pM-nM range) have been detected

during a natural dispersal event in *P. aeruginosa*. This is significant because bacteria are thought to be the most susceptible to therapeutics (including traditional antibiotics) during this dispersal phase. Therefore, the ability to induce a dispersal event in a mature biofilm by administering low concentrations of NO could lend itself to a synergistic approach between therapeutics, all of which would be at lower concentrations than what are necessary to cause bacterial inhibition or outright death of a mature biofilm.

One of the challenges with inducing biofilm dispersal is the inability to accurately determine if and when a dispersal event has occurred. Because biofilms have natural dispersal events (without the introduction of therapeutics), the first step is to determine at what point this natural event takes place under the given experimental conditions. Once this is determined, the therapeutic can be administered prior to that time point. Regardless of a dispersal event occurring naturally or induced by an administered therapeutic, the more challenging aspect is the actual determination of a dispersal event. Currently there are three main methods for this, all of which contain complications. Since dispersal is marked by release of planktonic bacteria, some research groups have investigated this phenomenon by monitoring the increase in planktonic bacteria (increase in cellular viability in solution). Likewise, some research groups have quantified a decrease in biofilm bacteria and attributed that to a dispersal event. Lastly, some groups will take the ratio of biofilm to planktonic bacteria (denoted as biofilm/planktonic or simply b/p) and determine that if that ratio is less than one, a dispersal event has occurred because that value indicates that there is more planktonic than biofilm bacteria. Each of these techniques contains inherent challenges that are not easily eradicated by method development. In many cases, assumptions are made about starting concentrations of planktonic and biofilm bacteria and causes of reductions on either type of bacteria.

An examination of the dispersal methods provided is not intended to discredit the ongoing research but rather to draw attention to the fact that there are valuable analytical experiments to consider that would greatly enhance the discussion. Quantification and verification methods to determine both natural and induced dispersal events could consume an entire graduate career. This focus of research would be extremely useful to truly exploit the susceptibility of biofilms while in their dispersal phase.

Antibacterial surfaces – dual approach. The ongoing research related to antibacterial surfaces has demonstrated that multiple methods must be employed to improve current biomaterials. It is likely that a combination of approaches 1 and 2 (discussed in Chapter 1), where both a released therapeutic and non-biocidal releasing surface is necessary to inhibit and kill approaching bacteria. This allows for initial reductions in cellular viability in solution by the released drug and impediment of remaining bacteria to halt the biofilm formation process. It may also allow for low doses of drug to be initially impregnated into the material substrate, lessening the likelihood for toxicity concerns. This approach could easily be an extension of the work presented in Chapter 4 (*Adv. Funct. Mater*. **2017**, 27, 1702255-1702264), where a water-stable MOF was impregnated into a chitosan substrate to impede bacterial attachment. Another drug-eluting therapy could be blended into the MOF-containing system, or the chitosan backbone could be functionalized to contain additional antifouling properties. With the growing concern around superbugs, a shift away from developing single-action antibacterial agents (such as antibiotics) and a movement towards dual therapies with multiple mechanisms of action is of vital importance.